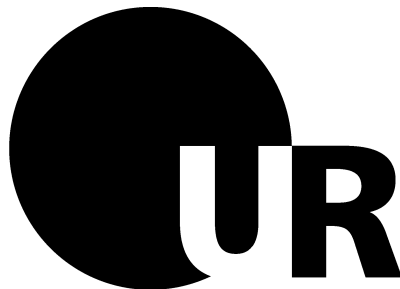# New Materials for Temperature and Pressure Sensitive Fluorescent Paints

Dissertation zur Erlangung des Doktorgrades der Naturwissenschaften

(Dr. rer. nat.)

an der

naturwissenschaftlichen Fakultät IV

- Chemie und Pharmazie -

der Universität Regensburg

vorgelegt von

**Lorenz Fischer**

aus Regensburg

im Juli 2012

# New Materials for Temperature and Pressure Sensitive Fluorescent Paints

Dissertation zur Erlangung des Doktorgrades der Naturwissenschaften

(Dr. rer. nat.)

an der

naturwissenschaftlichen Fakultät IV

- Chemie und Pharmazie -

der Universität Regensburg

vorgelegt von

**Lorenz Fischer**

aus Regensburg

im Juli 2012

Diese Doktorarbeit entstand in der Zeit von Januar 2009 bis Juli 2012 am Institut für Analytische Chemie, Chemo- und Biosensorik an der Universität Regensburg.

Die Arbeit wurde angeleitet von Prof. Dr. Otto S. Wolfbeis

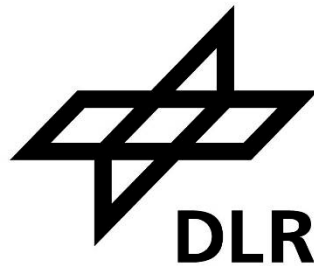**Promotionsgesuch eingereicht am**    20. Juni 2012
**Kolloquiumstermin**    19. Juli 2012

**Prüfungsausschuss**

| | |
|---|---|
| **Vorsitzender** | Prof. Dr. Bernhard Dick |
| **Erstgutachter** | Prof. Dr. Otto S. Wolfbeis |
| **Zweitgutachter** | Prof. Dr. Joachim Wegener |
| **Drittgutachter** | Prof. Dr. Achim Göpferich |

# Acknowledgements

**Für meine Eltern**

# Contents

# Chapter 1

# Introduction

## 1.1    Historical Background

The determination of oxygen partial pressure ($pO_2$) is of great interest in a variety of medical, biological and technical applications. The first continuous measurements of $pO_2$ in liquids were conducted by Leland Clark in 1953[1]. He developed the famous Clark oxygen electrode which represents the first oxygen sensor. These days, millions of solid state oxygen sensors, measuring the $pO_2$ in exhaust fumes, can be found in cars all over the world. However, these techniques are not capable of determining the oxygen distribution on surfaces.

The visualization of $pO_2$ distributions (and consequently distributions of air pressure) on surfaces gained a lot of interest with the growing field of aircraft development.[2-4] Aerodynamic tests are most often conducted in wind tunnels. There are a large number of wind tunnel facilities all over the world. The largest of them run by the NASA at the Langley Research Center in Virgina. It is capable of testing planes with a wing span of up to 30 m. This wind tunnel is driven by six 15-bladed fans with a diameter equal to the height of a four-story building. Each fan is powered by a 22,500-horsepower engine. Efforts like these make it obvious that wind tunnels play an essential role in aeronautic construction. Among the research conducted in wind tunnels, one of the major interests is the distribution of air pressure and temperature on surfaces of aero plane models. One can obtain the pressure values by using pressure taps, small perpendicular holes drilled into the model that are connected to pressure transducers. However, this method has some serious disadvantages:

- Taps and transducers only allow measurements at discrete points of the model surface. Pressure values in between the taps have to be interpolated.
- Taps are influencing the airflow. Measurements can not be carried out downstream of a pressure tap.
- Applying a large number of pressure taps distributed over the model is very time consuming and very expensive. Fabrication costs of an average model for wind tunnel testings are $500,00 to $1,000,000 , with the mounting of the taps causing 30% of the price.

An approach to overcome these problems is using a "pressure sensitive paint" (PSP).[5] The idea is coating the surface of interest with a photoluminescent dye in a polymer matrix. The luminescence is quenched by oxygen and depends on the partial oxygen pressure. The quenching of luminescence by oxygen was first described by Kautsky and Hirsch in 1935[6]. This dynamic quenching effect was first proposed to visualize the flow over a surface by Peterson and Fitzgerald in 1980[7]. The method was first used to obtain the pressure distribution on the surface of an aircraft model by Ardasheva and his group during the 1980s[2]. The temperature distribution is of interest because it can also be used to visualize aerodynamic effects. More than that it is necessary to correct the temperature effect on the PSP.[8] Compared to conventional temperature measurement techniques (e.g. infrared cameras), a temperature sensitive paint (TSP) offers a much higher lateral resolution. The principle is quite similar to that of a PSP. The luminescence of a dye in a polymer matrix is thermally quenched and the data is processed in a way analog to PSP measurements.[9]

## 1.2    Motivation

PSP/TSP measurements are applied and refined by all major aerodynamic research facilities in the world such as ONERA (France), JAXA (Japan), NASA (USA) and DLR (Germany). At the Institute of Analytical Chemistry, Chemo- and Biosensors of the University of Regensburg, optical chemical sensors especially for oxygen as well as for temperature, pH, metal ions or carbon dioxide partial pressure have been developed and studied intensely.

This work aims on the preparation and evaluation of new materials for PSPs and TSPs as well as dual pressure and temperature sensitive paints and the application of appropriate imaging techniques including RGB imaging. New materials for PSPs and TSPs Have to be developed in cooperation with the Institute of Aerodynamics and Flow Technology of the German Aerospace Center (Institut für Aerodynamik und Strömungsmechanik, Deutsches Zentrum für Luft- und Raumfahrt, DLR). The spectral separability of the pressure and temperature signal can be improved by applying new indicators for oxygen partial pressure and temperature. Therefore, new complexes that have not been used in PSPs or TSPs so far, have to be investigated. Furthermore it was aimed to improve the lateral signal homogeneity of PSPs and TSPs. New dyes with blue to green emission and good photostability and thermostability are needed for referencing purposes in intensity imaging and RGB imaging. In the course of this research project, a series of Ir(III) and Pt(II) complexes is investigated, resulting in a dual PSP/TSP based exclusively on Ir(III) complexes, different methods of read out are compared, a novel water based dual paint and the first dual PSP/TSP for RGB imaging is prepared and evaluated.

## 1.3 References

[1]    L. C. Clark, Jr., R. Wolf, D. Granger, Z. Taylor, *J. Appl. Physiol.* **1953**, *6*, 189-193.

[2]    J. W. Holmes, *J. Fluoresc.* **1993**, *3*.

[3]    R. H. Engler, C. Klein, O. Trinks, *Meas. Sci. Technol.* **2000**, *11*.

[4]    R. H. Engler, U. Fey, U. Henne, C. Klein, W. E. Sachs, *J. Visual-Japan* **2005**, *8*, 277-284.

[5]    J. H. Bell, E. T. Schairer, L. A. Hand, R. D. Mehta, *Annu. Rev. Fluid Mech.* **2001**, *33*.

[6]    H. Kautsky, A. Hirsch, *Z. anorg. u. allg. Chem.* **1935**, *222*, 126.

[7]    J. I. Peterson, R. V. Fitzgerald, *Rev. Sci. Instrum.* **1980**, *51*, 670-671.

[8]    S. Gouin, M. Gouterman, *J. Appl. Polym. Sci.* **2000**, *77*, 2805-2814.

[9]    M. I. Stich, O. S. Wolfbeis *Fluorescence Sensing and Imaging Using Pressure-Sensitive Paints and Temperature-Sensitive Paints; Standardization and Quality Assurance in Fluorescence Measurements I* Springer, 2008; Vol. 5.

# Chapter 2

# Imaging of Photoluminescent Coatings

## 2.1    Photoluminescence

Photoluminescence is the phenomenon of radiative relaxation of an electronically excited state generated by absorption of light. Photoluminescence is used in a huge number of applications[1] and methods in medical[2,3] and technological research[4-7] as well as in life science[8]. The basic principles of luminescence will not be discussed in detail in this work as they are extensively described in physical-chemistry textbooks.[9-11]

In this thesis, organic fluorophores were employed as temperature indicators and reference dyes. Metal-ligand complexes were employed as oxygen and temperature indicators. In case of organic fluorophores the emission is from a $S_1$-$S_0$ transition.[12] In metal-ligand complexes with a transition metal atom being the center, a slightly different electronic transition plays a very important role. The electron in the ground state $S_0$ located in the metal atom's d-orbital is excited to the $\pi^*$-orbital of a ligand molecule. This transition is called metal-to-ligand-charge-transfer (MLCT). In the crystal field of the ligands, the d-orbitals of the metal center get split. For example, in an octahedral ligand field, the d-orbitals split into three degenerated $t_{2g}$ and two degenerated $e_g$ orbitals.[12] A MLCT can only occur if the crystal field of the complex is sufficiently strong to raise the $e_g$-orbitals energetically above the $\pi^*$-orbital of the ligand as shown in Figure 2.1.
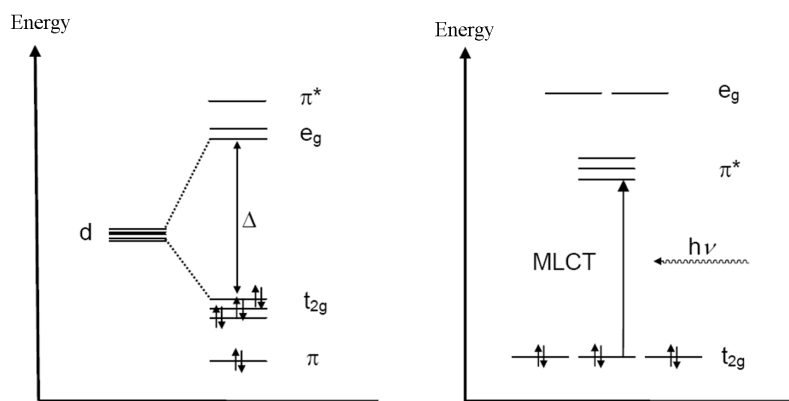
**Figure 2.1.** Jablonski diagram (a) of the crystal field splitting of a six-d-electron metal atom (e.g. Ru, Os) in an octahedral ligand field and (b) of the MLCT.[13]

In the MLCT the electron is excited to the singlet MLCT ($^1$MLCT) followed by intersystem crossing to the triplet MLCT ($^3$MLCT) (see Figure 2.2). Due to the stronger spin orbit coupling in transition metal complexes, the phosphorescence from this $^3$MLCT is shorter lived ($10^{-6} - 10^{-3}$ s) than the phosphorescence of common organic compounds.
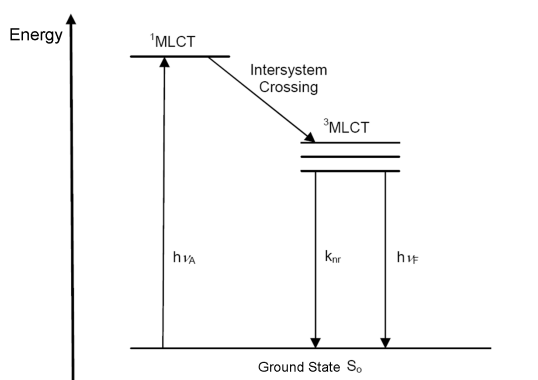


**Figure 2.2**. Jablonski diagram of the phosphorescence from the $^3$MLCT; $h\nu_A$ excitation energy; $h\nu_F$ energy of the phosphorescence; $k_{nr}$ rate of nonradiative decay.[13]

The quantum yields and lifetimes of phosphorescence can be described by first order kinetic equations. All rate constants and Abbreviations refer to the Jablonski diagram in Figure 2.3.
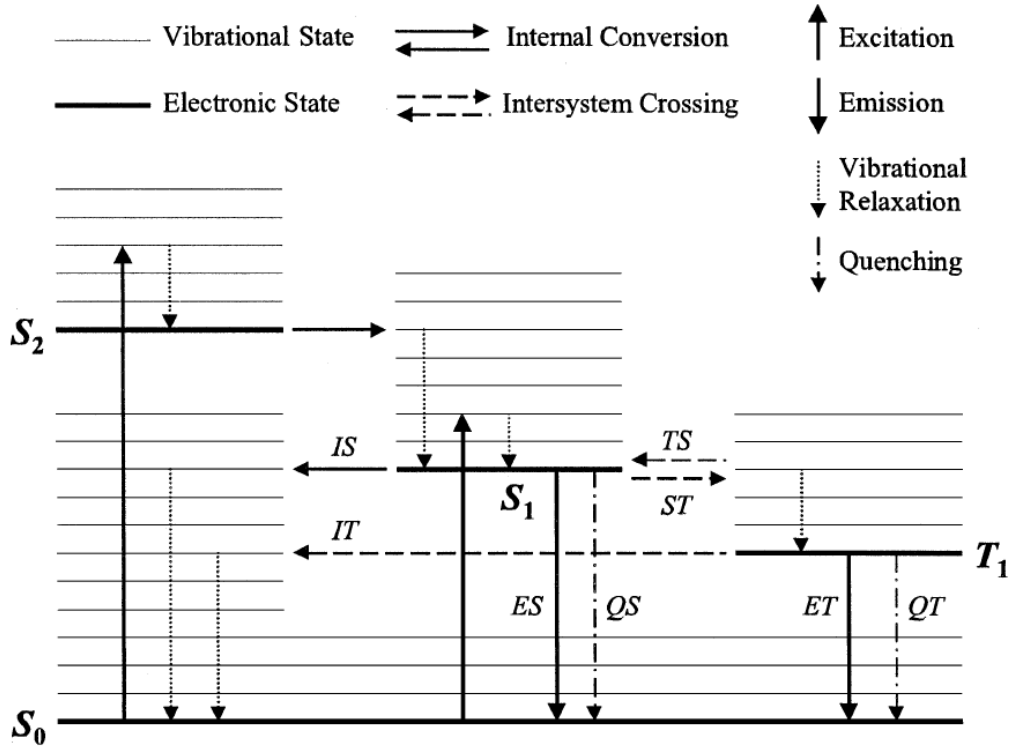
**Figure 2.3.** Jablonski diagram of basic electronic transitions. ES fluorescence; ET phosphorescence; QS quenching of fluorescence; QT quenching of phosphorescence.[12]

- $k_{ES}$: rate of fluorescence ($10^6 – 10^9$ s$^{-1}$)
- $k_{IS}$: rate of internal conversion from $S_1$ to $S_0$ ($10^5 – 10^9$ s$^{-1}$)
- $k_{QS}$: rate of quenching; a transition to $S_0$ by collision with an oxygen molecule described later ($k_{QS}$[O2] $= 0 – 10^{-8}$ s$^{-1}$). The rate is proportional to the concentration of oxygen and $k_{QS}$ is called the bimolecular quenching rate
- $k_{ST}$: rate of intersystem crossing ($10^4 – 10^{12}$ s$^{-1}$)
- $k_{ET}$: rate of phosphorescence ($10^2 – 10^6$ s$^{-1}$)
- $k_{IT}$: rate of intersystem crossing to $S_0$ ($10^1 – 10^9$ s$^{-1}$)
- $k_{QT}$: rate of quenching to $S_0$ as above ($k_{QS}$[O2] $= 0 – 10^8$ s$^{-1}$)
- $k_{TS}$: rate of intersystem crossing from $T_1$ back to $S_1$ ($A_{TS}$exp[$-\Delta_{TS}$/RT]).

The rate $k_{TS}$ depends on the energy gap and the temperature according to the Arrhenius equation given ($A_{TS} = k_{ST}$ /3)

The reciprocal values for the lifetimes of the $S_1$ ($\tau_S$) and the $T_1$ ($\tau_T$) are:

$$1/\tau_S = k_{ES} + k_{IS} + k_{QS} + k_{ST} \qquad \text{eq. 2.1}$$

$$1/\tau_T = k_{ET} + k_{IT} + k_{QT} \qquad \text{eq. 2.2}$$

The triplet quantum yield ($\Phi_T$) is the fraction of absorbed photons that produces dye molecules in the triplet state:

$$\Phi_T = \frac{k_{ST}}{k_{ES} + k_{IS} + k_{QS} + k_{ST}} = k_{ST}\tau_S \qquad \text{eq. 2.3}$$

The phosphorescence quantum yield ($\Phi_P$) is the fraction of absorbed photons that produces phosphorescence:

$$\Phi_P = k_{ET}\,\tau_T\,\Phi_T = \Theta_P\,\Phi_T \qquad \text{eq. 2.4}$$

$\Theta_P$ is the phosphorescence quantum efficiency. It indicates the fraction of molecules in the triplet state that relax to the $S_0$ via phosphorescence.[9,12]

## 2.2    Pressure Sensitivity

Unlike the name suggests, a PSP is not sensitive to (mechanical) pressure, but rather to oxygen partial pressure.[14] The luminescence of the indicator molecules is quenched by oxygen.[15] There are two basic types of quenching: dynamic and static quenching. Static quenching (quencher and luminophore form a complex) is not of interest with regard to oxygen sensing in PSP and will thus not be discussed. In case of a PSP the quencher is oxygen.[15] If the quencher collides with an excited luminophore, energy can be transferred to the ground state oxygen molecule.[16] An oxygen molecule in its ground state forms a triplet and in addition it has two excited singlet states at only 1 eV above the ground state. If a triplet oxygen molecule hits an excited indicator molecule an energy transfer occurs, and it will be raised to one of its excited singlet states. The dye emerges from the collision in its ground state $S_0$. The energy is finally degraded by either intersystem crossing followed by vibrational relaxation or IR-luminescence at wavelengths above 1240 nm.[17] The nonradiative triplet-triplet energy transfer is managed by the Dexter mechanism[18] shown in Figure 2.4. The premise for a Dexter transfer is an overlap of the wave functions of the energy donor (D) and the

energy acceptor (A). The overlap is required because the energy transfer is based on an electron exchange. Consequently, donor molecule and acceptor molecule have to come very close, for example by colliding. The distance between D and A ($R_{DA}$) has to be 20 Å or less. [9,19-21]
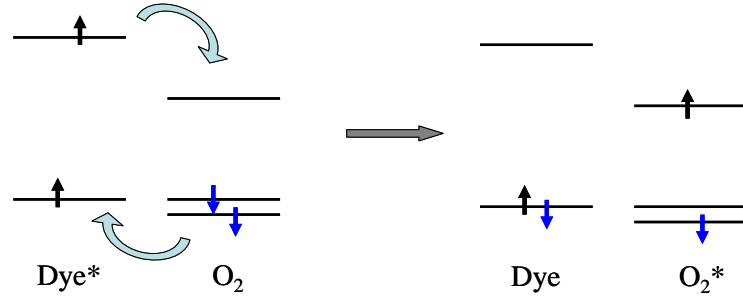


**Figure 2.4.** Sketch of the electron exchange in a Dexter energy transfer

The rate for the Dexter energy transfer $k_{DA}$ is given by:

$$k_{DA} \propto \left[\frac{h}{2\pi}\right] P^2 \exp\left[\frac{-2R_{DA}}{L}\right] J \qquad \text{eq. 2.5}$$

$L$ and $P$ are constants that can not easily be related to experimentally determinable quantities, and $J$ is the spectral overlap integral.[19] This is only one postulated mechanism for collisional quenching by oxygen. There are various other mechanisms discussed like the Förster decline model or the discrete exponential model.[22,23] The decrease of luminescence intensity and lifetime as a result of collisional quenching is given by the Stern-Volmer equation:

$$\frac{I_0}{I} = \frac{\tau_0}{\tau} = 1 + K_{SV}[Q] \qquad \text{eq. 2.6}$$

$I_0$ is the intensity and $\tau_0$ is the lifetime in absence of the quencher respectively the intensity and lifetime under reference conditions. Correspondingly $I$ and $\tau$ are intensity and lifetime in the presence of the quencher at the concentration $[Q]$. $K_{SV}$ is the Stern-Volmer constant. This equation is valid for a homogenous population of indicator

molecules. This means they are all in the same non-quenching matrix. For luminophores with different environments the so called multi-site model is an accurate description:

$$\frac{I}{I_0} = \frac{\tau}{\tau_0} = \sum_{i=1}^{n} \frac{f_i}{1 + K_{SV,i}[Q]}$$

eq. 2.7

With $i$ being the number of different matrices, $f_i$ is the fraction of dye in the respective matrix and $K_{SV;i}$ is the corresponding Stern-Volmer constant. $K_{SV}$ itself is the product of $\tau_0$ and the bimolecular quenching constant $\kappa_{QT}$ :

$$K_{SV} = \tau_0 \kappa_{QT}$$

eq. 2.8

$\kappa_{QT}$ is described by the Smoluchowski equation,

$$\kappa_{QT} = 4\pi N \alpha r D$$

eq. 2.9

where $N$ is Avogadro's number ($N = 6; 022 \times 10^{23}$ mol$^{-1}$) and $r$ is the radius of interaction between oxygen molecules and luminophore. $D$ is the sum of oxygen diffusivities in the matrix of the dye and the dye itself. The diffusivity in the indicator can usually be neglected. Finally, $\alpha$ is the quenching efficiency (the fraction of excited dye molecules that are quenched once they collided with oxygen). Typical values would ideally be 1/9 for triplet states and 1 for singlet states. But as stated above, the triplet states of transition metal complexes show singlet characteristics due to strong spin orbit coupling. As a result, the quenching efficiencies of these triplet states are much higher and can reach the corresponding singlet values for $\alpha$.

Furthermore, the oxygen concentration in the PSP is proportional to the partial oxygen pressure above it (Henry's law). With the mole fraction $\chi$ of oxygen in the air being constant 0.21, the partial oxygen pressure $\chi p$ is proportional to the air pressure $p$ (Dalton's law). In consequence, the quenching rate is proportional to $p$:

$$k_{QT} = \kappa_{QT}[O_2] = \kappa_{QT} S \chi p = 4\pi N \alpha r D S \chi p = 4\pi N \alpha r P \chi p$$

eq. 2.10

*S* is the solubility of oxygen in the matrix and *P = DS* is the oxygen permeability of the matrix.[12,19,20,24,25]

## 2.3    Temperature Sensitivity

The temperature sensitivity of luminescence is based on the temperature dependence of the intersystem crossing rate $k_{IT}$ to the $S_0$ state. It is given by the following Arrhenius equation:

$$k_{IT}(T) = A_{IT} \exp\left(-\frac{\Delta E_{IT}}{RT}\right) \cong k_{IT}(T_0)\left(1 + \frac{\Delta E_{IT}}{R_{T0}}\frac{\Delta T}{T_0}\right) \qquad \text{eq. 2.11}$$

$\Delta E_{IT}$ is the activation energy for the intersystem crossing, $T_0$ is a random reference temperature and $\Delta T = T - T_0$ is small relative to $T_0$ [12]. This means, the phosphorescence intensity and lifetime decrease with rising temperature. This is also referred to as thermal quenching. As a matter of principle every dye is more or less temperature sensitive and pressure sensitive. Hence, a matrix material with very low oxygen permeability is required for temperature indicators.[26-29]

## 2.4    Pressure Sensitive and Temperature Sensitive Paints

Considering the phenomena described above, an indicator in a film of polymer binder is the simplest paint conceivable. To increase the signal strength, a reflective white layer (base coat) is cast on the solid support (the model) first (see Figure 2.5).[4,20,30,31]
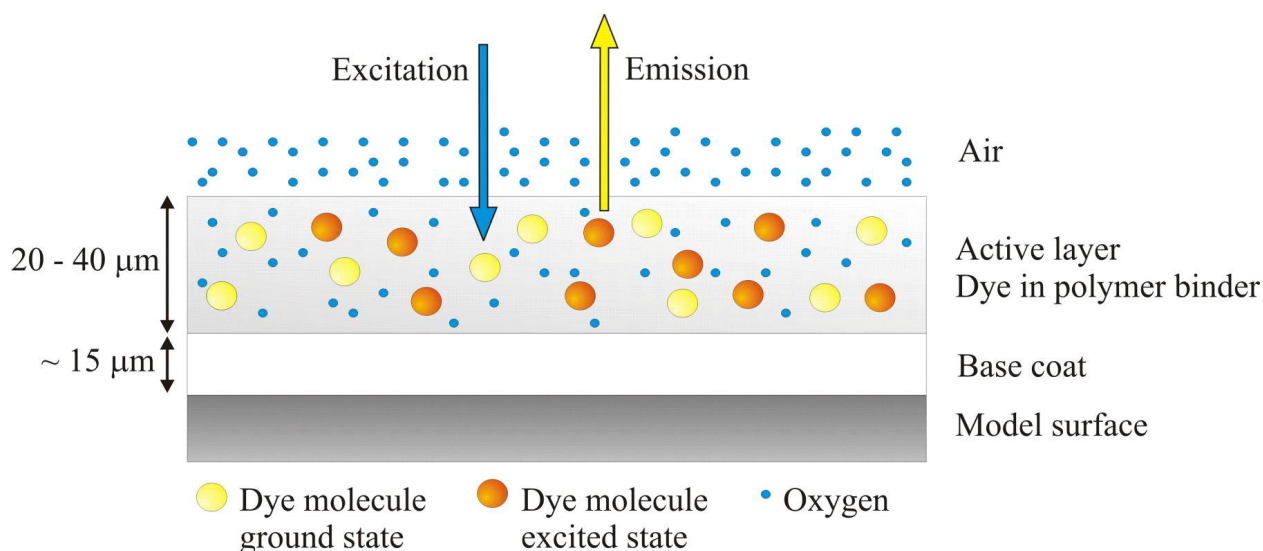
**Figure 2.5.** Sketch of a single luminophore PSP/TSP and its typical dimensions.

A dually sensitive film can not be composed by simply mixing two indicators in a polymer solution and casting a film from that mixture. A polymer for pressure sensing has to be chosen according to the oxygen sensitivity of the dye and the desired dynamic range of the sensor. A polymer that is as oxygen blocking as possible is the matrix of choice for temperature sensing to circumvent cross sensitivity towards oxygen. A cross section of a typical dually sensitive coating is shown in Figure 2.6.
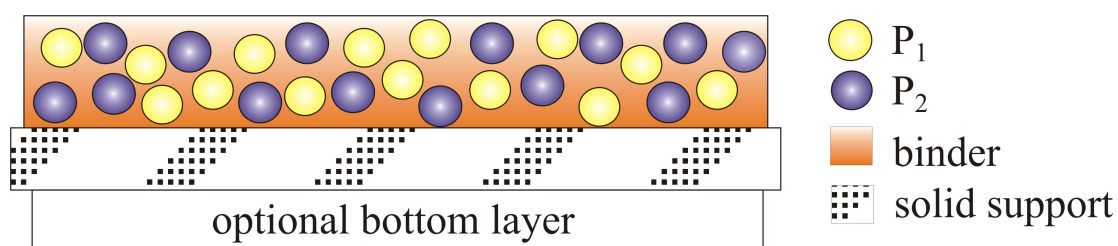


**Figure 2.6.** Cross section of a dually optical chemical sensor film. The particles ($P_1$, $P_2$) are responsive to the respective analyte and yield the optical information. The particles are incorporated into a matrix polymer (the binder) whose choice is quite critical. The sensor matrix usually is deposited on an optically transparent support so that the optical signal also may be gathered from the bottom. If gathered from top, the sensor layer also

may contain a reflective bottom layer that prevents sample fluorescence (which is strong in case of most biomatter) to interfere with the optical readout.

Two luminescent probes located in close proximity (less than 10 nm) can lead to fluorescence resonance energy transfer (FRET) which is highly undesirable. In order to avoid FRET it is necessary that at least the temperature indicator is encapsulated in polymer micro particles for measuring pressure and temperature simultaneously. Also, both pressure and temperature sensitive dyes can be embedded in different micro particles with tailored properties and cast together in a polymer binder.[32-35]

## 2.5    Polymers and Indicators for PSPs
### 2.5.1    Polymers for PSPs

The oxygen permeability is the foremost quality upon which the polymers for PSPs are chosen. For pressure sensing the permeability has to fit the oxygen sensitivity of the dye in respect to the favored dynamic range of the sensor. The relevant Figure is the permeability coefficient $P$.

$$P = \frac{(thickness\ of\ the\ polymer\ film)\cdot(quantity\ of\ oxygen)}{(area)\cdot(time)\cdot(pressure\ drop\ across\ the\ film)}$$    eq. 2.12
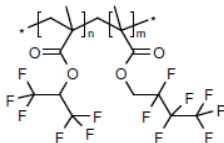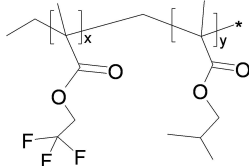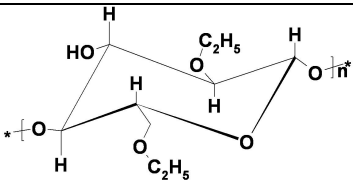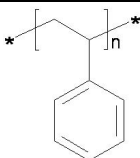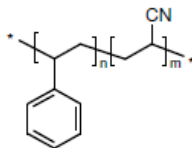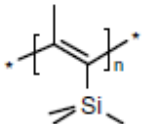
This coefficient $P$ is also temperature dependent.

$$P = P_0 \exp\left(-\frac{E_P}{RT}\right)$$    eq. 2.13

$P_0$ is a pre-exponential factor, $E_P$ is the activation energy of permeation, $R$ is the gas constant and $T$ is the absolute temperature in Kelvin.[24] This means, the cross sensitivity of a PSP towards temperature is also influenced by the temperature dependence of the oxygen permeability of the polymer and not only by the properties of dye itself. Further, the solubility of the polymer plays an important role as the particular dye has to be soluble in the same solvent. The polymer has to be mechanically robust and transparent. Some functional groups, e.g. carboxy groups, can quench the

luminescence of an indicator dye. Furthermore, some fluorophores are solvatochromic, meaning their spectral properties change depending on the matrix they are embedded in. The structures, the oxygen permeabilities, and the manufacturers of the used polymers are shown in table 2.1.
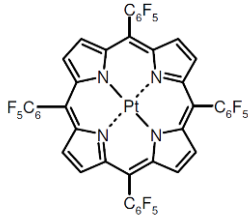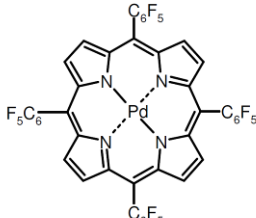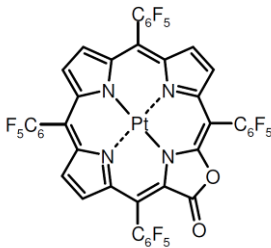
**Table 2.1.** Names, acronyms, chemical structures, and permeabilities *P* of polymers used in pressure sensitive paints.
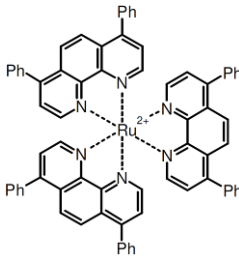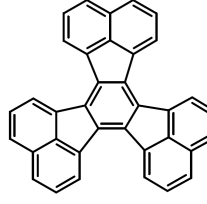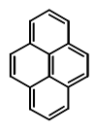
| Polymer [acronym] | Chemical Structure | $P$ [$10^{-13}$cm$^2$s$^{-1}$Pa$^{-1}$] | Ref. |
|---|---|---|---|
| Poly(hexafluoroisopropyl methacrylate-co-heptafluoro-n-butyl methacrylate) **[FIB]** |  | n.s. | [36] |
| Poly(isobutyl methacrylate-co-trifluoroethyl methacrylate) **[Poly(IBM-co-TFEM]** |  | n.s. | [37] |
| Etyhl cellulose **[EC]** |  | 11 | [38] |
| Poly(styrene) **[PS]** |  | 1.9 | [39] |
| Poly(styrene-co-acrylonitrile) **[PSAN]** |  | 0.0032 | [40] |
| Poly(trimethylsilyl propyne) **[PTMSP]** |  | n.d. | [41] |

## 2.5.2    Indicators for PSPs

Foremost Pt,Pd and Ru containing dyes and polycyclic aromatic hydrocarbons (PAHs) are employed for pressure sensing. For lifetime imaging the luminescence lifetime should be in the µs range. Nanosecond lifetimes require very sophisticated camera equipment and hardware to determine the changes in lifetime properly. A dye as bright as possible is favorable with respect to high signal strengths. The brightness of a dye is the product of the molar absorbance ($\varepsilon$) at the excitation wavelength and the quantum yield $\Phi$. In general, metal-ligand complexes display lower brightness than PAHs whereas the lifetime of the metal-ligand complexes is usually longer (µs) and thus more appropriate for lifetime imaging. Some common oxygen probes are listed in table 2.2.

**Table 2.2.** Common oxygen probes to be used in PSPs and their absorbance and emission maxima (S: Soret-band; Q: Q-band).

| Compound [acronym] | Chemical Structure | $\lambda_{abs}$ (max) | $\lambda_{em}$(max) | Ref. |
|---|---|---|---|---|
| Platinum(II)-5,10,15,20-tetrakis(2,3,4,5,6-pentafluorophenyl) porphyrin **[PtTFPP]** |  | 395 nm (S) 541 nm (Q) | 648 nm | [36] |
| Palladium(II)-5,10,15,20-tetrakis(2,3,4,5,6-pentafluorophenyl) porphyrin **[PdTFPP]** |  | 407 nm (S) 518 nm (Q) 552 nm (Q) | 653 nm | [42] |
| Platinum(II)-5,10,15,20-tetrakis(2,3,4,5,6-pentafluorophenyl) porpholactone **[PtTFPL]** |  | 392 nm (S) 572 nm(S) | 745 nm | [34] |

| Ruthenium(II)-tris(4,7-diphenyl-1,10-phenanthroline) **[Ru(dpp)3 2+]** | | 337 nm 457 nm | 610 nm | [43,44] |
|---|---|---|---|---|
| Decacyclene | | 385 nm | 510 nm | [45,46] |
| Pyrene | | 335 nm | 395 nm | [30,47] |
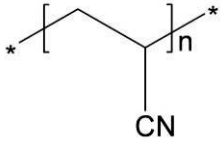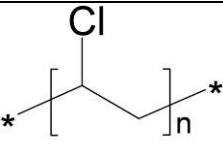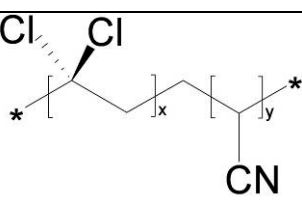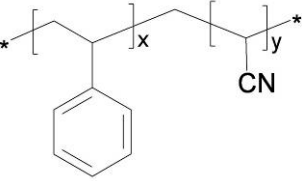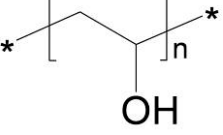
PtTFPP is most often applied due its superior characteristics in terms of brightness ($\Phi$ = 0.1; $\varepsilon$ = 323 10$^3$ (S) and 23.2 10$^3$ (Q)), photostability and sensitivity to oxygen.

## 2.6.    Polymers and Indicators for TSPs

### 2.6.1    Polymers for TSPs

The most important requirement for a polymer applied in a TSP is to have a low permeability for oxygen in order to suppress the cross-sensitivity towards oxygen.[20,31] Obviously, as well as in a PSP the polymer has to be mechanically stable and transparent at the excitation and emission wavelengths. In case one wants to combine the TSP with a pressure indicator to create a dually sensitive paint, the temperature indicator needs to be incorporated in polymer particles. Consequently, a polymer has to be applied for temperature sensing from which it is possible to synthesize micro particles or nano particles. Common polymers for use in TSPs are listed in table 2.3.
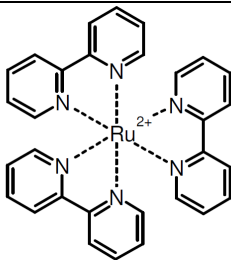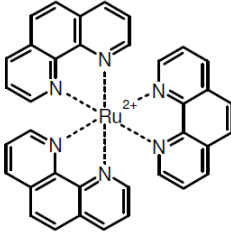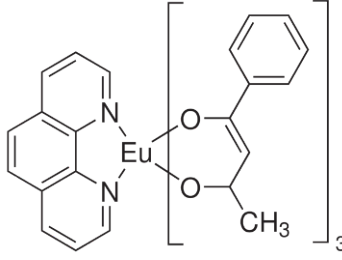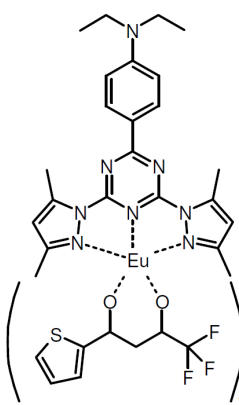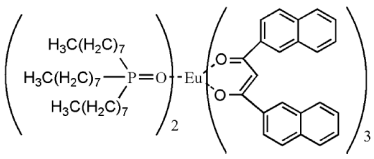
**Table 2.3.** Common polymers used for TSPs and their oxygen permeability $P$.

| Polymer [acronym] | Chemical Structure | $P$ [$10^{-13}$cm$^2$s$^{-1}$Pa$^{-1}$] | Ref. |
|---|---|---|---|
| Poly(acrylonitrile) [PAN] | | 0.00015 | [32] |
| Poly(vinyl chloride) [PVC] | | 0.034 | [24] |
| Poly(vinylidene chloride-co-acrylonitrile) [PVDCAN] | | n.s. | [48] |
| Poly(styrene-co-acrylonitrile) [PSAN] | | 0.0032 | [24] |
| Poly(vinyl alcohol) [PVA] | | 0.0065 | [24] |

## 2.6.2    Indicators for TSPs

Foremost complexes containing Ru(II) and Eu(III) are used for temperature sensing. The choice of the indicator depends on the desired temperature range. The oxygen sensitivity of a temperature indicator should be as low as possible because one can not suppress the oxygen cross-sensitivity by gas blocking polymers to any extend. A list of temperature indicators for use in TSPs is given in table 2.4.

**Table 2.4**. Indicators for use in TSPs, and their absorbance and emission maxima.

| Compound [acronym] | Chemical Structure | $\lambda_{abs}$(max) | $\lambda_{em}$(max) | Ref. |
|---|---|---|---|---|
| Ruthenium-tris(2,2'-bipyridine) [Ru(bpy)₃²⁺] | | 320 nm 425 nm | 588 nm | [29,49] |
| Ruthenium-tris(1,10-phenantroline) [Ru(phen)₃²⁺] | | 448 nm | 579 nm | [50] |
| Tris(benzoylacetonato)mono(phenanthroline)europium(III) [Eu(benzac)₃(phen)] | | 381 nm | 611 nm | [48] |
| Europium(III)-tris(thenoyltrifluoroacetylacetonato)-(2-(4-diethylaminophenyl)-4,6-bis(3,5-dimethylpyrazol-1-yl)-1,3,5-triazine) [Eu(tta)₃(dpbt)] | | 417 nm | 614 nm | [40,51] |
| Eu-tris(dinaphthoylmethane)-bis-(trioctylphosphine oxide) [Eu-DT] | | 375 nm | 616 nm | [52] |

In case the temperature indicator is supposed to be combined with a pressure indicator in a dually sensitive paint, it is important that the emissions of the two indicators are spectrally different. This is one of the most challenging tasks when choosing indicators because most probes for temperature and pressure emit in the red part of the spectrum. The investigation of new temperature probes with blue to green emission is supposed to be the most promising part for innovative improvements in dually sensitive paints.

## 2.7    Methods of Sensor Read Out

### 2.7.1    Intensity Imaging

In intensity imaging, the emission of a single luminescent probe under continuous excitation is gathered by a camera. It is the simplest read out method conceivable. The signal strength depends on the concentration of the analyte and on the concentration of the probe itself. All influences can be described by the law of Parker:

$$I_L = I_0 \, \Phi \, k \, \varepsilon \, l \, c \qquad \qquad \text{eq. 2.14}$$

$I_L$ is the luminescence intensity, $I_0$ is the intensity of the excitation light, $\Phi$ is the quantum yield of the fluorophore, $k$ is the geometric factor including the spatial setup, $\varepsilon$ is the molar extinction coefficient, and $l$ is the length of the medium that is penetrated by the emitted light. It is obvious from this equation that intensity imaging is not a robust method. It requires in situ calibrations and even slight changes to the setup make results incomparable. Apart from those two factors, the intensity strongly depends on the distance between the luminescent probe and the camera given by the inverse square law. If the distance between light source and camera is doubled, the intensity recorded is reduced by a factor of four. This will be crucial when imaging three-dimensional objects. Inhomogeneous coatings are another source for errors in intensity imaging. The dye itself can be inhomogeneously distributed inside the coating or the coating can be inhomogeneous in thickness. Also, the excitation intensity can be heterogeneous on the surface of the object to be imaged. Furthermore, the excitation light is by nature far more intense than the luminescence caused. The excitation light needs to be separated

from the luminescence by an optical filter in front of the camera. Reflected excitation light can leak through this filter and falsify the measurement. Furthermore, the degradation of the paint by photo bleaching and ambient light severely influence the results.[9,11,20,53,54]

## 2.7.2    Referenced Intensity Imaging

Some sources of error in intensity imaging can be avoided by adding a reference dye to the system.[30] This second luminophore has to be insensitive to the analyte concentration. A second picture has to be taken when using a reference. The emission of the analyte indicator is recorded in one picture and the emission of the reference in a second picture. The intensity ratio of these two pictures is the final analytical value. Obviously, the emissions of reference and indicator have to be separable. The spectral overlap has to be as small as possible and the emissions of the two dyes should be of comparable intensity. The emission intensity of every dye is temperature dependent and so is the emission of the reference. There are two strategies to cope with this fact. One can either use a reference dye with a temperature sensitivity as low as possible so the effect of temperature on the reference is insignificant. Or, one can try to find a reference dye with the exact same temperature dependence like the analyte indicator. This results in a temperature independent ratio of intensities. Using the intensity ratio eliminates the errors caused by inhomogeneous illumination, inhomogeneous thickness of paint, and deviations caused by geometrical reasons. Referenced intensity imaging is way more robust than unreferenced intensity imaging but it requires significantly more complex coatings and measurement setups. If both, reference and indicator are imaged with the same camera the optical filter in front of the lens needs to be changed in between the taking of the two pictures. If two cameras with suiting optical filters are used simultaneously, the two pictures are taken from slightly different angles and have to be aligned by sophisticated software for correct evaluation.

## 2.7.3 Lifetime-Based Imaging

Lifetime imaging is an intrinsically referenced (differential) measurement. Thus, time gated lifetime imaging can foreclose these errors. The lifetime is measured in the time domain by the rapid lifetime determination (RLD)[55] method shown in Figure 2.7.
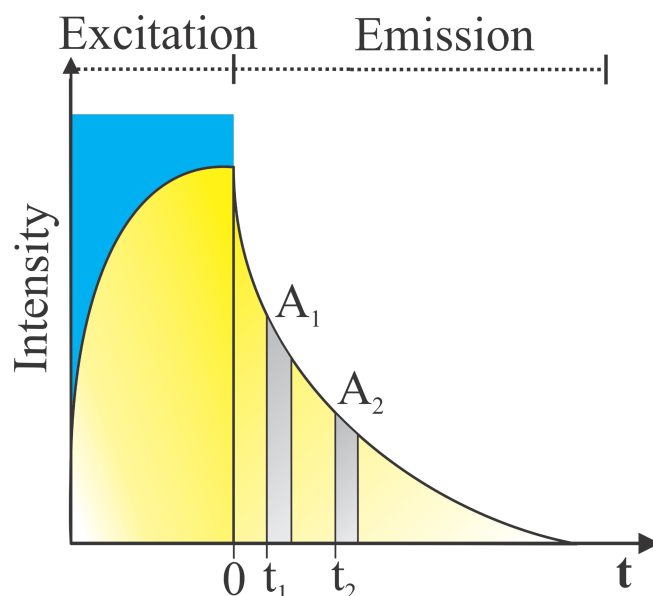


**Figure 2.7**. Scheme of the temporal properties of the rapid lifetime determination (RLD).

Almost ideally square-shaped excitation light pulses can be realized by using LED light sources. The phosphorescence lifetimes of metal-ligand complexes are in the microsecond scale and the response time of an LED is in the nanosecond scale. The phosphorescence intensity (after the excitation) is obtained in two precisely timed (microsecond scale) gates by a triggered CCD camera. These intensity values (*A1;A2*) indicate the integrated luminescence intensities within the gates. The lifetime can be estimated from the ratio of *A1/A2* according to the following formula:

$$\tau = \frac{t_2 - t_1}{\ln\dfrac{A1}{A2}} \qquad\qquad \text{eq. 2.15}$$

This equation is valid only if both gates have the same length. The calculated lifetimes can only be considered absolute in case of monoexponential decays.

Nevertheless, the RLD method is a reasonable choice for imaging applications, because it is hardly affected by the interferences mentioned above. Furthermore, it is not in the focus of interest if the decay is monoexponential, neither are the absolute lifetime values. The analytical purpose is an intrinsic referenced sensor that is calibrated against the air pressure (or against the oxygen partial pressure). Moreover, the obtained results are highly reproducible and they are impartial to the absolute intensities of both the excitation and the emission.[56] In addition, this differential measurement is not interfered by inhomogenities in thickness of the paint, dye distribution, photo degradation, reflections of excitation light ambient light and changes in the optical setup, turbidity, and alternating distances between camera and sensor film.[54] The images shown in Figure 2.8 demonstrate this principle.
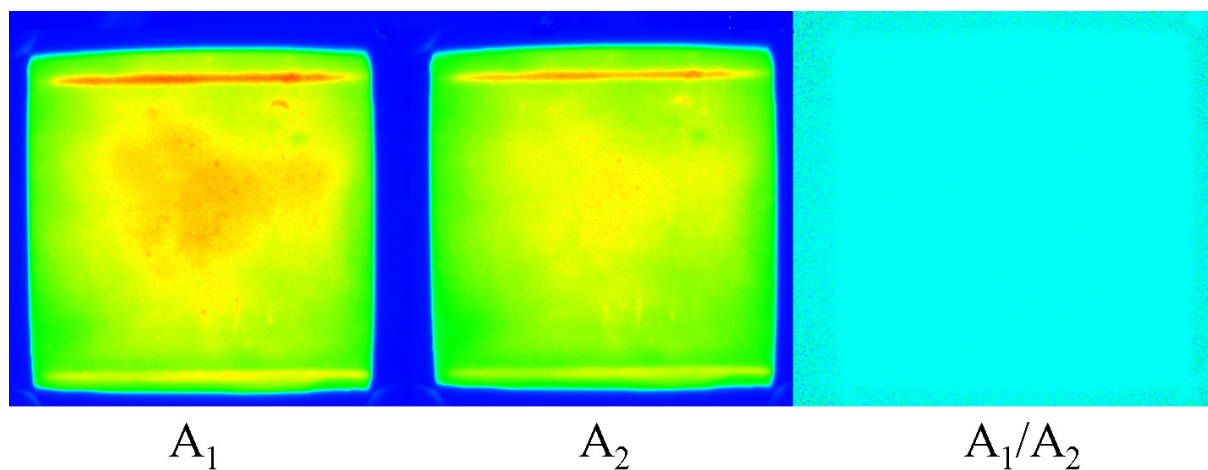


$A_1$        $A_2$        $A_1/A_2$

**Figure 2.8.** Pseudo-color images of a PSP sample taken within the gates (A1;A2), and the resulting image ratio (A1/A2). The inhomogeneities in the intensity in the two pictures are eliminated in the ratio image.

The two pictures A1 and A2 depict the intensity of a 3x3 cm sensor sample. The third image is the calculated pseudo-color picture displaying the intensity ratio A1/A2. It obviously is a very homogenous image that is not affected by any of the inhomogenities in intensity. The sensor sample was manufactured by knife coating a piece of Mylar foil. The stripes of high intensity at the top and bottom of the sensor film are due to the vacuum chamfers of the knife coating device. The foil is slightly dented by the vacuum, causing the film to be thicker in those areas. There are various other gated

imaging methods like phase delay rationing (PDR)[57], dual Lifetime referencing (DLR)[58], and dual lifetime determination (DLD).[55,59] Those schemes were not applied in this thesis and thus will not be discussed.[35,60,61]

### 2.4.7    RGB Imaging

A fairly new approach is to use color cameras for scientific imaging purposes. A colored image consists of three images. A red, a green, and a blue image that are merged or rather, are displayed simultaneously. These three images are recorded during the same exposure on one CCD or CMOS chip. The pixels on the chip are covered with three different optical filters. The filters can be arranged in various patterns on the pixels of the chip. The most common is the so called Bayer pattern displayed in Figure 2.9.[62,63] Herein, four pixels on the chip (two green, one blue, one red) make up one pixel of the picture. This means a lateral separation of the three images on the chip.
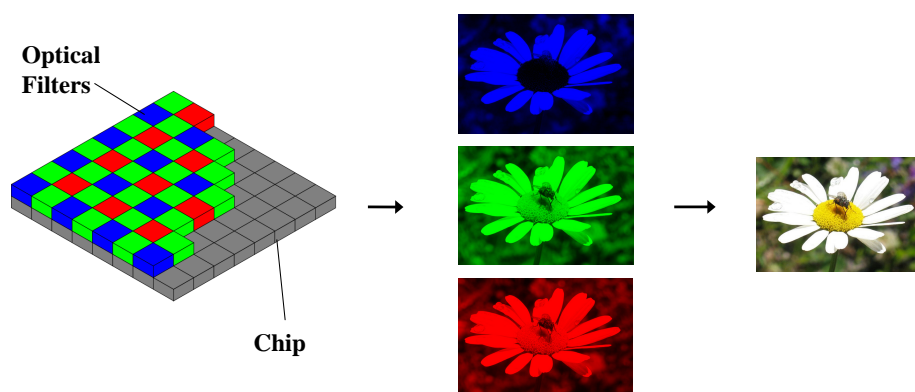


**Figure 2.9.** The Bayer color pattern (RGB) on a photo sensitive chip, the three pictures of the different color channels and the merged RGB image.[62-64]

When using a color camera for imaging of a sensor, the emission of the indicator has to match one of the channels. The emission of a reference dye has to match a different channel. For dual sensing of two analytes a third dye, the indicator for the second analyte has to emit in the remaining channel. This means that a color camera can be used to gather the emission intensities of up to three dyes simultaneously in one colored image. The separation of the emissions by optical filters in front of the lens is

oblivious and only a single image has to be taken. The ratio of reference and indicator intensity can be calculated without any alignment of the pictures. To be precise, RGB imaging is a special form of referenced intensity imaging. The output is the ratio of reference image and indicator image.[65-68]

## 2.8    Imaging Setup

The setup for luminescence imaging depends on the imaging method applied. In general a camera and a light source are needed. A scheme of the imaging setup used in this thesis is given in Figure 2.10. A setup like this can perform spectroscopic measurements, intensity imaging, lifetime imaging and RGB imaging. In case of this work, a two dimensional sensor film inside a calibration chamber is imaged but it could be any object of interest.
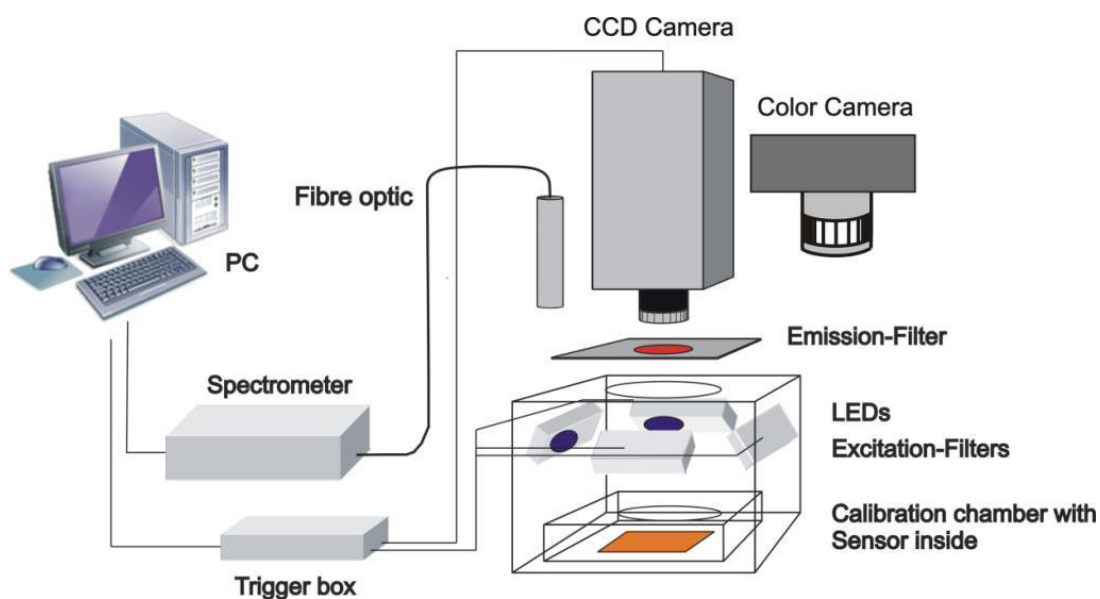


**Figure 2.10.** The experimental setup used in this thesis as an example for an imaging setup. A two dimensional sensor film in a calibration chamber was imaged in this case.

### 2.8.1    Camera Systems

The choice of camera depends on the imaging method. For intensity imaging CCD or CMOS cameras are used. The camera does not need a fast shutter technique. The

chips inside the camera are usually operated at room temperature. If the signal is too weak the exposure of the chip is prolonged. For lifetime imaging a fast shutter CCD or CMOS camera is obligatory. The fast shutter camera needs to be triggered in the low µs scale precisely together with the light source. The chips inside these cameras often are cooled (for example to -15 °C) in order to decrease the noise. The camera is connected to a computer via a trigger device controlling the temporal properties and the data acquisition by software. Obviously, for RGB imaging a color camera is needed. There are scientific color cameras available as well as a huge variety of standard color cameras in various resolutions and prices.

### 2.8.2    Light Sources

In view of Parkers law the light source is supposed to have a high brightness. Additionally, the object of interest should be illuminated as homogeneously as possible. It is desirable that the excitation light is monochromatic in order to grant a good separability from the indicator emission. For lifetime imaging it is mandatory that the light source can be pulsed.

Laser light sources usually can illuminate a relative small area only and are thus not suited for macroscopic imaging. They are available in wavelengths from 250 nm to above 2000 nm. Additionally, they have extremely high output, are monochromatic, and can be pulsed at very high frequencies which makes them a favorable light source for microscopic applications.

Mercury and xenon flash lamps are used for intensity imaging. Their emission ranges from 250 nm to 600 nm. The desired excitation wavelength has to be chosen by an appropriate optical filter in front of the lamp. However, LEDs are the most convenient light source for imaging applications. They are cheap and compact, cover a wavelength range from 245 nm to 4600 nm and are fairly monochromatic. LEDs can be pulsed in the nanosecond scale and they display high brightness. Furthermore, they can easily be bundled in LED arrays to illuminate larger areas due to their small size.

### 2.8.3    Calibration Chamber

The calibration chamber was built and provided by the German Aerospace Center (DLR) in Göttingen. It is equipped with a water cooling circuit, a Peltier- Element for temperature control, a pressure sensor, and a connection to an external pump. The sensor is clamped inside the chamber and can be calibrated at air pressures from 50 mbar to 2000 mbar. The temperature is adjustable via the peltier element from 1 °C to 55 °C. Pressure and temperature values are set by accordant control software.

### 2.10    References

[1]      M. Schaferling, *Angew. Chem. Int. Ed.* **2012**, *51*, 3532-3554.

[2]      S. Schreml, R. Meier, O. Wolfbeis, M. Landthaler, R. Szeimies, P. Babilas, *Exp. Dermatol.* **2010**, *19*, 222-222.

[3]      *FLIM Microscopy in Biology and Medicine*; A. Periasamy, R. M. Clegg, Eds.; CRC Press, Boca Raton: FL, 2009.

[4]      R. H. Engler, U. Fey, U. Henne, C. Klein, W. E. Sachs, *J. Visual-Japan* **2005**, *8*, 277-284.

[5]      K. Kontis, *Aeronaut. J* **2007**, *111*, 495-508.

[6]      Y. Mebarki, K. R. Cooper, T. M. Reichert, *J. Visual-Japan* **2003**, *6*, 381-393.

[7]      J. W. Gregory, K. Asai, M. Kameda, T. Liu, J. P. Sullivan, *P. I. Mech. Eng. G-J Aer.* **2008**, *222*, 249-290.

[8]      H. S. Peng, J. A. Stolwijk, L. N. Sun, J. Wegener, O. S. Wolfbeis, *Angew. Chem. Int. Ed.* **2010**, *49*, 4246-4249.

[9]      *Principles of Fluorescence Spectroscopy*; J. R. Lakowicz, Ed.; Kluwer Academic / Plenum Publishers: New York, London, Moscow, 1999.

[10]     *Physical Chemistry, 7th edn.*; P. W. Atkins, J. d. Paula, Eds.; Oxford University Press: Oxford, 2002.

[11]     *Molecular Fluorescence - Principles and Applications*; B. Valeur, Ed.; Wiley-VCH: Weinheim, 2002.

[12]     J. H. Bell, E. T. Schairer, L. A. Hand, R. D. Mehta, *Annu. Rev. Fluid Mech.* **2001**, *33*.

[13]     E. K. Kainmüller, Albert-Ludwigs-Universität Freiburg, 2006.

[14]     S.-K. Lee, O. Ichiro, *Anal. Sci.* **1997**, *13*.

[15]    J. I. Peterson, R. V. Fitzgerald, *Rev. Sci. Instrum.* **1980**, *51*, 670-671.

[16]    K. Eaton, B. Douglas, P. Douglas, *Sens. Actuat. B-Chem.* **2004**, *97*, 2-12.

[17]    D. R. Kearns, *Chem. Rev.* **1971**, *71*, 395-&.

[18]    D. L. Dexter, *J. Chem. Phys.* **1953**, *21*, 836.

[19]    A. D. McNaught, A. Wilkinson *IUPAC Compendium of Chemical Terminology*; Royal Society of Chemistry, Cambridge, UK, 1996.

[20]    M. I. Stich, O. S. Wolfbeis *Fluorescence Sensing and Imaging Using Pressure-Sensitive Paints and Temperature-Sensitive Paints; Standardization and Quality Assurance in Fluorescence Measurements I* Springer, 2008; Vol. 5.

[21]    S. H. Lin, W. Z. Xiao, W. Dietz, *Phys. Rev. E* **1993**, *47*, 3698-3706.

[22]    W. Ruyten, *Chem. Phys. Lett.* **2004**, *394*, 101-104.

[23]    A. A. Abdel-Shafi, M. D. Ward, R. Schmidt, *Dalton Trans.* **2007**, 2517-2527.

[24]    J. Brandrup, E. H. Immergut, E. A. Grulke *Polymer Handbook.*

[25]    E. R. Carraway, J. N. Demas, B. A. Degraff, *Langmuir* **1991**, *7*, 2991-2998.

[26]    M. A. Woodmansee, J. C. Dutton, *Exp. Fluids* **1998**, *24*.

[27]    L. M. Coyle, D. Chapman, G. Khalil, E. Schibli, M. Gouterman, *J. Lumin.* **1999**, *82*, 33-39.

[28]    L. M. Coyle, M. Gouterman, *Sens. Actuat. B-Chem.* **1999**, *61*, 92-99.

[29]    G. Liebsch, I. Klimant, O. S. Wolfbeis, *Adv. Mater.* **1999**, *11*, 1296-+.

[30]    C. Klein, R. H. Engler, U. Henne, W. E. Sachs, *Exp. Fluids.* **2005**, *39*, 475-483.

[31]    T. Liu, J. P. Sullivan *Pressure and Temperature Sensitive Paints*; Springer, 2004.

[32]    L. H. Fischer, S. M. Borisov, M. Schaeferling, I. Klimant, O. S. Wolfbeis, *Analyst* **2010**, *135*, 1224-1229.

[33]    L. H. Fischer, M. I. Stich, O. S. Wolfbeis, N. Tian, E. Holder, M. Schaferling, *Chemistry* **2009**, *15*, 10857-10863.

[34]    B. Zelelow, G. E. Khalil, G. Phelan, B. Carlson, *Sens. Actuators, B* **2003**, *B 96*, 304.

[35]    M. I. J. Stich, L. H. Fischer, O. S. Wolfbeis, *Chem. Soc. Rev.* **2010**, *39*, 3102-3114.

[36]    E. Puklin, B. Carlson, S. Gouin, *J. Appl. Polym. Sci.* **1999**, *77,13*.

[37]    K. Asai, Y. Amao, Y. Iijima, I. Okura, H. Nishide, *J. Thermophys. Heat Transfer* **2002**, *16*, 109-115.

[38]    G. Liebsch, I. Klimant, B. Frank, G. Holst, O. S. Wolfbeis, *Appl. Spectrosc.* **2000**, *54*, 548-559.

[39]    S. Gouin, M. Gouterman, *J. Appl. Polym. Sci.* **2000**, *77*, 2815.

[40]    S. M. Borisov, O. S. Wolfbeis, *Anal. Chem.* **2006**, *78*, 5094-5101.

[41]    Y. Amao, I. Okura, H. Shinohara, H. Nishide, *Polym. J. (Tokyo, Jpn.)* **2002**, *34*, 411-417.

[42]    X. Lu, M. A. Winnik, *Chem. Mater.* **2001**, *13*, 3449-3463.

[43]    Y. Sakamura, M. Matsumoto, T. Suzuki, *Meas. Sci. Technol.* **2005**, *16*, 759-765.

[44]    E. R. Carraway, J. N. Demas, B. A. Degraff, *Anal. Chem.* **1991**, *63*, 332-336.

[45]    O. S. Wolfbeis, H. E. Posch, H. W. Kroneis, *Anal. Chem.* **1985**, *57*, 2556-2561.

[46]    M. E. Cox, B. Dunn, *Appl. Opt.* **1985**, *24*, 2114-2120.

[47]    M. C. Merienne, Y. Le Sant, J. Ancelle, D. Soulevant, *Meas. Sci. Technol.* **2004**, *15*, 2349-2360.

[48]    X. D. Wang, X. H. Song, C. Y. He, C. J. Yang, G. N. Chen, X. Chen, *Anal. Chem.* **2011**, *83*, 2434-2437.

[49]    Z. Wang, A. R. McWilliams, C. E. B. Evans, X. Lu, S. Chung, M. A. Winnik, I. Manners, *Adv. Funct. Mater.* **2002**, *12*, 415-419.

[50]    *Pressure- and Temperature-Sensitive Paints*; T. Liu, Ed.; Wiley, 2011.

[51]    C. Yang, L. M. Fu, Y. Wang, J. P. Zhang, W. T. Wong, X. C. Ai, Y. F. Qiao, B. S. Zou, L. L. Gui, *Angew. Chem. Int. Ed. Engl.* **2004**, *43*, 5010-5013.

[52]    H. S. Peng, M. I. J. Stich, J. B. Yu, L. N. Sun, L. H. Fischer, O. S. Wolfbeis, *Adv. Mater.* **2010**, *22*, 716-+.

[53]    B. J. Basu, N. Vasantharajan, C. Raju, *Sens. Actuat. B-Chem.* **2009**, *138*, 283-288.

[54]    C. McDonagh, C. S. Burke, B. D. MacCraith, *Chem. Rev.* **2008**, *108*, 400-422.

[55]    C. Moore, S. P. Chan, J. N. Demas, B. A. DeGraff, *Appl. Spectrosc.* **2004**, *58*, 603-607.

[56]    J. Hradil, C. Davis, K. Mongey, C. McDonagh, B. D. MacCraith, *Meas. Sci. Technol.* **2002**, *13*, 1552-1557.

[57]    M. Schaferling, M. Wu, J. Enderlein, H. Bauer, O. S. Wolfbeis, *Appl. Spectrosc.* **2003**, *57*, 1386-1392.

[58]    G. Liebsch, I. Klimant, C. Krause, O. S. Wolfbeis, *Anal. Chem.* **2001**, *73*, 4354-4363.

[59]    M. I. J. Stich, S. Nagl, O. S. Wolfbeis, U. Henne, M. Schaeferling, *Adv. Funct. Mater.* **2008**, *18*, 1399-1406.

[60]    R. H. Engler, C. Klein, O. Trinks, *Meas. Sci. Technol.* **2000**, *11*, 1077-1085.

[61]    K. K. Sharman, A. Periasamy, H. Ashworth, *Anal. Chem.* **1999**, *71 No.5*.

[62]    B. E. Bayer, U. P. 3971065, 1976.

[63]    C. M. L. Burnett; Bayer pattern on Sensor; Wikimedia Commons: 2006.

[64]    Antaya; Leucanthemum-vulgare, Wikimedia Commons: 2006.

[65]    L. F. Capitan-Vallvey, A. J. Palma, *Anal. Chim. Acta* **2011**, *696*, 27-46.

[66]    R. J. Meier, S. Schreml, X. D. Wang, M. Landthaler, P. Babilas, O. S. Wolfbeis, *Angew. Chem. Int. Ed.* **2011**, *50*, 10893-10896.

[67]    Xudong Wang, H. H. Gorris, J. A. Stolwijk, R. J. Meier, D. B. M. Groegel, J. Wegener, O.    S. Wolfbeis, *Chem Sci* **2011**, *2*, 901-906.

[68]    Xudong Wang, R. J. Meier, M. Link, O. S. Wolfbeis, *Angew. Chem. Int. Ed.* **2010**, *49*, 4907-4909.

# Chapter 3

# Referenced Fluorescence Imaging with Digital Color Cameras: A Comparative Study

**Summary:** We have performed a comparative study on read out techniques for optical chemical sensors with the aim to assess the utility of red-green-blue (RGB) color cameras for quantitative analysis. A luminescent film for sensing barometric pressure (via quenching by oxygen) was used as a model system and calibrated by four different fluorescence imaging methods including intensity imaging, referenced intensity imaging, lifetime imaging, and RGB digital imaging using a common color camera. The results are compared in terms of standard deviation, lateral signal homogeneity and achievable resolution of the sensor film. The four methods were applied to the same sensor film under identical experimental conditions in order to warrant the comparability of the results.

## 3.1   Introduction

Optical chemical imaging by means of luminescent sensors is a versatile, fast-developing technique to visualize the distribution of analytes such as pH value[1], $H_2O_2$[2], $CO_2$[3] and oxygen[4]. It can be applied to biology[5], medicine[6], aerodynamics[7,8], and the chemical industry[9], to name a few. In optical chemical sensing, the emission of a probe luminophore (an "indicator") is affected by the concentration of an analyte, which exhibits no intrinsic fluorescence. The probe can be applied in either molecular form or

in the form of sensor nano particles. Alternatively, a sensor layer (a polymer containing the probe) can deposited as a very thin film (0.5 – 5 μm) on the sample.[10] Typical examples of sensor applications are the imaging of oxygen on (tumorous) skin[11],  or in bioreactor fluids[12], and of barometric pressure on aerodynamic models[13]. In all cases, the indicator molecules have to be accessible for the analyte. Thus, the sensor film hosting the indicator has to be permeable to the analyte. When imaging a sensor film, it has to be in direct contact with the sample. Read-out, in contrast, is contact-less.

The most important parameter to be determined via optical chemical imaging is oxygen partial pressure ($pO_2$). However, several other species that do not display intrinsic fluorescence may also be imaged now by using appropriate sensor materials, examples being pH-value in cells [14] or of wound[15] hydrogen peroxide and enzymes producing it[16], biogenic amines[17] , heavy metal ions[18], and even temperature.[19]

In recent years the use of digital color cameras for chemical sensing and imaging became a valuable alternative to scientific CCD cameras. These cameras are based on the use of chips containing red/green /blue (RGB) channels that are sensitive to the red, green, and blue parts of the visible spectrum. The final color picture is composed of the three virtually independent RGB data sets. The distribution of the brightness of the colors is recorded in the RGB image channels and reflected in the form of histograms. The progress of CMOS based detector arrays which are assembled in digital RGB cameras enable the application of more cost-effective and compact devices also for analytical applications. Most notably, the data acquisition using digital cameras is more straightforward and does not require computer-controlled guidance. Their employment is particularly useful for the imaging of multiple or intrinsically referenced optical sensors if the luminescence emissions of the probes and the reference can be adjusted to the maximum sensitivity of the RGB channels. Thus, with RGB cameras dual wavelength (2-λ) fluorescence measurements can be performed. In order to identify the merits and limitations of the RGB imaging method for quantitative analysis, we have performed a comparative study on four common techniques for imaging fluorescent sensor layers using a referenced oxygen-sensitive film as a model.

The four most commonly used methods for imaging sensor films are based on the measurement (a) of luminescence intensity[20], (b) of referenced 2-λ luminescence intensities,[13] (c) of luminescence lifetime,[21] or (d) by making use of the fact that digital cameras store data in the  red-green-blue (RGB) format and such data can be analyzed to create ratiometric pseudo images (see section 2.7). Intensity imaging is usually

performed with black/white CCD or CMOS cameras with a suiting optical filter mounted in front of the camera[22]. In case of referenced intensity imaging the emission of a reference dye is separated from the indicator emission by optical filters[23]. The ratio of both emissions is used as signal. Lifetime imaging requires a high speed camera (fast shutter) that can be gated in the μs range, equipped with an appropriate optical filter. Furthermore, rather complex hardware and software is needed to operate such a camera and a precisely pulsed light source is obligatory[24].

In RGB imaging, which is evaluated here, a color camera is used to photograph up to three different emissions, all matching the different color channels[25-29]. One of the dyes can be a reference signal. This supersedes the use of optical filters for each emission as well as elaborate and bulky hardware or triggered light sources. The RGB camera does not need to be connected to a computer, and a portable LED light source can be mounted directly on the camera.

## 3.2    Results and Discussion

Oxygen partial pressure (and thus barometric pressure) can be imaged with so-called pressure sensitive paints (PSPs). The active layer of the new paint introduced and evaluated here consists of a thin (5 μm) layer of a polyurethane hydrogel that contains (a) micro particles dyed with diphenylanthracene (DPA) in poly(acrylonitrile) (PAN) micro particles ( DPA-PAN, 0.1 – 1 μm) and (b) polystyrene micro particles containing platinum(II) meso-tetrakis(pentafluorophenyl)porphyrinato (PtTFPP) (Pt-PS, 0.1 – 5 μm). The DPA-PAN micro particles act as reference, the Pt-PS as oxygen-sensitive probe. Transmission electron microscopy images of the particles are shown in Figure 3.1. The luminescence intensity and lifetime of PtTFPP is strongly quenched by oxygen (Fig. 3.2). The sensor film was manufactured via knife coating on a foil of poly(ethylene terephtalate) (Mylar®) which acts as an inert and transparent support.
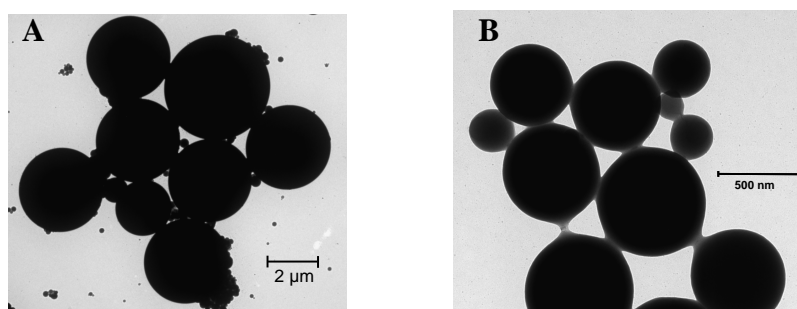
**Figure 3.1.** Transmission electron microscopy images of the particles applied in the pressure sensitive paint. (A) Polystyrene particles doped with PtTFPP and (B) Poly(acrylonitrile) particles doped with diphenylanthracene.
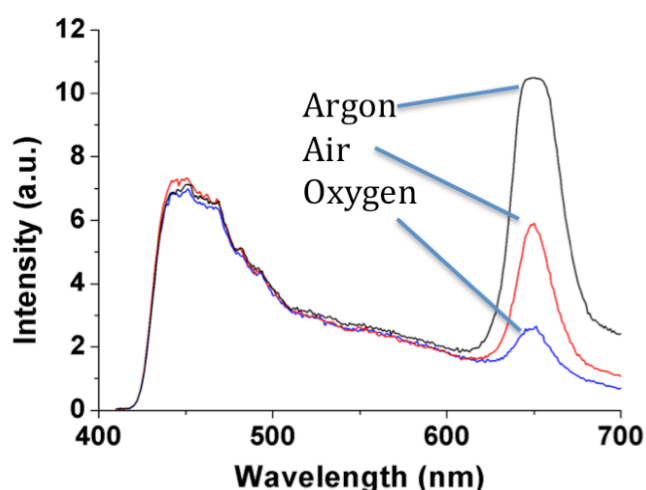


**Figure 3.2.** Emission spectrum of the polyurethane sensor film consisting of DPA (emission $\lambda_{max}$ = 456 nm) in PAN micro particles and the oxygen indicator PtTFPP (emission $\lambda_{max}$ = 650 nm) in PS micro particles dispersed in a film of polyurethane hydrogel. The emission was recorded under various atmospheres (argon, normal air and oxygen). The emission of the DPA reference matches the blue channel and the emission of PTTFPP matches the red channel of the digital color camera.

An oxygen sensitive paint sensitive paint of 2 x 3 cm size was used for the evaluation of the four described imaging methods. The intensity data of the probe PtTFPP (emission $\lambda_{max}$ = 650 nm) were acquired with a single CCD camera and the appropriate filter (high pass 630 nm) being mounted in front of it. These reflect the performance of the pure and non-referenced sensor layer. The intensity of the blue fluorescing inert reference dye was imaged with the same camera after changing the

optical filter. Lifetime measurements were performed as gated measurements according to the RLD scheme[24] given in Figure 2.7. Herein, the analytical information is obtained by rationing the intensities in the two gates ($A_1/A_2$) after a short excitation pulse. The lifetime ($\tau$) can be estimated from this ratio by the equation (eq. 2.15). In all cases the dyes were excited with 405 nm LEDs.

For better comparability, the results were not converted into the lifetime values. Rather, the relative changes of the ratiometric signal $A_1/A_2$ were used as sensor response. RGB imaging was performed with a regular digital color camera with a LED ring as excitation light source mounted in front of the lens.

The calibration plots of the four methods are displayed in Figure 3.3.
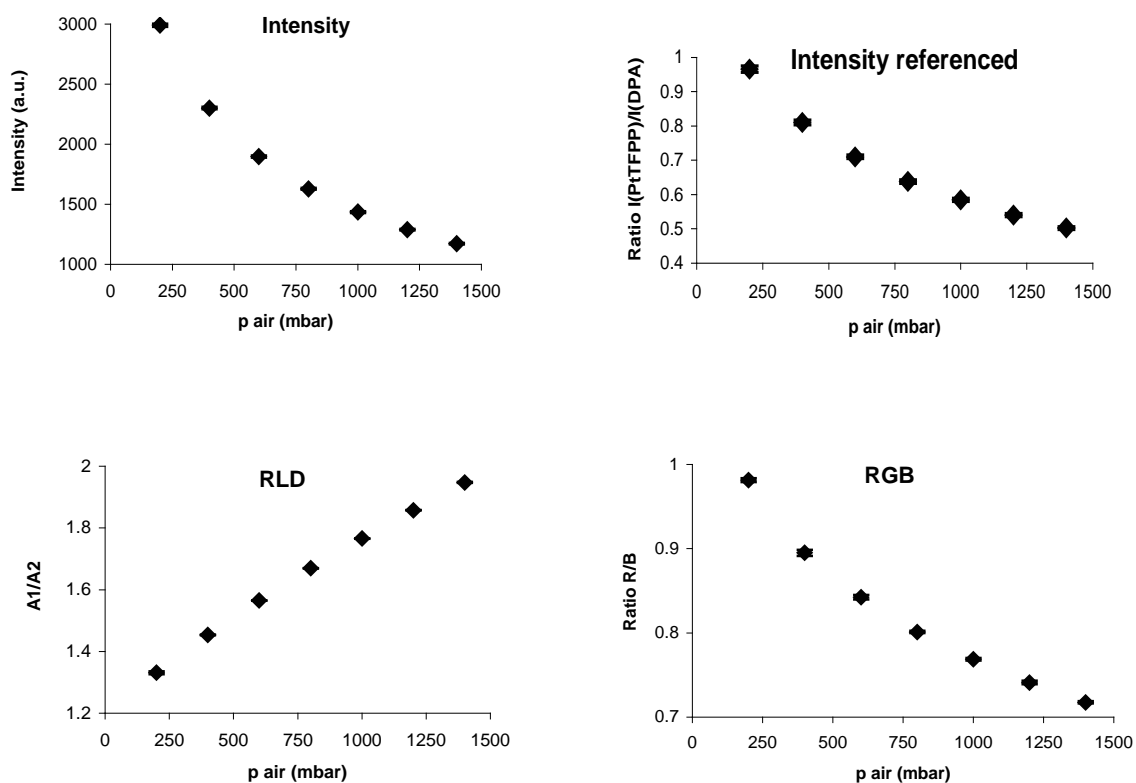


**Figure 3.3.** Calibration plots of the four imaging methods applied (intensity, referenced intensity, rapid lifetime determination, RGB camera). Displayed are the average values of five calibrations together with the standard deviation. For intensity imaging only the emission of the oxygen indicator PtTFPP is recorded. Imaging the emission of the reference dye DPA enables for calculating the ratio of indicator / reference (intensity referenced). Rapid lifetime determination (RLD) is a gated method with the ratio of two gates being the signal. In RGB imaging the indicator emission in the red channel is divided by the reference emission gathered in the blue channel.

The PSP was calibrated from 200 mbar to 1400 mbar air pressure at 25 °C in five consecutive calibrations with each method. After adjusting a certain pressure in the calibration chamber, a single measurement was performed and the next pressure value was set until one run of the calibration was finished. After that, the pressure was set to the first value (200 mbar) again and the second calibration cycle was done in the same way. Thus, the measurements were not performed five times after setting a pressure value once but five independent calibration runs were accomplished to determine the standard deviation of each imaging technique. A region of interest (ROI) of 1.5 x 1.5 cm was used for the quantitative evaluation of the sensor responses.

The lateral homogeneity of the signal in terms of standard deviation (SD) from pixel to pixel was investigated under both homogeneous and inhomogeneous illumination with a 405-nm chip LED as the excitation light source. The SD was evaluated at 25 °C and 1000 mbar air pressure. Inhomogeneous illumination was generated by masking a part of the LED with a strip of black tape. Approximately half of the ROI was illuminated much less than the rest of the area. The results are summarized in Table 3.1.

**Table 3.1.** Comparison of the lateral signal homogeneity of the PSP at 25 °C and 1000 mbar air pressure at homogeneous and inhomogeneous illumination (*), read out with the four different methods. The standard deviation of the pixels was converted into the deviation of the pressure value. Additionally, the standard deviation (SD) is given (percentage related to the average signal of the integrated area).

| Read out method | Average/ROI | SD/pixels | % SD/ pixels | Signal/noise ratio | SD converted to air pressure (mbar) |
|---|---|---|---|---|---|
| Intensity | 1435[a] | 13.4 | 0.93 | 107 | 15.7 |
| Intensity * | 1440[a] | 309 | 21.5 | 4.7 | 363 |
| Referenced int. | 0.584[b] | 0.0095 | 1.62 | 61 | 38.5 |
| Referenced int.* | 0.586[b] | 0.075 | 12.7 | 7.8 | 304 |
| RLD | 1.766[c] | 0.0005 | 0.03 | 3532 | 0.98 |
| RLD* | 1.766[c] | 0.031 | 1.8 | 57 | 66.5 |
| RGB | 0.761[d] | 0.003 | 0.39 | 254 | 20.2 |
| RGB* | 0.769[d] | 0.048 | 6.3 | 16 | 320 |

* under inhomogeneous illumination; [a] a.u., [b] ratio I(Indicator)/I(Reference), [c] ratio $A_1/A_2$, [d] ratio R/B channels of color camera.

The results underline the superior capability of the RLD method using CCD cameras to compensate inhomogeneities of the sensor set up.  However, also the RGB camera provides quite homogenous images.

The most significant parameter to compare the four methods for sensor read out is the resolution that is achieved. Herein the resolution is defined as the ratio of the SD from five consecutive calibrations divided by the slope of the calibration plot. Figure 3.3 shows that the calibration plots are not linear. The resolution consequently differs depending on the pressure ($pO_2$) value. Here, the average values, the SDs, and resolutions at 25 °C and 1000 mbar air pressure are evaluated and merged in Table 2.

**Table 2.** Average values of 5 calibration runs, standard deviations, and resolutions achieved with the four different imaging methods . The resolution is defined as the ratio of the SDs divided by the slope of the calibration plot. All values refer to 25 °C and 1000 mbar air pressure.

| Method | Average | SD/calibration | Signal/noise ratio | Resolution (mbar) |
|---|---|---|---|---|
| Intensity | 1436[a] | 13.4[a] | 107 | 15 |
| Referenced intensity | 0.58[b] | 0.009[b] | 61.8 | 38 |
| RLD | 1.77[c] | 0.0005[c] | 3838 | 1 |
| RGB | 0.77[d] | 0.003[d] | 253 | 20 |

[a] a.u., [b] ratio I(Indicator)/I(Reference), [c] ratio $A_1/A_2$, [d] ratio R/B channels of color camera.

Obviously, the RLD method provides the highest accuracy and precision for a quantitative read out in terms of signal homogeneity and resolution of the sensor. Nevertheless, the performance will to some extent also depend on the choice of materials. Different dyes and matrix polymers will display different resolutions. Thus, there are various options for a further optimization of RGB imaging.

## 3.3   Conclusions and Outlook

The advantages and disadvantages of the four techniques are summarized in Table 3.3.

**Table 3.3.** Overview on the advantages and disadvantages of the four imaging techniques.

|  | Advantages | Disadvantages |
|---|---|---|
| **Intensity Imaging** | Relatively simple hardware; inexpensive; large number of indicators available; high signals in case of strong excitation light. | Unreferenced; error prone due to inhomogenities, setup geometry; requires very homogeneous illumination. |
| **Referenced Intensity Imaging** | Less prone to errors; relatively simple hardware; inexpensive; high signals in case of strong excitation light. | The choice of dyes is limited; requires the acquisition of two images; demands sophisticated image alignment. |
| **Lifetime Imaging** | Very high resolution and homogeneity; very robust; highly reproducible; intrinsically referenced; even tolerates changes in the setup. | Complex hardware necessary; limited choice of indicators; expensive. |
| **RGB Imaging** | Very simple and cheap hardware; portable and hand held; very convenient and easy to use. | Lower resolution; very limited choice of indicators. |

The results clearly reveal that the accuracy of 2-$\lambda$ measurements with RGB cameras is sufficient for certain applications and useful for imaging of the distribution of an analyte on a surface. Though, the quantitative evaluation of sensor responses can only be carried out with some restrictions compared to fluorescence lifetime imaging using a time-gated CCD camera. The efficiency to inhibit interferences such as inhomogeneous illumination of the sensor area or stray light is also limited.

We are currently working intensely on the improvement of the RGB imaging method for sensor applications. In contrast to the other methods, RGB imaging can be performed with a simple hand held device, which consists of only the camera. Cameras including an excitation light source are portable, applicable for in the field measurements. Of course RGB imaging is not limited to oxygen sensing. Any pair of luminescent indicator and

reference dye that matches the color channels of a camera can be imaged. Even two indicators plus one reference can be used to simultaneously image two different analytes.

## 3.4   Experimental

The polystyrene (PS) microparticles were prepared by a known method[30] by dissolving $\alpha,\alpha'$-azoisobutyronitrile (62.5 mg) in a mixture of styrene (7.0 mL) and methacrylic acid (60 mL) and mixing the solution with ethanol (25 mL) containing dissolved poly(vinyl pyrrolidone) (0.188 g; type K-30) in order to reduce agglomeration of the particles. The solution was deoxygenated and subsequently polymerized (24 h; 70 °C). The resulting particles (0.1 – 1 μm) were separated by centrifugation, washed three times with ethanol, and stained using a soaking procedure.[31] PS particles (300 mg), distilled water (20 mL), and tetrrahydrofurane (THF; 15 mL) were mixed and sonicated (30 min) to swell the microbeads. A solution of platinum 5,10,15,20-tetrakis-(2,3,4,5,6-pentafluorophenyl)porphyrin (Pt-TPFPP) in THF (5 mL; 1.0 mg/mL$^{-1}$) was added dropwise (0.2 mL/s$^{-1}$) under sonication for 20 min. As a result, virtually all dye molecules are incorporated inside the hydrophobic PS particles. The THF was then removed using rotary evaporation.

The DPA-PAN reference particles were synthesized by incorporating diphenylanthracene (DPA) in poylacrylonitrile (PAN) using a precipitation method.[32] The dyed particles precipitate from a solution of DPA (30 mg) and PAN (300 mg) in dimethylformamide (30 mL) upon slow addition (1 mL/s$^{-1}$) of distilled water (70 mL) and subsequent addition of brine (20 mL). They can be separated by centrifugation. All sensor particles were washed four times with ethanol and four times using distilled water (each washing step followed by centrifugation for 10 min at 1030 g). Particles were freeze-dried before storage. Particle sizes were determined by transmission electron microscopy. All chemicals were purchased from sigma-aldrich (www.sigma-aldrich.com) and used without further purification.

The sensor film was prepared by dispersing Pt-PS (50 mg) and DPA-PAN (20 mg) in 4 ml of a 5% solution of polyurethane hydrogel (type D4; from AdvanSource Biomaterials;   formerly CardioTech; www.advbiomaterials.com) in an ethanol-water

mixture (9:1 v/v). This cocktail was cast, in a wet thickness of 100 μm, onto a foil of poly(ethylene terephtalate) (type Mylar®; from www.goodfellow.com) by knife coating. The sensor film is ready after evaporation of the solvent and has a thickness of around 5 μm.

The RGB imaging setup[26] consists of a standard digital camera (Canon EOS50D), a modified ring light with 28 LEDs (405 nm peak wavelength; UV5TZ-405-15 BIVAR), and a GG435 emission filter (www.schott.com). Camera parameters were set as follows: Raw+jpg; ISO 160; white balance 2450 K. Excessive ambient light is to be avoided. The image data were stored as 16-bit TIFs using the Adobe Camera Raw plug-in for Adobe Photoshop and data were further processed with ImageJ software. The images are split into the three color channels. The ratios of R/B are calculated and plotted vs. the air pressure. The calibration chamber was provided by the German Aerospace Center (DLR) in Göttingen (www.dlr.de, see section 2.8.3). Intensity imaging and lifetime imaging was performed with a PCO SensiCam 12 bit b/w CCD camera (PCO, Kelheim; www.pco.de) equipped with a Schneider- Kreuznach Xenon 0.95/17 lens (Schneider Optische Werke; www.schneiderkreuznach.com) and a 405-66-60 405 nm LED from Roithner Lasertechnik (Vienna; www.roithner-laser.com).

## 3.4   References

[1]      M. I. J. Stich, M. Schaeferling, O. S. Wolfbeis, *Adv. Mater.* **2009**, *21*, 2216.

[2]      P. Niethammer, C. Grabher, A. T. Look, T. J. Mitchison, *Nature* **2009**, *459*, 996.

[3]      G. Liebsch, I. Klimant, B. Frank, G. Holst, O. S. Wolfbeis, *Appl. Spectrosc.* **2000**, *54*, 548.

[4]      L. H. Fischer, S. M. Borisov, M. Schaeferling, I. Klimant, O. S. Wolfbeis, *Analyst* **2010**, *135*, 1224.

[5]      *FLIM Microscopy in Biology and Medicine*; A. Periasamy, R. M. Clegg, Eds.; CRC Press, Boca Raton: FL, 2009.

[6]      M. C. Hung, G. B. Mills, D. H. Yu, *Nat. Med. (N. Y., NY, U. S.)* **2009**, *15*, 246.

[7]      T. Liu, J. P. Sullivan *Pressure and Temperature Sensitive Paints*; Springer, 2004.

[8]      J. W. Holmes, *J. Fluoresc.* **1993**, *3*.

[9]     *Optical Sensors for Industrial, Environmental and Clinical Applications*; R. Narayanaswamy, O. S. Wolfbeis, Eds.; Springer: Berlin, 2003.

[10]    M. Schaferling, *Angew. Chem. Int. Ed.* **2012**, *51*, 3532.

[11]    S. Schreml, R. J. Meier, O. S. Wolfbeis, T. Maisch, R. M. Szeimies, M. Landthaler, J. Regensburger, F. Santarelli, I. Klimant, P. Babilas, *Exp. Dermatol.* **2011**, *20*, 550.

[12]    D. Sud, G. Mehta, K. Mehta, J. Linderman, S. Takayama, M. A. Mycek, *J. Biomed. Opt.* **2006**, *11*.

[13]    C. Klein, R. H. Engler, U. Henne, W. E. Sachs, *Exp. Fluids.* **2005**, *39*, 475.

[14]    H. S. Peng, J. A. Stolwijk, L. N. Sun, J. Wegener, O. S. Wolfbeis, *Angew. Chem. Int. Ed.* **2010**, *49*, 4246.

[15]    S. Schreml, R. J. Meier, O. S. Wolfbeis, M. Landthaler, R. M. Szeimies, P. Babilas, *Proc. Natl. Acad. Sci. U. S. A.* **2011**, *108*, 2432.

[16]    M. Wu, Z. H. Lin, M. Schaferling, A. Durkop, O. S. Wolfbeis, *Anal. Biochem.* **2005**, *340*, 66.

[17]    M. S. Steiner, R. J. Meier, A. Duerkop, O. S. Wolfbeis, *Anal. Chem.* **2010**, *82*, 8402.

[18]    T. Mayr, C. Igel, G. Liebsch, I. Klimant, O. S. Wolfbeis, *Anal. Chem.* **2003**, *75*, 4389.

[19]    H. S. Peng, M. I. J. Stich, J. B. Yu, L. N. Sun, L. H. Fischer, O. S. Wolfbeis, *Adv. Mater.* **2010**, *22*, 716.

[20]    C. McDonagh, C. S. Burke, B. D. MacCraith, *Chem. Rev.* **2008**, *108*, 400.

[21]    M. I. J. Stich, L. H. Fischer, O. S. Wolfbeis, *Chem. Soc. Rev.* **2010**, *39*, 3102.

[22]    J. H. Bell, E. T. Schairer, L. A. Hand, R. D. Mehta, *Annu. Rev. Fluid Mech.* **2001**, *33*.

[23]    G. E. Khalil, C. Costin, J. Crafton, G. Jones, S. Grenoble, M. Gouterman, *Sens. Actuat. B-Chem.* **2004**, *97*, 13.

[24]    M. I. Stich, O. S. Wolfbeis *Fluorescence Sensing and Imaging Using Pressure-Sensitive Paints and Temperature-Sensitive Paints; Standardization and Quality Assurance in Fluorescence Measurements I* Springer, 2008; Vol. 5.

[25]    X. D. Wang, R. J. Meier, M. Link, O. S. Wolfbeis, *Angew. Chem. Int. Ed.* **2010**, *49*, 4907.

[26]    R. J. Meier, S. Schreml, X. D. Wang, M. Landthaler, P. Babilas, O. S. Wolfbeis, *Angew. Chem. Int. Ed.* **2011**, *50*, 10893.

[27]    X. D. Wang, H. H. Gorris, J. A. Stolwijk, R. J. Meier, D. B. M. Groegel, J. Wegener, O. S. Wolfbeis, *Chem. Sci.* **2011**, *2*, 901.

[28]    M. I. J. Stich, S. M. Borisov, U. Henne, M. Schaferling, *Sens. Actuat. B-Chem.* **2009**, *139*, 204.

[29]    A. Lapresta-Fernandez, L. F. Capitan-Vallvey, *Analyst* **2011**, *136*, 3917.

[30]    Z. L. Zhang, Y. Long, J. B. Pan, X. M. Yan, *J. Mater. Chem.* **2010**, *20*, 1179.

[31]    T. Behnke, C. Wurth, K. Hoffmann, M. Hubner, U. Panne, U. Resch-Genger, *J. Fluoresc.* **2011**, *21*, 937.

[32]    S. M. Borisov, T. Mayr, G. Mistlberger, K. Waich, K. Koren, P. Chojnacki, I. Klimant, *Talanta* **2009**, *79*, 1322.

# Chapter 4

# Evaluation of Reference Dyes for Imaging Purposes

**Summary:** Various dyes were investigated with respect to their suitability as reference dye for ratiometric intensity imaging or RGB imaging. The response of the luminescence intensity to barometric pressure and temperature was calibrated. Furthermore the dyes are compared in terms of photostability and thermostability.
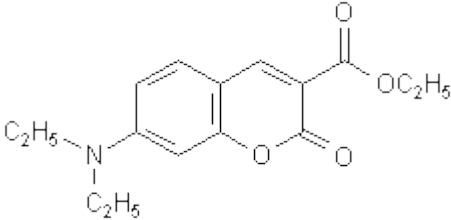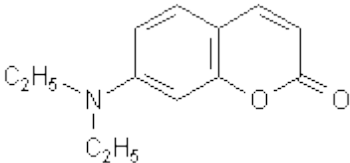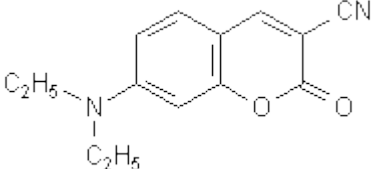
## 4.1    Introduction

Reference dyes are often used in referenced intensity imaging[1-3] and RGB imaging[4-7]. It has to be distinguished between two situations, sensing of a single analyte and multiple chemical sensing. All dyes investigated herein are organic fluorophores with nanosecond fluorescence lifetimes.[8] In contrast to metal ligand complexes, these dyes are not suited for lifetime imaging in the μs range.[9] The intention is to find blue or green emitting dyes suited for reference purposes in referenced intensity imaging or RGB imaging.
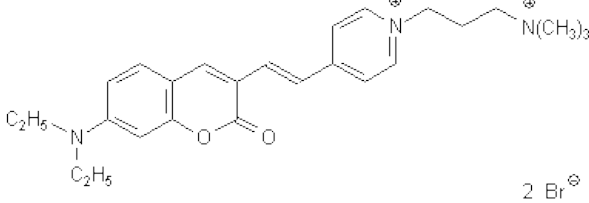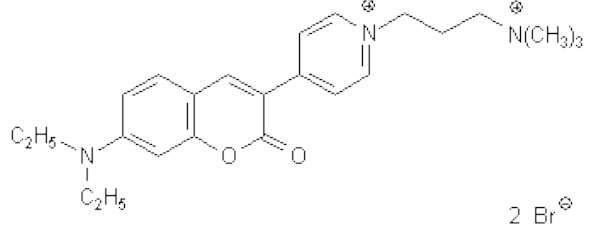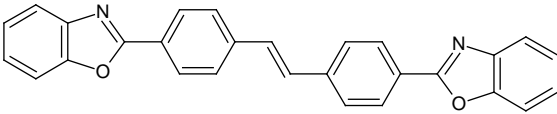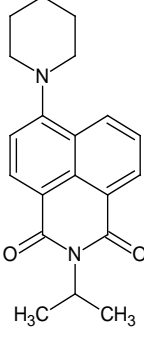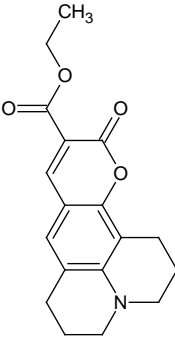
When sensing a single analyte the emission of the reference dye can be analyte dependent as long as the dependence differs from that of the indicators behaviour. If reference dye and indicator display the same decrease or increase with the analyte concentration, the ratio of indicator emission divided by the reference will not change. A change of the ratio as high as possible is desirable for sensing purposes. In terms of single analyte sensing it would be ideal if the emission intensity of the reference
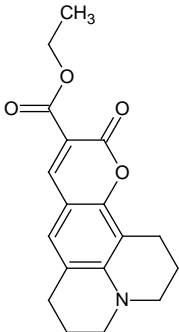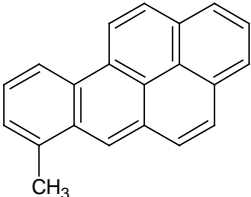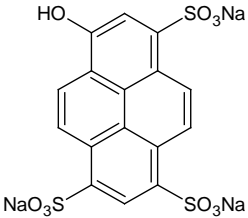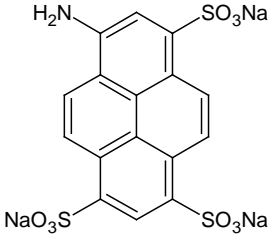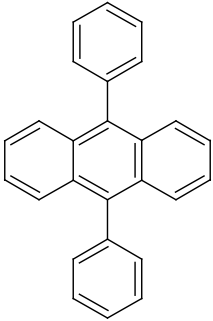
responds inversely to the indicator emission. This would result in very high changes of the intensity ratio with the analyte concentration. However, this never is the case when sensing oxygen or temperature. When sensing multiple analytes, the emission of the reference should ideally be independent of all analytes. This section describes a search for a blue or green emitting reference dye. The blue or green emission is obligatory in order to combine it with a good temperature indicator (e.g. Eu-complexes) or pressure indicator (pO$_2$, e.g. Pt-porphyrins), as they are all red emitters. The blue or green emission can be separated from red emission by optical filters in case of referenced intensity imaging. For RGB imaging the emission of the reference dye has to match one of the color channels of the camera (see section 2.7.4). All dyes were incorporated in a film of polystyrene (PS) (thickness 6μm) manufactured by knife coating. In order to be combined with a second fluorophore the dye has to be incorporated in polymer micro particles. A list of all the dyes investigated is given in Table 4.1.

**Table 4.1**. The dyes investigated in search for a blue or green emitting reference dye.

| Dye [acronym] | Structure | $\lambda_{max}$abs (nm) | $\lambda_{max}$em (nm) |
|---|---|---|---|
| 7-Diethylamino-2-oxo-2H-chromene-3-carboxylic acid ethyl ester **[S 0679]** | | 412 | 447 |
| 7-Diethylamino-4a,8a-dihydro-chromen-2-one **[S 2142]** | | 369 | 420 |
| 7-Diethylamino-2-oxo-2H-chromene-3-carbonitrile **[S 2145]** | | 420 | 457 |

| | | | |
|---|---|---|---|
| 4-(2-(7-(Diethylamino)-2-oxo-2H-chromen-3-yl)vinyl)-1-(3-(trimethylammonio)propyl)pyridinium dibromide **[S 2166]** | | 493 | 542 |
| 4-(7-(Diethylamino)-2-oxo-2H-chromen-3-yl)-1-(3-(trimethylammonio)propyl)pyridinium dibromide **[S 2167]** | | 494 | 545 |
| 4,4'-Bis(2-benzoxazolyl)stilbene **[BBS]** | | 371 | 429 |
| Naphthalimide DG43 **[DG43]** | | 408 | 510 |
| Coumarin 314 **[C 314]** | | 425 | 462 |

| | | | |
|---|---|---|---|
| Coumarin 343<br><br>**[C 343]** | | 442 | 476 |
| 7-<br>Methylbenzo[a]pyren<br>**[MBP]** | | 391 | 429 |
| 8-Hydroxypyren-1,3,6-<br>trisulfonat<br>**[HPTS]** | | 404 | 422 |
| 8-Aminoypyren-1,3,6-<br>trisulfonat<br>**[APTS]** | | 427 | 484 |
| 9,10,-<br>Diphenylanthracene<br>**[DPA]** | | 395 | 429 |

Four of these dyes are discussed in detail due to their outstanding properties. All other dyes are not suitable for reference purposes in imaging applications. Their response to oxygen partial pressure or to temperature is too high for reference

applications. The emission of HPTS displayed pronounced temperature dependence. The emissions of DG43, S 2145, and DPA showed only small temperature dependence and small dependence on barometric pressure ($pO_2$) as well.

## 4.2    8-Hydroxypyrene-1,3,6-trisulfonate (HPTS)

HPTS is a well known pH indicator dye. It is excitable with a 405 nm LED and displays blue emission if dissolved in a nonprotic solvent or polymer. Due to these spectral properties it was calibrated with respect to its temperature and oxygen sensitivity. HPTS is hydrophilic and is not soluble in PS. Therefore, it was dissolved in ethanol and incorporated into a film of polyurethane hydrogel. The spectra and the temperature dependence of the fluorescence intensity of HPTS are given in Figure 4.1.
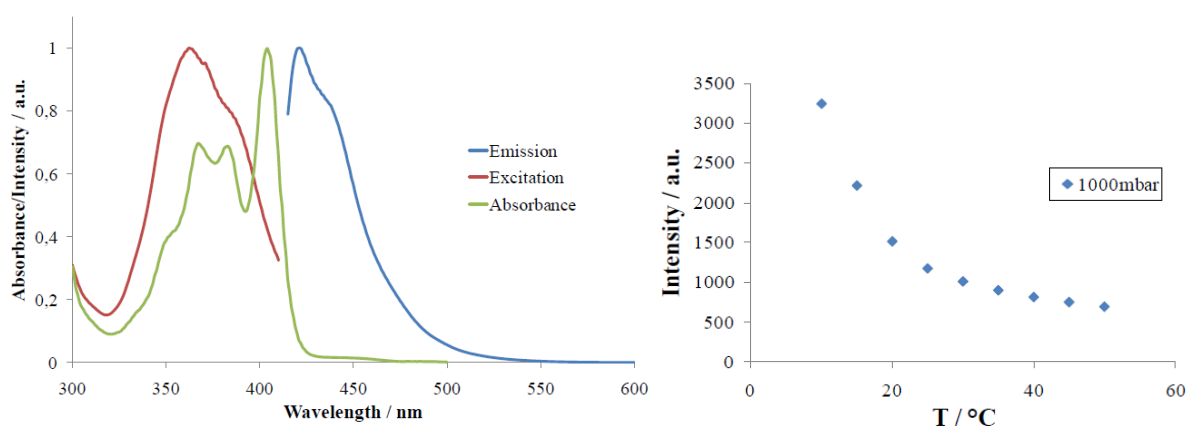


**Figure 4.1.** Spectra and temperature dependence of the fluorescence intensity of HPTS at 1000 mbar air pressure, incorporated into a film of polyurethane hydrogel.

The short wave emission of HPTS is perfectly separable from red emitting indicators. The pronounced temperature dependence of HPTS is not desirable for reference purposes. HPTS can be used as blue emitting temperature indicator. In order to combine it with a second luminophore and to apply it in other matrix materials, HPTS has to be incorporated in polymer micro particles. The favourable polymer for

temperature sensing is poly(acrylonitrile) (PAN) due to its low oxygen permeability. Dyed PAN micro particles can be synthesized by coprecipitation[10] if the dye is soluble in dimethylformamide (DMF) but insoluble in water. HPTS is soluble in DMF and water. It has to be modified in order to become less polar remain soluble in DMF but not in water. This was achieved with an ion pair extraction. The sodium ions were replaced by tetraoctylammonium (TOA) ions. By this ion exchange, HPTS becomes hydrophobic enough to render dyed PAN particles by coprecipitation. The PAN micro particles dyed with HPTS were incorporated into a film (thickness 5 µm) of polyurethane hydrogel and calibrated. The results of the calibration are displayed in Figure 4.2.
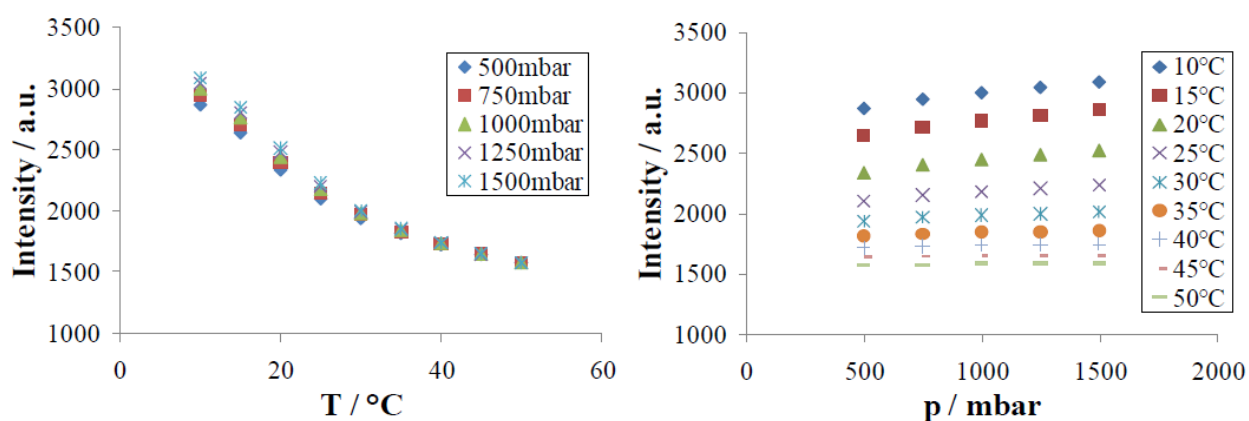


**Figure 4.2.** Calibration plots of HPTS in PAN micro particles in a 5 µm polyurethane hydrogel film.

The luminescence intensity of HPTS in PAN displays pronounced temperature sensitivity and only a verry small cross sensitivity towards oxygen. HPTS can be used as blue emitting temperature indicator.

## 4.3    Naphthalimide DG43 (DG43)

The dye DG43 was synthesized by Domink Groegel in the course of the development of a probe for hydrogen peroxide. The spectra and the calibration plot of

DG43 are shown in Figure 4.3. The emission spectra of this sample at 30 °C and different air pressures are shown in Figure 4.4.
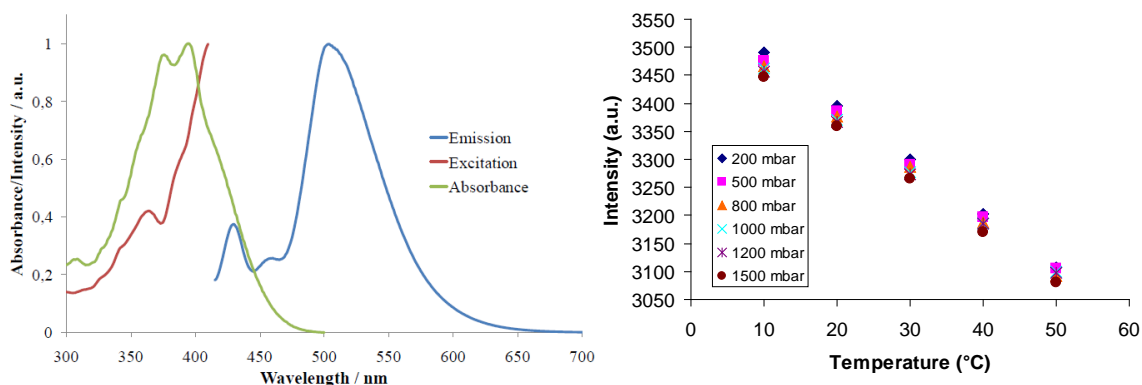


**Figure 4.3.** Spectra (left) of DG43 in THF and calibration plot (right) of DG43 in a film of PS.
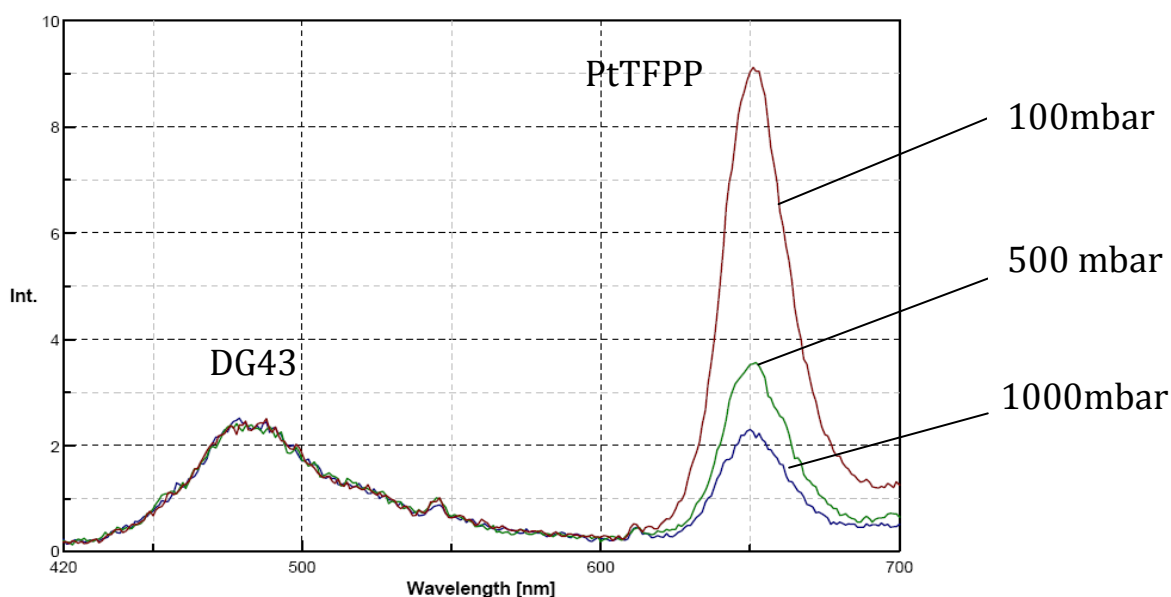


**Figure 4.4.** Emission spectra of DG43 in PAN micro particles and of the pressure indicator PtTFPP in a PS film at 30 °C and various air pressures.

The temperature dependence of the luminescence intensity of DG43 is small. The sensitivity towards oxygen is even smaller. To supress this small oxygen sensitivity

51

and to be able to combine DG43 with other dyes, it was incorporated into PAN micro particles by coprecipitation[10]. The PAN beads were dispersed in polystyrene and cast on a solid support by knife coating. The oxygen indicator PtTFPP was dissolved in the PS film as well to check the separability of the reference and indicator emission. The reference luminophore displayed virtually no oxygen sensitivity and only small temperature sensitivity, making it a very suiting reference dye. As it can be seen in Figure 4.4, the emission of DG43 in PAN is well separated from that of PtTFPP. DG43 is a suitable dye for referencing red indicators.

## 4.4      7-Diethylamino-2-oxo-2H-chromene-3-carbonitrile (*S 2145*)

The luminescence intensity of S2145 displays small temperature dependence and very small oxygen sensitivity. The spectra and the calibration plot of S2145 are shown in Figure 4.5.
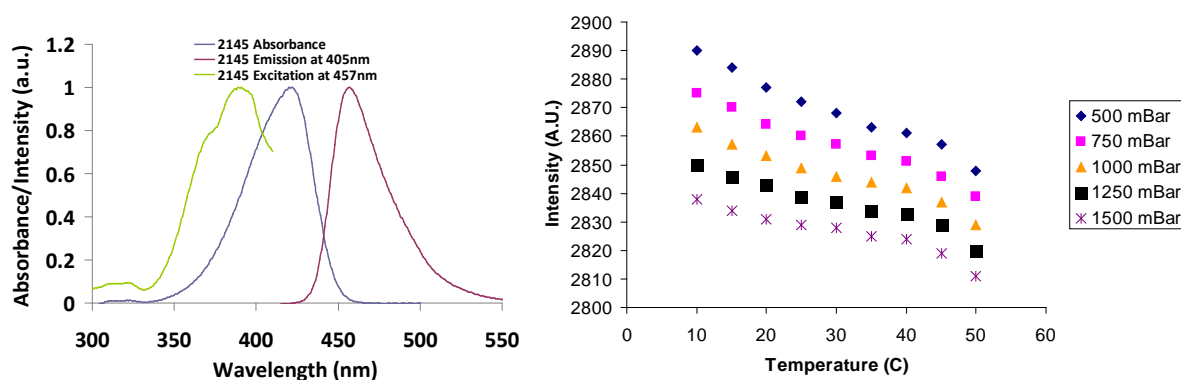


**Figure 4.5.** Spectra of S 2145 (left) in THF and calibration plot of S2145 in PS film (right).

In order to check the separability of the emission from the emission of PtTFPP, S 2145 was incorporated into PAN micro particles and dispersed in a film of PS containing PtTFPP. The results are shown in Figure 4.6.
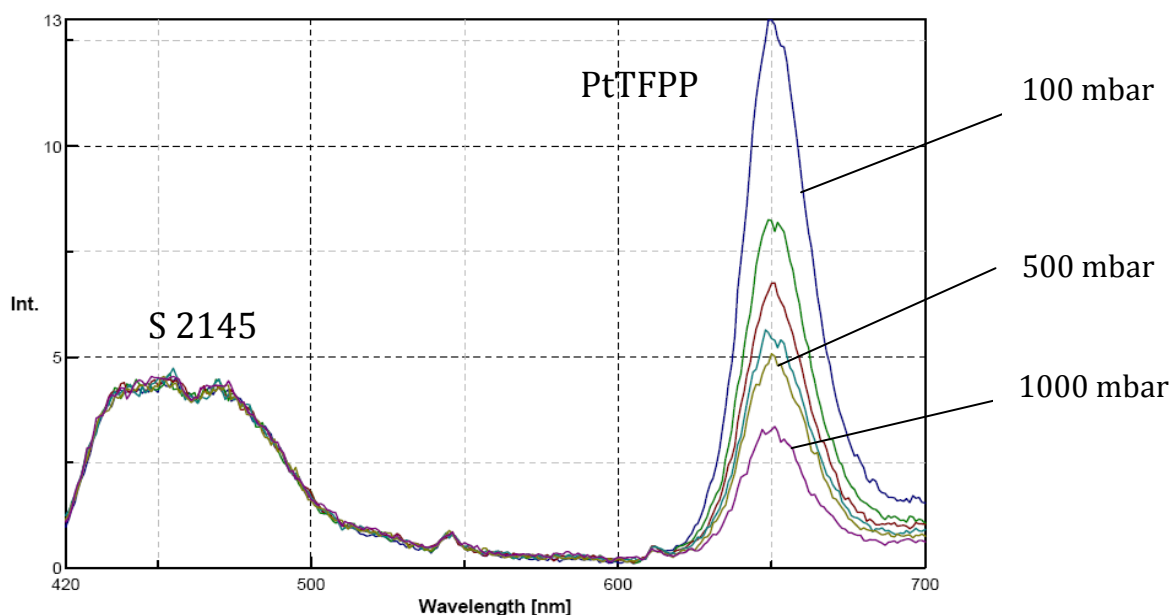
**Figure 4.6.** Emission spectra of S 2145 in PAN microparticles and the pressure indicator PtTFPP in a PS film at 30 °C and various air pressures.

The emission of S 2145 can be separated from red emitting indicators by optical filters. The emission intensity of S 2145 in PAN micro particles is insensitive towards oxygen and the temperature sensitivity is extremely small. S 2145 is a very adequate dye for referencing of red emitting indicators.

## 4.5    9,10-Diphenylanthracene (DPA)

DPA is a blue emitting organic semiconductor used in organic electronics. It is perfectly excitable with a 405 nm LED. The spectra of DPA dissolved in THF and the calibration plot of DPA in a film of PS are shown in Figure 4.7.
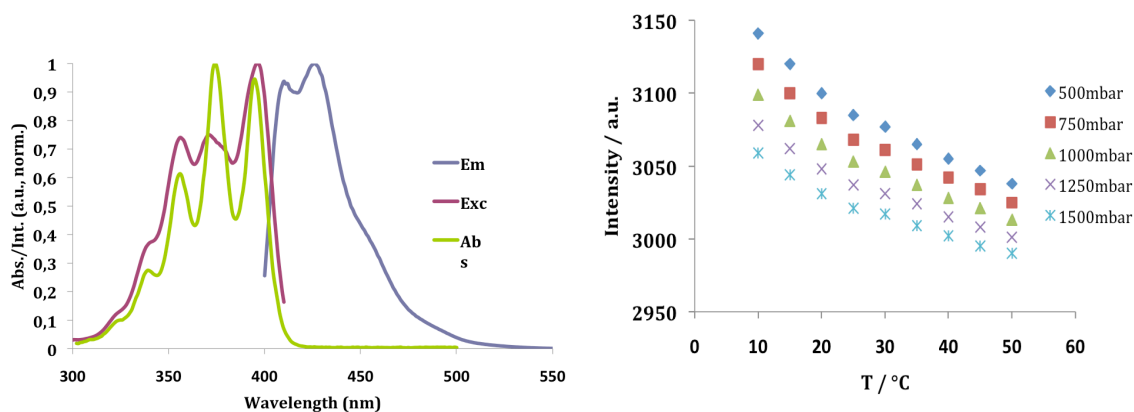
**Figure 4.7.** Spectra of DPA dissolved in THF (left) and calibration plot of DPA in PS film (right).

DPA is easy to incorporate in PAN micro particles by coprecipitation in order to suppress its slight oxygen sensitivity. The PAN particles dyed with DPA were dispersed in a PS film containing PtTFPP. The emission spectra of the film under excitation with 405 nm and various atmospheres are displayed in Figure 4.8.
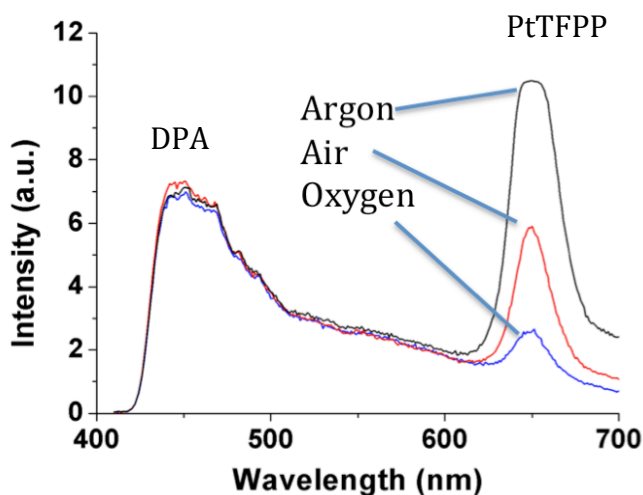


**Figure 4.8.** Emission spectra of DPA in PAN micro particles dispersed in a film of PS containing the oxygen indicator PtTFPP.

## 4.6        Comparison of DG43, S 2145, and DPA

DG43, S 2145, and DPA are suitable reference dyes for referenced intensity imaging or RGB imaging with red emitting indicators. Herein, the three dyes are compared with respect to their photo stability, thermo stability, and temperature sensitivity. The photo stability was tested by illuminating the samples (dyed 6 μm PS film of 3 x 3 cm size) with a 405 nm LED for 3 hours at 30 °C and 1000 mbar air pressure. The Luminescence intensity of the films was recorded every 30 minutes. The ratio of the start value ($I_0$) divided by the value ($I$) after the respective time was plotted vs. time. The plot is shown in Figure 4.9. All three dyes are very photo stable with S 2145 being the most stable.
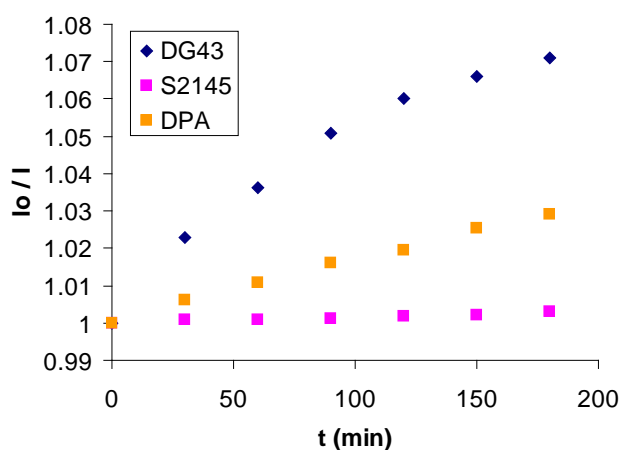


**Figure 4.9.** Results of the photostability test. The samples were illuminated at 405 nm for 3 hours at 30 °C and 1000 mbar air pressure. $I_0$ is the luminescence intensity of the film at the start of the experiment and $I$ is the intensity after the respective time $t$.

The thermostability was tested by heating the samples to 55 °C at 1000 mbar air pressure for two hours. The luminescence intensity was recorded at 30 °C and 100 mbar air pressure before and after the heating. Results are shown in Figure 4.10. The decrease of intensity is very small for all of the dyes. Especially, S 2145 and DPA display excellent thermostability.
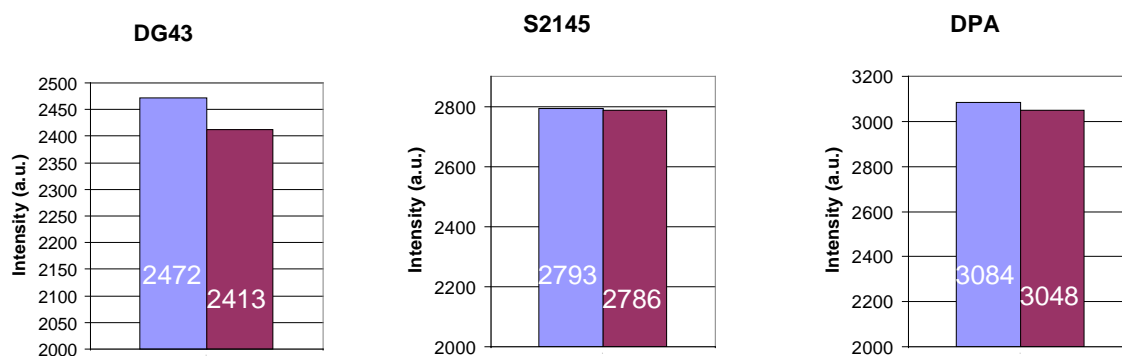
**Figure 4.10.** Thermostability test of the reference dyes DG43, S 2145, and DPA. The intensities were recorded at 30 °C and 1000 mbar air pressure. The samples were heated to 55 °C for two hours between two measurements. The bars indicate the intensity before (left) and after (right) heating.

The temperature sensitivities of the three dyes at 1000 mbar air pressure are shown in Figure 4.11. The ratio of the intensity at 10 °C ($I_0$) divided by the intensity($I$) at the respective temperature. This ratio is plotted vs. temperature. The temperature dependencies of DG43 and DPA are almost identically low. The luminescence intensity of S 2145 is remarkably insensitive to temperature.
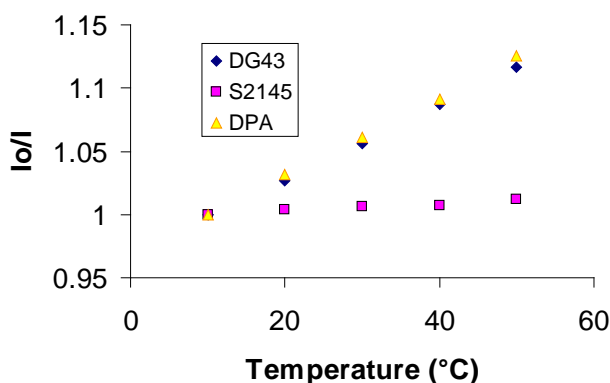


**Figure 4.11.** Temperature dependencies of the three reference dyes in PS film (6 µm) at 1000 mbar air pressure. $I_0$ is the luminescence intensity at 10 °C and $I$ is the intensity at the respective temperature.

The three dyes DG43, S 2145, and DPA are very promising candidates as reference dyes a red emitting indicator. The emission of DG43 is solvatochromic as the peak changes from 510 nm in THF solution to 480 nm in PS film. DG 43 is the least photo stable and least thermostable amongst them. The dyes can easily be incorporated into PAN microparticles by coprecipitation. In PAN microparticles they display virtually no sensitivity towards oxygen. S 2145 is the dye that is by far least sensitive to temperature out of all dyes studied.

## 4.7      Experimental

All spectra were recorded in THF unless stated different. The sensor films were manufactured by casting the respective sensor cocktail onto a foil of poly(ethylene terephtalate) (type Mylar®; from www.goodfellow.com) by knife coating. Thickness of the films is approximately 5 μm. Samples of 3 x 3 cm size were imaged in the calibration chamber.

The dyed PAN reference particles were synthesized by incorporating the respective dye in poylacrylonitrile (PAN) using a precipitation method.[10] The dyed particles precipitate from a solution of dye (20 mg) and PAN (300 mg) in dimethylformamide (30 mL) upon slow addition (1 mL/s$^{-1}$) of distilled water (70 mL) and subsequent addition of brine (20 mL). They can be separated by centrifugation. All sensor particles were washed four times with ethanol and four times using distilled water (each washing step followed by centrifugation for 10 min at 1030 g). Particles were freeze-dried before storage.

.The calibration chamber was provided by the German Aerospace Center (DLR) in Göttingen (www.dlr.de). Inside the chamber a three by three cm sample can be mounted. The temperature can be adjusted from 1 to 60 °C and air pressure values between 50 mbar and 2000 mbar can be set. Intensity imaging was performed with a PCO SensiCam 12 bit b/w CCD camera (PCO, Kelheim; www.pco.de) equipped with a Schneider- Kreuznach Xenon 0.95/17 lens (Schneider Optische Werke; www.schneiderkreuznach.com) and a 405-66-60 405 nm LED from Roithner Lasertechnik (Vienna; www.roithner-laser.com)

The ion pair extraction of HPTS was performed by the following procedure [11]. 200 mg of HPTS trisodium salt were dissolved in 30 mL of an 1% (w/w) solution of sodium carbonate in water. TOABr was added to the solution in the 4-fold molar amount (834 mg). The solution was mixed with 30 mL of $CH_2Cl_2$ in a separatory funnel. The ion pair is extracted from the aqueous phase into the organic phase. After 30 minutes the organic phase is washed three times with 0.05 M NaOH and separated from the aqueous phase. The solvent is removed by rotary evaporation, yielding the crystalline ion pair HPTS(TOA)$_4$.

All solvents and the dyes BBS, C 314, C 343, MBP, HPTS, APTS, DPA, and polystyrene were purchased from Sigma-Aldrich ([www.sigma-aldrich.com](www.sigma-aldrich.com)). The dyes S 2145, S 0679, S 2142, S 2166 and, S 2167 were a kind gift of Dr. H. Mustroph of FEW chemicals (www.few.de).

## 4.8    References

[1]     G. E. Khalil, C. Costin, J. Crafton, G. Jones, S. Grenoble, M. Gouterman, *Sens. Actuat. B-Chem.* **2004**, *97*, 13.

[2]     R. H. Engler, C. Klein, O. Trinks, *Meas. Sci. Technol.* **2000**, *11*, 1077.

[3]     C. Klein, R. H. Engler, U. Henne, W. E. Sachs, *Exp. Fluids.* **2005**, *39*, 475.

[4]     A. Lapresta-Fernandez, L. F. Capitan-Vallvey, *Analyst* **2011**, *136*, 3917.

[5]     L. F. Capitan-Vallvey, A. J. Palma, *Anal. Chim. Acta* **2011**, *696*, 27.

[6]     X. D. Wang, R. J. Meier, M. Link, O. S. Wolfbeis, *Angew. Chem. Int. Ed.* **2010**, *49*, 4907.

[7]     R. J. Meier, S. Schreml, X. D. Wang, M. Landthaler, P. Babilas, O. S. Wolfbeis, *Angew. Chem. Int. Ed.* **2011**, *50*, 10893.

[8]     U. Resch-Genger, M. Grabolle, S. Cavaliere-Jaricot, R. Nitschke, T. Nann, *Nat. Meth.* **2008**, *5*, 763.

[9]     M. Schaferling, *Angew. Chem. Int. Ed.* **2012**, *51*, 3532.

[10]    S. M. Borisov, T. Mayr, G. Mistlberger, K. Waich, K. Koren, P. Chojnacki, I. Klimant, *Talanta* **2009**, *79*, 1322.

[11]    G. J. Mohr, T. Werner, I. Oehme, C. Preininger, I. Klimant, B. Kovacs, O. S. Wolfbeis, *Adv. Mater.* **1997**, *9*, 1108.

# Chapter 5

# Pressure and Temperature Sensitivity of Various Homoleptic and Heteroleptic Ir(III) Complexes

**Summary:** A series of iridium-derived luminophores was investigated in order to find new indicators for oxygen and temperature. Iridium complexes are promising dyes for indicator applications.[1-6] They provide photostability and tunable emission. The diversity of emission wavelengths is important to enable the separation from a second luminescent signal in a dually sensitive paint. The pressure ($pO_2$) and temperature dependency of the phosphorescence lifetimes of seven heteroleptic iridium complexes and of three homoleptic iridium complexes was evaluated.

## 5.1   Compounds and Calibration

The seven heteroleptic compounds were synthesized by the group of Prof. E. Holder at the University of Wuppertal. They consist of two identical cyclometalating ligands and different ancillary ligands. The cyclometalating ligands are (1-phenylisoquinoline, piq), 2-(naphthalen-1-yl)pyridine (npy) and 2-phenylpyridine (ppy), respectively. The structures of the complexes $Ir(ppy)_2B$, $Ir(ppy)_2C$, $Ir(ppy)_2D$, $Ir(npy)_2B$, $Ir(npy)_2C$, $Ir(npy)_2D$, $Ir(piq)_2(acac)$ are shown in Figure 5.1. The three homoleptic iridium(III)

complexes ([*tris*[2-(benzo[*b*]thiophen-2-yl)pyridinato-C$^3$,N]iridium(III)], (Ir(btpy)$_3$), [*tris*[2-(4,6-difluorophenyl)pyridinato-C$^2$,N]iridium(III)], (Ir(Fppy)$_3$), and [*tris*[2-phenylpyridinato-C$^2$,N]iridium(III)], (Ir(ppy)$_3$) are commercially available. Their structures are shown in Figure 5.1 as well. The emission spectra of the dyes are shown in Figure 5.2. The emission spectra of the heteroleptic complexes with the same cyclometalating ligand but with a different ancillary ligand only slightly differ from each other. For better visual clarity only six emission spectra are displayed in Figure 5.2.
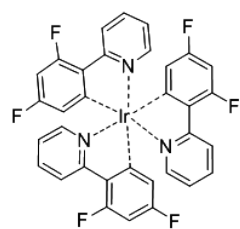
Ir(Fppy)₃
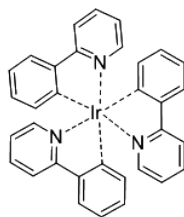
Ir(ppy)₃
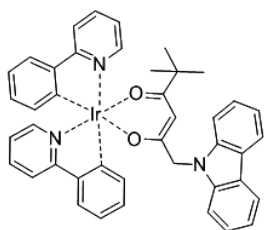
Ir(ppy)₂B
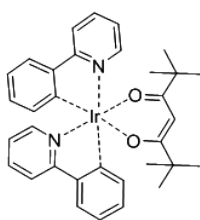
Ir(ppy)₂C
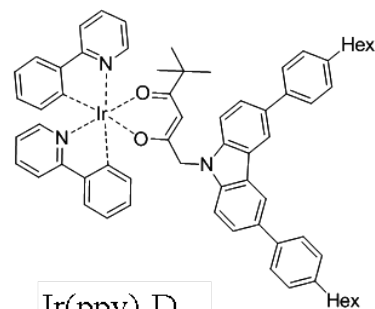
Ir(ppy)₂D
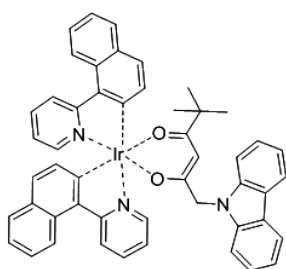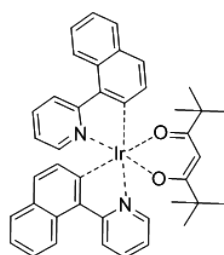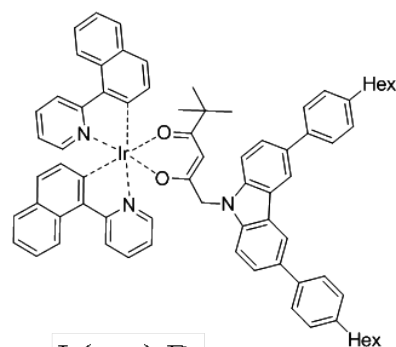
Ir(npy)₂B

Ir(npy)₂C

Ir(npy)₂D
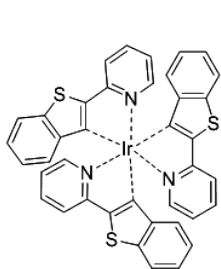
Ir(btpy)₃
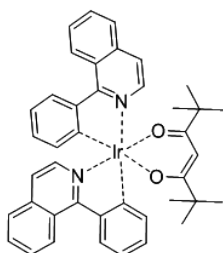
Ir(piq)₂acac

**Figure 5.1.** Structures of the ten iridium complexes characterized.
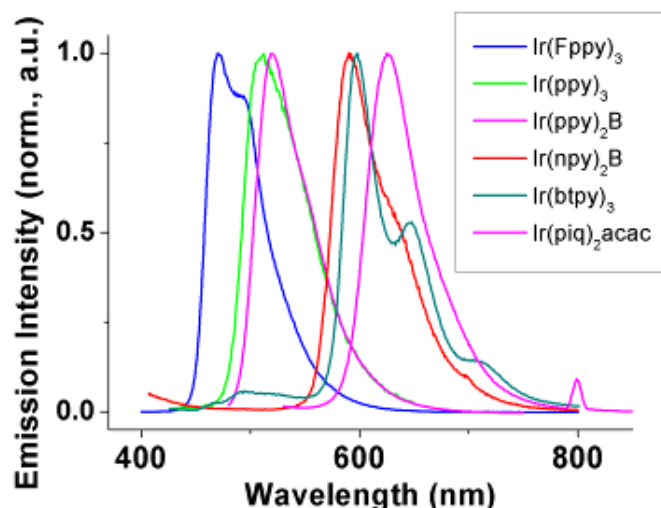
**Figure 5.2.** Emission spectra of the characterized iridium complexes. The emission spectra of the missing heteroleptic complexes with the same cyclometalating ligand but with a different ancillary ligand are only slightly different from the ones shown and thus are not displayed above.

The dyes were incorporated into standardized polystyrene films of 6 µm thickness. These were fabricated with a knife coating device on a solid poly(ethylene-terephtalate) (PET) support. The backside of the PET foil was coated with a high reflective silicone/$TiO_2$ screen layer. The luminescence lifetimes were obtained according the rapid lifetime determination (RLD) method.[7,8] This ratiometric method provides intrinsic referenced signals and can be used to calculate the average luminescence lifetimes. For this purpose, the sensor films are photo-excited by means of a pulsed 405 nm LED with an internal frequency of 125 kHz. The luminescence intensity is integrated by a triggered CCD camera within two precisely timed gates ($A_1$ and $A_2$) of 1.4 µs with delay times of 0 µs ($t_1$) and 0.7 µs ($t_2$), respectively. This is followed by the acquisition of the corresponding dark images for background subtraction.[9] More precisely, after a short light pulse of 5 µs the luminescence intensity is acquired in the first gate $A_1$. This is repeated several hundred times within an integration time of 250 ms and the measured intensities are accumulated and displayed as the first image.[9] Likewise, the intensity in the second gate $A_2$ and the dark images are recorded.

It has to be emphasized that luminescence decays of metal-ligand complexes are not monoexponential and the lifetimes determined by this simple ratiometric method do

not represent exact values as obtained with single photon counting measurements. However, the values acquired at identical experimental settings reflect changes of luminescence lifetimes within a series of measurements. For comparison, *Baranoff et al.* reported a lifetime $\tau_0$ of the triplet emission of Ir(btpy)$_3$ at 596 nm of 4.0 µs in toluene solution at 298  K .[10]

In this study, the pressure and temperature calibration of the iridium(III) phosphors in a PS film was performed with square samples of $3 \times 3$ cm size. These were placed in a calibration chamber, in which the air pressure can be adjusted from 50 to 2000 mbar and the temperature from 1 to 60 °C. The assembly of the calibration chamber and of the imaging set up has been outlined in a recent publication.[11]

The results of the temperature calibrations are shown in Figure 5.3. The resulting lifetimes were normalized to the first value (1 °C at 1000 mbar) of the series of measurements in order to display the graphs in one plot. The results of the pressure calibrations are shown in Figure 5.4 in the form of Stern-Volmer plots.
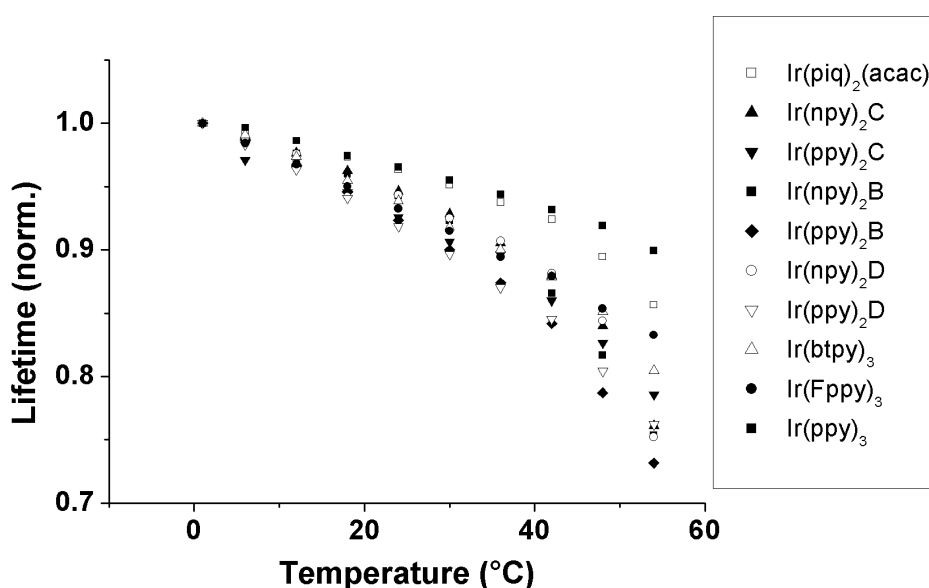


**Figure 5.3.** Temperature dependence of the normalized luminescence lifetimes of the iridium(III) complexes in 6 µm PS films at 1000 mbar.
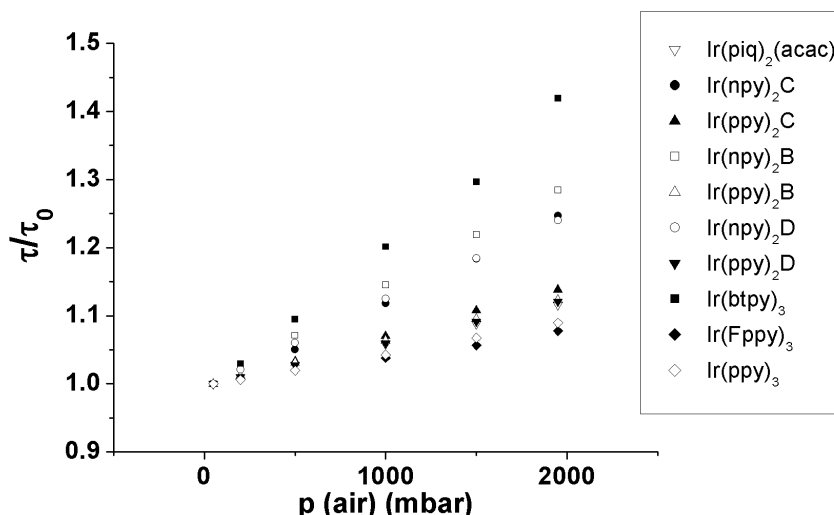
**Figure 5.4.** Air pressure dependence of the luminescence lifetimes of cyclometalated iridium(III) complexes in 6 μm PS films at T = 30 °C. All plots are referenced to the according lifetime values at 50 mbar air pressure and 1 °C.

The respective Stern-Volmer ($K_{SV}$) constants and the temperature coefficients were calculated according to linear fits. The fits are very consistent in case of pressure dependency with correlation coefficients $R^2$ higher than 0.99. Although the temperature plots are apparently not linear, the calculated linear temperature coefficients are a suitable quantity for the temperature sensitivity. Furthermore, the oxidation potential of the complexes was measured *via* cyclic voltammetry *vs.* ferrocene (Fc/Fc$^+$) in dried tetrahydrofuran. All parameters are summarized in Table 5.1.

Generally, in case of metal-ligand complexes, the emission maximum is determined by the energy gap between the excited triplet state and the ground state, which can be correlated with the energy difference of the frontier molecular orbitals (HOMO-LUMO gap). It is obvious that increasing HOMO-LUMO gaps result in emission maxima of higher energy. Furthermore, within this series, decreasing energy gaps from blue to red emission cause increased lifetimes. The oxidation potential, which depends on the energy level of the HOMO, is clearly decreasing in this order (see Table 5.1).

Unfortunately, reduction potentials could not be measured with our set-up. They occur at potentials lower than -2.0 V.[32]

**Table 5.1.** Reversible oxidation potentials, phosphorescence emissions maxima, and lifetimes of cyclometalated iridium(III) complexes and their pressure and temperature sensitivities.

| | $\lambda_{em}$ [nm] | $E_{ox}$ Fc/Fc+ [V] | vs.T-coeff. [%(t)/°C] | $K_{sv}$ mbar-1 [a] | $[10^{-4}\tau$ [µs] [b] |
|---|---|---|---|---|---|
| **Ir(Fppy)₃** | 470 | 0.64 | 0.31 | 0.4 | 1 |
| **Ir(ppy)₃** | 512 | 0.31 | 0.19 | 0.47 | 1.2 |
| **Ir(ppy)₂B** | 521 | 0.28 | 0.48 | 0.65 | 1.2 |
| **Ir(ppy)₂C** | 526 | 0.25 | 0.37 | 0.73 | 1.2 |
| **Ir(ppy)₂D** | 522 | 0.27 | 0.43 | 0.63 | 1.1 |
| **Ir(npy)₂B** | 590 | 0.27 | 0.43 | 1.49 | 3.5 |
| **Ir(npy)₂C** | 600 | 0.27 | 0.4 | 1.33 | 3.4 |
| **Ir(npy)₂D** | 595 | 0.27 | 0.4 | 1.26 | 3.3 |
| **Ir(btpy)₃** | 596 | 0.25 | 0.35 | 2.17 | 6.6 |
| **Ir(piq)₂acac** | 625 | - | 0.21 | 0.61 | 1.1 |

[a] in 6 µm PS film, [b] at 50 mbar air pressure and 30 °C.

## 5.2   Pressure Sensitivity

The series of homoleptic and heteroleptic Ir(III) complexes emitting from blue to red showed also an increasing oxygen (and pressure) sensitivity with increasing lifetimes of the excited triplet state. This can be expected as a consequence of the Stern-Volmer equation (eq. 2.6), which describes the dependency of the luminescence lifetime from oxygen partial pressure. The influence of the ancillary ligand on the temperature and oxygen sensitivity is very small. Within a series of complexes bearing the same cyclometalating ligand (ppy or npy respectively) $K_{SV}$ and temperature coefficients show only negligible deviations. In contrast, the cyclometalating ligands have a large impact on the sensing properties, as expected from their different photophysical properties. The red emitting series with the npy ligand shows much higher oxygen sensitivity compared to the green emitting series with the ppy cyclometalating ligand. With respect to the Stern-Volmer equation this is due to the longer lifetimes of the complexes with the npy ligand. The highest oxygen quenching efficiency is observed for $Ir(btpy)_3$ with a $K_{SV}$ of 2.17 [$10^{-4}$ mbar$^{-1}$] relating to air pressure. Stern-Volmer constants of several cyclometalated iridium(III) complexes have been reported, but they can hardly be compared because they have been determined at different experimental conditions and with various polymer matrices.[1,4,5,12-15] Generally, with the exception of $Ir(btpy)_3$ and the npy complexes, the iridium(III) complexes are not efficiently quenched by oxygen.

A general influence of the emission wavelength on the sensitivity to oxygen can not be deduced because the deep red emitting complex $Ir(piq)_2(acac)$ shows only slight oxygen sensitivity. It is apparent that the luminescence quenching by oxygen is a bimolecular process and affected by many factors.

Another very important aspect that determines the response is the oxygen permeability of the matrix polymer. In this study, all complexes were calibrated in PS, which possesses a oxygen permeability P of $1.9 \times 10^{-13}$cm$^3$ (STP) cm (cm$^2$sPa)$^{-1}$ (STP = standard temperature and pressure).[1] Because of this moderate oxygen permeability, PS is an appropriate polymer binder in order to compare the luminescence responses to temperature and oxygen of a series of dyes at standard conditions. If polymers with higher oxygen permeabilities are applied, the oxygen sensitivity and $K_{SV}$ values increase and also the differences between the single complexes are more pronounced. Figure 5.5

compares the response to oxygen of Ir(btpy)$_3$ in PS and ethyl cellulose (EC). The latter provides a very high oxygen permeability with P = 11 × 10$^{-13}$cm$^3$ (STP) cm (cm$^2$sPa)$^{-1}$).[16] This results in an increased K$_{SV}$ of 40 [10$^{-4}$ mbar$^{-1}$], which is very high compared to other luminescent probes used in optical oxygen sensors.
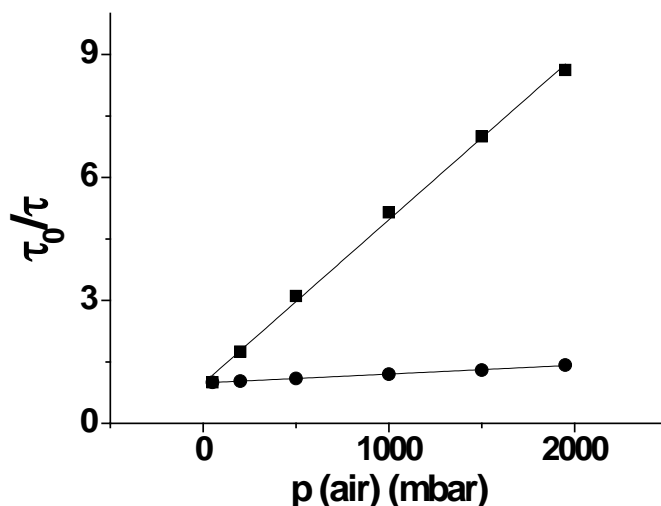


**Figure 5.5.** Stern-Volmer plots for Ir(btpy)$_3$ (10) in PS (dots) and EC 49 (squares) (EC with 49 % ethoxy grade) at 30°C.

## 5.3   Temperature Sensitivity

Nearly all luminescent dyes display a more or less strong sensitivity towards temperature (see section 2.3). The Boltzmann distribution is one factor for this phenomenon because it governs the populations of the different vibrational levels of the electronic states involved. At higher temperatures, nonradiative relaxation mechanisms are becoming dominant because deactivating states are thermally activated. For example, the decreasing energy difference between the electronic states can be converted more easily to vibrational energy in the complex ligand or in the polymer matrix. Furthermore, the energy of the excited electronic state can be transferred to fitting electronic states of the environment. Finally, the oxygen permeability of the matrix polymer increases with temperature. This results in a higher concentration of quenching oxygen molecules in the polymer binder at increased temperatures. Amongst the studied iridium(III) complexes, the green emitting series bearing ppy ligands show

the highest temperature sensitivity. The calibration plots for the temperature response are nonlinear and can be fitted by an Arrhenius-type equation.[17]

$$\frac{1}{\tau} = k_0 + k_1 \cdot \exp\left(-\frac{\Delta E}{R \cdot T}\right)$$

eq. 5.1

where $\tau$ is the lifetime, $k_0$ the temperature-independent decay rate for the deactivation of the excited state, $k_1$ the pre-exponential factor, $\Delta E$ the energy gap between the emitting level and an upper deactivating excited state, $R$ the gas constant, and $T$ the temperature in Kelvin. Figure 5.6 shows exemplary the Arrhenius fit of the thermal quenching of Ir(ppy)$_2$B in PS at 1000 mbar air pressure.
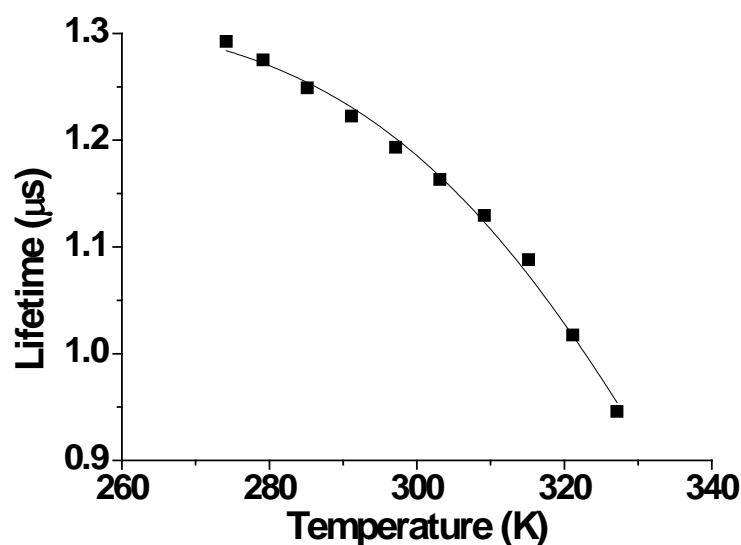


**Figure 5.6.** Temperature dependence of the luminescence lifetime of Ir(ppy)$_2$B in PS at 1000 mbar and Arrhenius fit according to eq. 5.1 (line). Fitting parameters: $k_0$ =0.76 $\mu s^{-1}$, $k_1$=19.5 $\times$ 10$^4$ $\mu s^{-1}$, and $\Delta E$=36.5 kJmol$^{-1}$. The correlation coefficient $R^2$ for the fit is 0.994.

Generally, the temperature sensitivity of cyclometalated iridium(III) complexes is very low compared to other luminescent metal-ligand complexes. Hence, the temperature coefficients of typical luminescent indicators for T such as ruthenium and

europium complexes[7,18,19] are up to two times higher compared to the green emitting iridium(III) complexes described here. The exceptional property of the green emitters, particularly of Ir(ppy)$_2$B, is their shortwave emission wavelengths, which make them easy to combine with the numerously available red emitting oxygen indicators for dual sensors. The high reproducibility and the very low standard deviations of the calibration plots and the broad dynamic range of the response are also noticeable.

## 5.4   Conclusion

A full series of neutral heteroleptic iridium(III) complexes equipped with 2-phenylpyridine, 2-(naphthalen-1-yl)pyridine, and 1-phenylisoquinoline as cyclo-metalating ligands was presented. In order to obtain unsymmetrical iridium(III) complexes, 2,2,6,6-tetramethylheptane-3,5-dione, 1-(9*H*-carbazol-9-yl)-5,5-dimethylhexane-2,4-dione and 1-(3,6-*bis*(4-hexylphenyl)-9*H*-carbazol-9-yl)-5,5-dimethylhexane-2,4-dione were utilized as ancillary ligands. These increase the unsymmetrical architecture of the Ir(III) complexes gradually. The photophysical and electrochemical properties of the Ir(III) complexes were investigated experimentally. Moreover, the properties of the synthesized heteroleptic iridium(III) complexes were compared to homoleptic Ir(III) complex structures revealing symmetrical architectures. These consist of three equal cyclometalating ligands. The emission intensities of the two classes of heteroleptic Ir(III) complexes respond to changes of partial oxygen pressure and, to a lower extent, to temperature changes. In addition, oxygen-sensitive Ir(III) emitters can be outlined due to the clear correlation of their oxygen-sensitivities with their phosphorescence lifetimes. A dually sensitive paint containing two Ir(III)-complexes as indicators is described in chapter 6.

## 5.5    Experimental

[*tris*[2-(benzo[b]thiophen-2-yl)pyridinato-C$^3$,N]iridium(III)],                     [*tris*[2-(4,6-difluorophenyl)pyridinato-C$^2$,N]iridium(III)],                     [*tris*[2-phenhylpyridinato-C$^2$,N]iridium(III)], ferrocene and, titanium dioxide were purchased from Sigma-Aldrich ([www.sigmaaldrich.com](www.sigmaaldrich.com)). All other complexes were synthesized by the group of Prof. Elisabeth Holder at the university of Wuppertal.[20] Absorption and emission spectra were recorded on a Lambda 14p Perkin-Elmer UV-vis spectrophotometer (Waltham, MA, USA, www.perkinelmer.com) and an Aminco AB 2 luminescence spectrometer (Thermo Scientific Inc., Waltham, MA, USA, www.thermo.com), respectively. The *p/T* calibration chamber was provided by the German Aerospace Center (DLR) in Göttingen.[8] All time-resolved measurements were performed with a PCO SensiCam 12 bit b/w CCD camera (PCO, Kelheim, Germany, www.pco.de) equipped with a Schneider-Kreuznach Xenon 0.95/17 lens (Jos. Schneider Optische Werke, Bad Kreuznach, Germany, www.schneiderkreuznach.com) and a 405-66-60 405nm LED from Roithner Lasertechnik (Vienna, Austria, www.roithner-laser.com). The excitation light was focused by a PCX 18_18 MgF2 TS lens from Edmund Optics (Karlsruhe, Germany, www.edmundoptics.com). It was filtered through a BG 12 filter (Schott, Mainz, Germany, www.schott.com) with a thickness of 2 mm. Emission was detected through a BP 475/40 band pass filter (Ir(Fppy)$_3$), a GG 475 high pass filter (all Ir(ppy)$_2$X complexes) and for all other complexes with a OG 530 high pass filter purchased from AHF Analysentechnik (www.ahf.de).

## 5.6    References

[1]    Y. Amao, Y. Ishikawa, I. Okura, *Anal. Chim. Acta* **2001**, *445*, 177-182.

[2]    M. C. DeRosa, P. J. Mosher, C. E. B. Evans, R. J. Crutchley, *Macromol. Symp.* **2003**, *196*.

[3]    S. M. Borisov, I. Klimant, *Anal. Chem.* **2007**, *79*, 7501-7509.

[4]    L. Huynh, Z. Wang, J. Yang, V. Stoeva, A. Lough, I. Manners, M. A. Winnik, *Chem. Mater.* **2005**, *17*, 4765-4773.

[5]  C. S. K. Mak, D. Pentlehner, M. Stich, O. S. Wolfbeis, W. K. Chan, H. Yersin, *Chem. Mater.* **2009**, *21*, 2173-2175.

[6]  K. Koren, S. M. Borisov, R. Saf, I. Klimant, *Eur. J. Inorg. Chem.* **2011**, 1531-1534.

[7]  M. I. Stich, O. S. Wolfbeis *Fluorescence Sensing and Imaging Using Pressure-Sensitive Paints and Temperature-Sensitive Paints; Standardization and Quality Assurance in Fluorescence Measurements I* Springer, 2008; Vol. 5.

[8]  C. Moore, S. P. Chan, J. N. Demas, B. A. DeGraff, *Appl. Spectrosc.* **2004**, *58*, 603-607.

[9]  G. Liebsch, I. Klimant, B. Frank, G. Holst, O. S. Wolfbeis, *Appl. Spectrosc.* **2000**, *54*, 548-559.

[10] E. Baranoff, J. H. Yum, M. Graetzel, M. K. Nazeeruddin, *J. Organomet. Chem.* **2009**, *694*, 2661-2670.

[11] L. H. Fischer, M. I. J. Stich, O. S. Wolfbeis, N. Tian, E. Holder, M. Schaferling, *Chem. Eur. J.* **2009**, *15*, 10857-10863.

[12] A. L. Medina-Castillo, J. F. Fernandez-Sanchez, C. Klein, *Analyst* **2007**, *132*.

[13] S. M. Borisov, I. Klimant, *Anal. Chem.* **2007**, *79*, 7501-7509.

[14] G. D. Marco, M. Lanza, M. Pieruccini, S. Campagna, *Adv. Mater.* **1996**, *8 No.7*.

[15] G. D. Marco, M. Lanza, A. Mamo, *Anal. Chem.* **1998**, *70,23*.

[16] J. Brandrup, E. H. Immergut, E. A. Grulke *Polymer Handbook*.

[17] J. N. Demas, B. A. Degraff, *Anal. Chem.* **1991**, *63*, A829-A837.

[18] M. E. Köse, B. F. Carroll, K. S. Schanze, *Langmuir* **2005**, *21*, 9121-9129.

[19] B. Zelelow, G. E. Khalil, G. Phelan, B. Carlson, *Sens. Actuat. B-Chem.* **2003**, *B 96*, 304.

[20] N. Tian, D. Lenkeit, S. Pelz, L. H. Fischer, D. Escudero, R. Schiewek, D. Klink, O. J. Schmitz, L. Gonzalez, M. Schaferling, E. Holder, *Eur. J. Inorg. Chem.* **2010**, 4875-4885.

# Chapter 6

# Red and Green Emitting Iridium(III) Complexes for a Dual Barometric and Temperature Sensitive Paint

**Summary:** A new dual luminescent sensitive paint for barometric pressure and temperature (T) is presented. The green-emitting iridium(III) complex [Ir(ppy)$_2$(carbac)] is applied as a novel probe for T along with the red-emitting complex [Ir(btpy)$_3$] that functions as a barometric (in fact oxygen-sensitive) probe. Both iridium complexes are dissolved in different polymer materials to achieve optimal response. The probe [Ir(ppy)$_2$(carbac)] is dispersed in gas-blocking poly(acrylonitrile) micro-particles in order to suppress any quenching of its luminescence by oxygen. The barometric probe [Ir(btpy)$_3$], in turn, is incorporated in a cellulose acetate butyrate film which exhibits good permeability for oxygen. Effects of temperature on the response of the oxygen probe can be corrected by simultaneous optical determination of T as the poly(acrylonitrile) micro-particles containing the temperature indicator are incorporated into the film. The phosphorescent signals of the probes for T and barometric pressure, respectively, can be separated by optical filters due to the ~75 nm difference in their emission maxima. The dual sensor is applicable to luminescence lifetime imaging of T and barometric pressure. It is the first luminescent dual sensor material for barometric pressure/T exclusively based on the use of Ir(III) complexes in combination with luminescence lifetime imaging.

## 6.1    Introduction

Oxygen partial pressure and temperature can be measured by using luminescent sensitive materials.[1-5] Luminescent probes for oxygen are usually incorporated in a gas-permeable polymer matrix and can be applied in various formats such as sensor foils or as fiber optic sensors.[6-8] The measurement of barometric pressure plays a essential role in aerodynamics and in fluid mechanics.[9,10]

Imaging offers a spatial resolution unsurpassed by any other method for determination of barometric pressure, and respective coatings ("PSPs") – unlike other sensors – do not disturb the gas flow in wind tunnels. However, luminescent probes for barometric pressure are sensitive to temperature as well. It therefore has been suggested that – by analogy to PSPs – a temperature indicator should be incorporated into a similar sensor layer in order to measure T (a so-called temperature sensitive paint; TSP), or in order to correct for the effect of T on the response of the PSP. TSPs use gas blocking matrix polymers, in order to avoid the quenching of luminescence by oxygen.[11,12] The relationship between polymer structure, oxygen permeation and diffusion in the polymer, and oxygen quenching efficiencies has been reviewed by *Lu et al.*[8] Finally, dual PSP/TSP sensors have been reported[13-15] based on the possibility of optical sensors to give several signals simultaneously (in this case one for barometric pressure and one for T) that can be separated by optical filters provided the probes emit at sufficiently different wavelengths and with insignificant spectral overlap, or if the decay times of the luminescence lifetimes differ by a certain amount.[16]

Several problems that occur in sensing based on measurement of luminescence intensity can be overcome by making use of time-resolved gated lifetime detection. In detail, lifetime imaging is insensitive towards variations in thickness of the sensor layer, inhomogenous sample surface and illumination, reflections and scatter of excitation light, photobleaching of fluorescent probes and leaching of the dyes, and interferences by strong ambient light.[17] Luminescence lifetime imaging is an intrinsically referenced method that is not influenced by varying distances between sample and detector, nor by applying different detectors or excitation light sources.[18] Luminescence lifetime imaging is often performed by the rapid lifetime determination (RLD) method (see section 2.7.3).[19]

Here, we report on the preparation and calibration of a dual sensor for barometric pressure and T that consists of two organometallic iridium(III) probes

dissolved in appropriate "binder" polymers. Various organometallic complexes have been used so far as indicator probes in PSPs and TSPs. Foremost, Pt(II) and Pd(II) porphyrins and porpholactones were employed as probes for sensing barometric pressure because their luminescence is strongly quenched by oxygen even in polymer solution.[20-24] Complexes of Eu(III) and Ru(II) have been presented for use in sensing T.[25,26] Iridium(III) probes, in contrast, have not been widely investigated with respect to their suitability for sensing oxygen or barometric pressure[1,27-31] and – up to now – they have not been employed for purposes of sensing T even though they display bright and tunable emission colors and phosphorescence lifetimes in the range from 1 to 10 μs[32-35] which are perfectly suited for lifetime imaging applications.

## 6.2    Results and Discussion

### 6.2.1    Sensor Composition

The dual sensor material consists of the green-emitting temperature probe di[2-phenylpyridinato-C2,N](1-(9*H*-carbazol-9-yl)-5,5-dimethylhexane-2,4-dione)iridium(III) = [Ir(ppy)$_2$(carbac)], and the red-emitting oxygen probe [*tris*[2-(benzo[b]thiophen-2-yl)pyridinato-C$^3$,N]iridium(III)] = [Ir(btpy)$_3$]. The temperature sensitive probe [Ir(ppy)$_2$(carbac)] was applied in gas-blocking poly(acrylonitrile) (PAN) micro-particles with a diameter of about 1 μm prepared by precipitation. These [Ir(ppy)$_2$(carbac)] / PAN micro-particles were dispersed in a solution of cellulose acetate butyrate (CAB) and the oxygen probe [Ir(btpy)$_3$] in THF. This "cocktail" was spread on a solid poly(ethylene terephthalate) (PET) support via knife coating. After evaporation of the solvent, the one layer sensor was obtained with optical response to either temperature (T) or barometric pressure (p).

The thickness of the sensor film is approximately 6 μm. The cross-section of the sensor device is shown in Figure 6.1, and the chemical structures of the fluorophores are depicted in Figure 6.2. The bottom of the substrate foil was coated with a high reflective 100-μm TiO$_2$/silicone screenlayer. PAN has a very low gas permeability[36] (P is 0.00015 × 10$^{-13}$ cm$^3$ (STP) cm (cm$^2$ s Pa)$^{-1}$. It shields the temperature probe from undesired oxygen quenching.
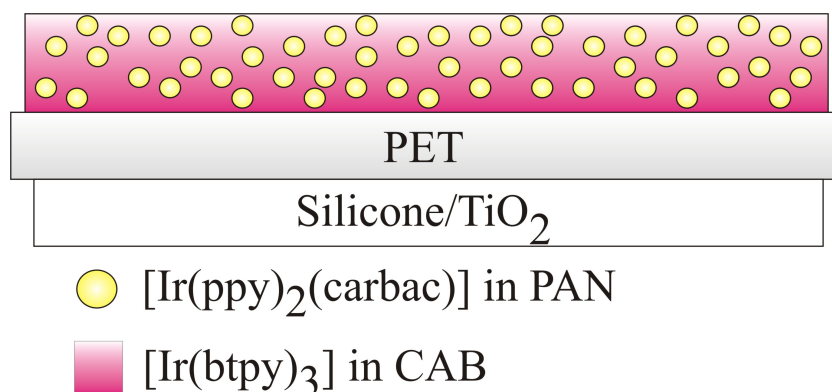
**Figure 6.1.** Scheme of the dual sensitive sensor layer. The cellulose acetate butyrate (CAB) film is cast on a poly(ethylene terephthalate) (PET) support by knife-coating. It contains the probe for barometric pressure (in fact for oxygen). The micro-particles made of poly(acrylonitrile) (PAN) doped with the temperature probe are dispersed in the CAB film. The bottom side of the PET layer is coated with a high reflective silicone/TiO$_2$ screen layer in order to improve optical readout which is performed from top.

The dual sensor layer was cast from a 5% solution (w/w) of CAB in tetrahydrofurane doped with [Ir(btpy)$_3$] and [Ir(ppy)$_2$(carbac)]. The permeability of the polymer hosting the oxygen probe is one of the major factors governing the quenching of the luminescence of the fluorophor. In this case, the sensor material was optimized for determination of air pressures up to 1500 mbar. Almost all established probes for luminescent barometric sensors are quenched to a wide extent at atmospheric pressure which makes them useful for pressures up to maximally 1 bar only. CAB was found to be a suitable polymer with a oxygen permeability[36] of $3.56 \times 10^{-13}$ cm$^3$ (STP) cm (cm$^2$ s Pa)$^{-1}$.

**(A) [Ir(ppy)₂(carbac)]**                    **(B) [Ir(btpy)₃]**

**Figure 6.2.** Structures of the indicators. (A) temperature indicator [Ir(ppy)$_2$(carbac)][33]; (B) oxygen indicator [Ir(btpy)$_3$].

## 6.2.2    Signal Separation

The emission of the luminescence of [Ir(ppy)$_2$(carbac)] peaks at 521 nm, that of [Ir(btpy)$_3$] at 596 nm. As the emission band of [Ir(ppy)$_2$(carbac)] is fairly narrow, the two signals can be almost quantitatively separated by optical filters as shown in Figure 6.3. The emission of [Ir(ppy)$_2$(carbac)] was optically isolated from other light using a BP 530/50 bandpass filter (530 nm indicating the center wavelength, 50 indicating the spectral bandpass). The oxygen-sensitive emission of [Ir(btpy)$_3$] was separated by a RG 610 longpass filter. It minimizes the interference by the emission of the temperature probe, however, at the expense of the intensity of the pressure signal. The luminescence properties of the two Ir(III) compounds are summarized in Table 6.1.
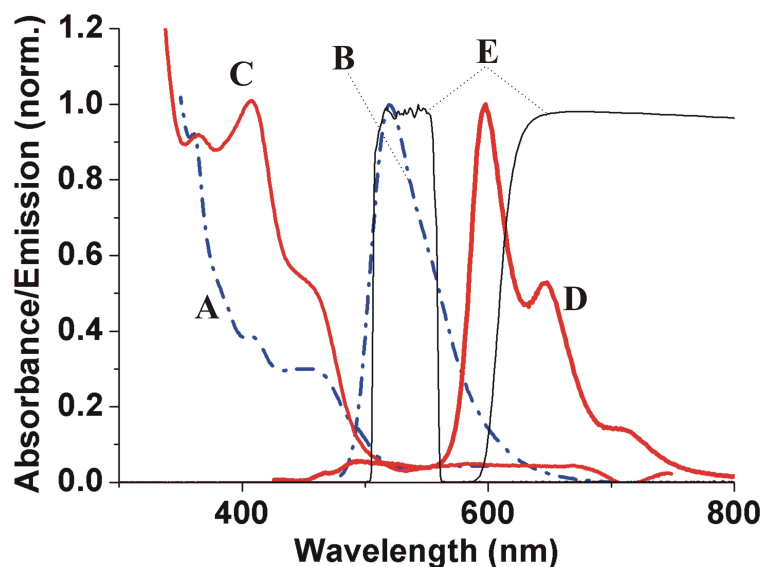
**Figure 6.3.** Optical spectra of the sensor system. (A) Absorbance and (B) emission of [Ir(ppy)$_2$(carbac)]. (C) Absorbance and (D) emission of [Ir(btpy)$_3$]. (E) Transmittance of the optical filters employed (BP 530/50 and RG 610).

**Table 6.1.** UV-vis absorption and emission maxima (in nm) of 10 µM chloroform solutions, decomposition temperatures ($T_d$), and luminescence lifetimes ($\tau$) of the iridium(III) complexes.

| Compound | Absorbance [nm] (log $\varepsilon$, [L × mol$^{-1}$ × cm$^{-1}$]) | $\lambda_{em}$ [nm] | $T_d$ [°C] | Lifetime [a) $\tau$ [µs] |
|---|---|---|---|---|
| [Ir(ppy)$_2$(carbac)] | 270 (4.71), 342 (4.06), 408 (3.58), 459 (3.45) | 521 | 337 [b)] | 3.65 |
| [Ir(btpy)$_3$] | 292 (4.83), 366 (4.31), 408 (4.34) | 596, 645 | 465 [b)] | 8.60 |

The single pressure sensitive film was then investigated in more detail using a fibre optic spectrometer. Emission spectra were acquired at different pressures at 24 °C. Figure 6.4 displays the pressure dependency of the emission spectrum of [Ir(btpy)$_3$] and shows that all maxima are quenched with equal efficiency.
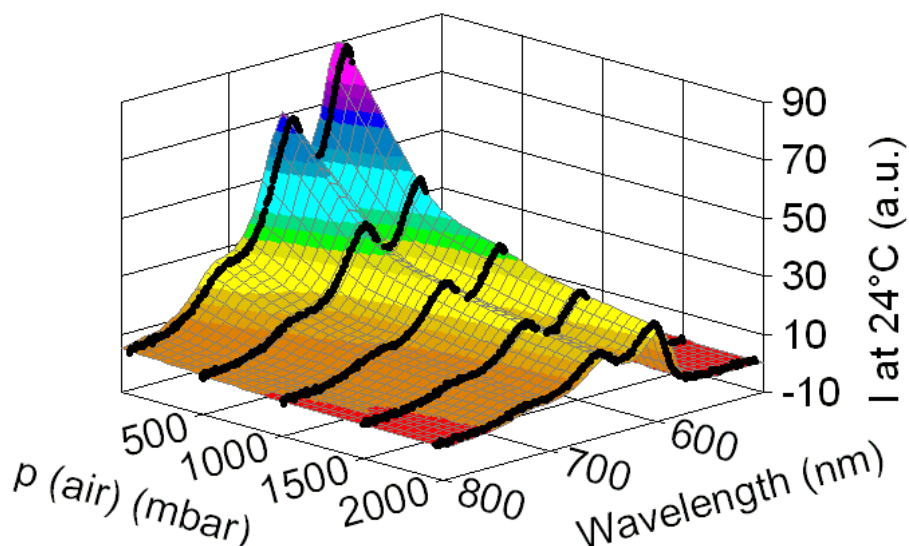
**Figure 6.4.** 3D intensity (I) plot of the pressure dependency of the emission spectra of the single pressure sensor [Ir(btpy)$_3$] in 6 μm CAB film at 24 °C.

The emission spectrum of the temperature probe has one maximum only. Its temperature dependence is given in Figure 6.5. The dynamic range covers the range of highest practical interest (0 to >50 °C).
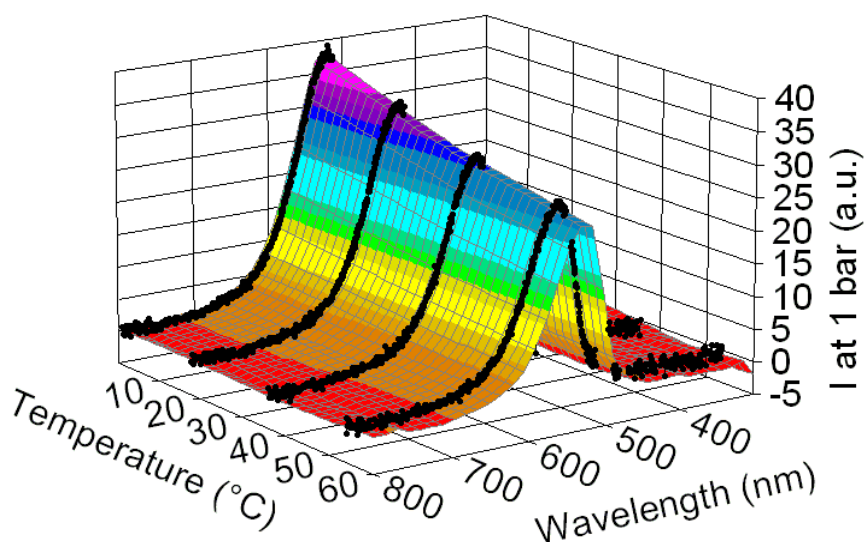


**Figure 6.5.** 3D intensity (I) plot of the temperature dependency of the emission spectra of the single temperature sensor of [Ir(ppy)$_2$(carbac)] in 6 μm PAN film at 24 °C.

## 6.2.3    Calibration of the Dual Sensor

The calibration of the sensor was performed by time-gated lifetime imaging using the RLD method.[18,37] Thereby, the decay of the luminescence intensity is considered to be monoexponential allowing a simple calculation of the luminescence lifetimes. Furthermore, the intrinsic reference accomplished by calculating an intensity ratio of two gates severely reduces the signal noise. The decay times of the phosphorescence of the metal-ligand complexes described here are in the range from 2.5 to 8 μs. Rather than using large (or expensive) lasers, we prefer to use small and inexpensive LED light sources for photoexcitation. The intensity of luminescence is measured in two precisely timed gates by a triggered CCD camera followed by a dark image for background substraction (see Figure 6). After the light pulse has decayed, luminescence intensity is acquired in the first gate. This is repeated several times over a certain period of time (the integration time) and the measured intensities are accumulated and displayed as the first image. Afterwards, the second gate and the dark image are recorded likewise.

The integration time has to be carefully chosen because it defines, for example, the overall intensities of the images taken. The complete RLD acquisition process typically takes three times the integration time. The RLD imaging parameters are summarized in Table 6.2.

**Table 6.2.** Basic settings for luminescence lifetime imaging according to the RLD scheme displayed in Figure 2.7.

|  | Excitation (μs) | Gate width (μs) | $t_1$ (μs) | $t_2$ (μs) | Integration time (ms) |
|---|---|---|---|---|---|
| [Ir(ppy)$_2$(carbac)] (T) | 5 | 1.4 | 0 | 0.7 | 150 |
| [Ir(btpy)$_3$] (barometric pressure) | 5 | 1 | 0 | 0.5 | 265 |

There are, however, two good reasons to use the RLD method: It is a fast method that also is hardly affected by the usual interferences in intensity measurements; secondly, we are not interested in exact lifetime values but rather in

their relative change to obtain an intrinsically referenced optical signal. Not the least, the results are highly reproducible and are not adversely affected by variations in the intensity of the excitation light. The sensing layer (with a sensing area of $3 \times 3$ cm) was mounted inside the calibration chamber. It can be calibrated at barometric pressures ranging from 50 to 2000 mbar. The temperature was adjusted using a Peltier element from 1 to 55 °C. The wavelength of the excitation light was 405 nm throughout all measurements.

The phosphorescence intensity and lifetime decrease with rising temperature. This is also referred to as thermal quenching.[11] The results of the temperature calibration from 1 – 54 °C are shown in Figure 6.6. The T-sensitive probe displayed almost no cross-sensitivity towards barometric pressure in the range from 50 to 1950 mbar.
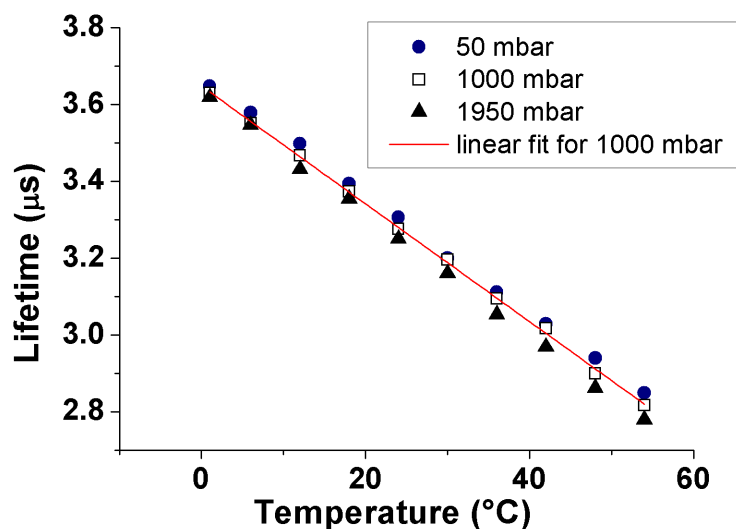


**Figure 6.6**. Temperature dependency of the luminescence lifetime of [Ir(ppy)$_2$(carbac)] in PAN micro-particles with linear fit for 1000 mbar air pressure.

The pressure dependency of the temperature probe is displayed in Figure 6.7. Unlike for other temperature sensors,[3,38,39] its calibration plot is linear over a rather wide temperature range, with a correlation coefficient $R^2$ of 0.999. The temperature coefficient of the decay time is 0.42 %/°C. There are various temperature sensors for imaging applications described in the literature, for example based on Eu(III) or Ru(II)

complexes[3,4,38] with somewhat higher temperature coefficients, but these display also much higher cross-sensitivities towards oxygen.
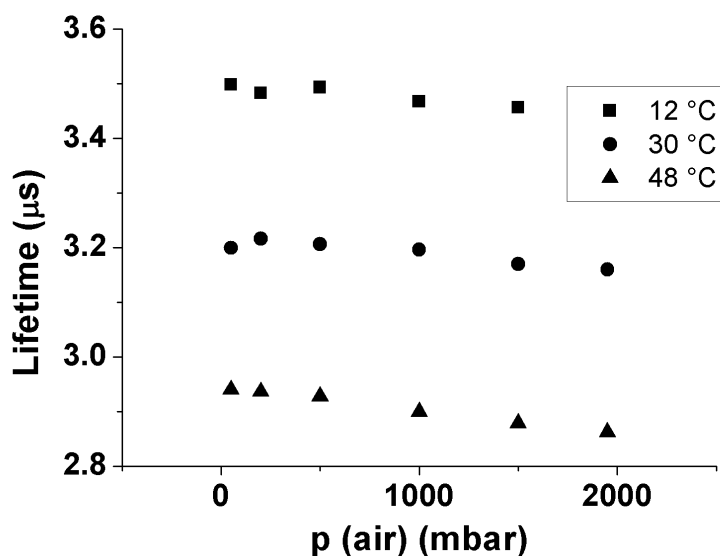


**Figure 6.7**. Pressure dependency of the luminescence lifetime of [Ir(ppy)$_2$(carbac)] in PAN micro-particles.

The quenching of the lifetime and the intensity of the luminescence of the oxygen probe Ir(btpy)$_3$ is due to collisional quenching by oxygen and can be described by the Stern-Volmer equation. The deviation from linearity is described by the so called "two site model":[11]

$$\frac{I}{I_0} = \frac{\tau}{\tau_0} = \frac{f_1}{1 + K^1_{SV}[Q]} + \frac{f_2}{1 + K^2_{SV}[Q]} \qquad \text{eq. 6.1}$$

Figure 6.8 gives lifetime calibration plots at various temperatures. Such plots do not reveal whether quenching follows Stern-Volmer (SV) kinetics. Therefore, SV plots were generated as shown in Figure 6.9. The standard deviation of the lifetimes (<4%) is not really significant. SV constants and correlation coefficients ($R^2$) are summarized in Table 6.3.
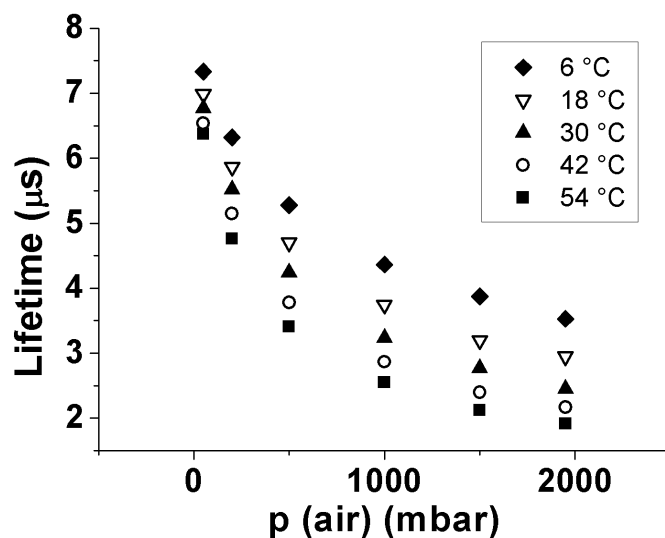
**Figure 6.8.** Pressure dependency at various temperatures of the phosphorescence lifetime of [Ir(btpy)$_3$] dissolved in a CAB film (thickness 6 μm).
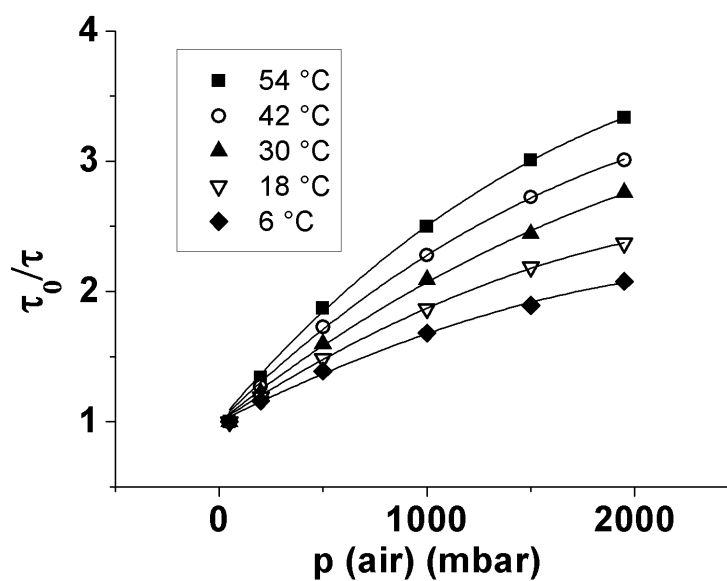


**Figure 6.9.** Stern-Volmer plots of the quenching, at various temperatures, by oxygen (expressed as air pressure) of the emission of [Ir(btpy)$_3$] dissolved in CAB polymer.

**Table 6.3.** Stern-Volmer constants ($K_{SV}$; in $10^{-4}$ mbar$^{-1}$) of the quenching of the luminescence of [Ir(btpy)$_3$] in CAB calculated from the fits in Figure 9 according the two site model. Fitting parameters were set to $f_1 = 0.9$ and $f_2 = 0.1$.

| T [°C] | $K^1_{SV}$ [$10^{-4}$ mbar$^{-1}$] | $K^2_{SV}$ [$10^{-4}$ mbar$^{-1}$] | $R^2$ |
|---|---|---|---|
| 54 | 21.2 ± 0.9 | -1.0 ± 0.3 | 0.997 |
| 42 | 17.6 ± 0.7 | -1.1 ± 0.3 | 0.997 |
| 30 | 14.2 ± 0.6 | -1.0 ± 0.3 | 0.997 |
| 18 | 11.7 ± 0.4 | -1.6 ± 0.2 | 0.998 |
| 6 | 9 ± 0.8 | -1.8 ± 0.3 | 0.996 |

## 6.2.4   Discussion

The metal-ligand complex (MLC) [Ir(ppy)$_2$(carbac)] is found to be a very useful luminescent probe for T. Dissolved in polyacrylonitrile polymer, its luminescence lifetime is linear over a large range and displays a remarkably low cross sensitivity towards oxygen. While several probes for T described before[3,4,38] have higher temperature coefficients, these also suffer from a much stronger cross-sensitivity to oxygen or barometric pressure. The fairly narrow emission band of [Ir(ppy)$_2$(carbac)] peaks at 521 nm, and this facilitates its spectral separation from the luminescence of the oxygen sensitive probe emitting in the deep red. The [Ir(btpy)$_3$] complex is shown to be a viable probe for oxygen and barometric pressure. Dissolved in the polymer CAB it covers a pressure range from 0 up to 2000 mbar if not more. It is possible to reduce the cross-sensitivity of this probe towards T by employing fluoroacrylic matrix polymers like FIB,[18,23] albeit at the expense of a smaller dynamic range.[4] Established oxygen probes such as Pt[5,10,15,20-tetra-(pentafluorophenyl) porphyrin] (PtTFPP)[3,38] are more sensitive to oxygen but have distinctly smaller dynamic ranges when used in comparable matrix polymers. The dynamic range of PtTFPP may be extended to about 1000 mbar barometric pressure by applying less permeable matrices, but then its temperature dependence becomes distinctly higher[3] compared to the [Ir(btpy)$_3$]/CAB sensor system.

## 6.3    Conclusion

A novel dual p (air)/T sensor system was prepared. It consits of two different iridium complexes as luminescent indicators. These indicators are incorporated into two different polymer matrices controlling the dynamic range, the sensitivity, and to avoid interferences. The sensor was calibrated using the RLD method for imaging. The signals for barometric pressure and temperature can be separated by optical filters. The homogeneity of the sensor layer along with the benefits of the intrinsically referenced lifetime imaging provides highly accurate and simultaneous determination of barometric pressure and temperature at a very high spatial resolution. The results obtained at the calibration of this new sensor system are very promising for future applications in fluid mechanics as dual one layer PSP/TSP.

## 6.4    Experimental

**Materials**. All synthesis procedures were performed under an atmosphere of dry argon by employing usual Schlenk techniques. Solvents were carefully dried and distilled from appropriate drying agents prior to use. Commercially available reagents were used without further purification unless otherwise stated. 2-Phenylpyridine, *N,N*-dimethylformamide, tetrahydrofuran, [*tris*[2-(benzo[b]thiophen-2-yl)pyridinato-$C^3$,N]iridium(III)] [Ir(btpy)$_3$], poly(vinyl alcohol), cellulose acetobytorate (CAB), and titanium dioxide were purchased from Sigma-Aldrich (www.sigmaaldrich.com). IrCl$_3$ × $n$H$_2$O, 2-ethoxyethanol and pinacolone were purchased from ABCR (www.abcr.de). Ethyl bromoacetate, sodium hydride and 9*H*-carbazole were purchased from Acros (www.acros.com). Poly(acrylonitrile) was purchased from Polysciences (www.polysciences.com), Elastosil A07 silicone from Wacker (www.wacker.com), PET foil (Mylar®) from Goodfellow (www.goodfellow.com).

**Instrumentation and Methods**. $^1$H NMR and $^{13}$C NMR spectra were acquired on a Bruker ARX 400, (www.bruker.com) chemical shifts are given relative to the internal standard tetramethylsilane (Me$_4$Si) in CDCl$_3$ solutions. Chemical shifts in NMR spectra are given in Hertz (Hz; s = singlet, d = doublet, t = triplet, q = quartet, and m = multiplet). Fourier transform infrared (FT-IR) spectra were recorded on a Jasco FT/IR-4200

Fourier transform spectrometer (www.jasco.de). The UV-vis spectra were measured with a JASCO V-550 UV-vis spectrophotometer (www.jasco.de; 1 cm cuvettes, $CHCl_3$) at concentrations of about $1 \times 10^{-5}$ mol/L. The emission spectra were performed using a CARY Eclipse fluorescence spectrophotometer (www.varianinc.com) at concentrations of about $1 \times 10^{-5}$ mol/L. Thermogravimetric analysis (TGA) was performed on a Mettler Toledo TGA/DSC STAR System (www.mettler-toledo.de; heating rate: 10 K/min; argon; $T_d$ @ 5% weight loss). Mass spectra were obtained using a Varian MAT 311 instrument (www.varianinc.com) with an electrospray source (ESI-MS), a Voyager-DE PRO Biospectrometry (www.appliedbiosystems.com; MALDI-TOFMS) and a microTOF instrument from Bruker Daltonik (Bremen, Germany; www.bruker.de) equipped with a multi-purpose ion source (MPIS)[41] made by the machine shop at the University of Wuppertal. In this case the APLI method was used as ionization technique.[40,41] Elemental analyses (EA) were performed on a Perkin Elmer 240 B setup.

**Synthetic methods**.

*Synthesis of PAN micro-particles containing [Ir(ppy)₂(carbac)].*

200 mg of PAN were dissolved in 40 mL of *N,N*-dimethylformamide (DMF). after the polymer was fully dissolved, 7 mg of [Ir(ppy)₂(carbac)] were added to the solution. 140 mL of double distilled water were added dropwise under vigorous stirring of the solution. The precipitated micro-particles were centrifuged and washed with water four times. They were then dispersed in double distilled water and were subsequently freeze dried. Prior to use in the dual sensor the micro-particles were washed three times with ethanol and three times with THF, dispersed in double distilled water and freeze dried again.

**Experimental setup for sensor calibration**. Absorption and emission spectra were recorded on a Lambda 14p Perkin-Elmer UV-vis spectrophotometer (Waltham, MA, USA, www.perkinelmer.com) and an Aminco AB 2 luminescence spectrometer (Thermo Scientific Inc., Waltham, MA, USA, www.thermo.com), respectively. The *p/T* calibration chamber was provided by the German Aerospace Center (DLR) in Göttingen. All time-resolved measurements were performed with a PCO SensiCam 12 bit b/w CCD camera (PCO, Kelheim, Germany, www.pco.de) equipped with a Schneider-Kreuznach

Xenon 0.95/17 lens (Jos. Schneider Optische Werke, Bad Kreuznach, Germany, www.schneiderkreuznach.com) and a 405-66-60 405nm LED from Roithner Lasertechnik (Vienna, Austria, www.roithner-laser.com). The excitation light was focused by a PCX 18_18 MgF2 TS lens from Edmund Optics (Karlsruhe, Germany, www.edmundoptics.com). It was filtered through a BG 12 filter (Schott, Mainz, Germany, www.schott.com) with a thickness of 2 mm. Emission was detected through a BP 530/50 band pass filter and a RG 610 high pass filter purchased from AHF Analysentechnik (www.ahf.de).

## 6.5    References

[1]     Y.Amaoa, Y. Ishikawa, and I. Okura, *Anal. Chim. Acta* **2001**, *445*, 177-182.

[2]     K. Mitsuo, K. Asai, A. Takahashi, and H. Mizushima, *Meas. Sci. Technol.* **2006**, *17*, 1282-1219.

[3]     M. I. Stich, S. Nagl, O. S. Wolfbeis, U. Henne, and M. Schaeferling, *Adv. Funct. Matter* **2008**, *18*, 1399-1406.

[4]     B. Zelelow, G. E. Kahlil, G. Phelan, B. Carlson, M. Gouterman, J. B. Callis, and L. R. Dalton, *Sens. Actuat. B* **2003**, *B96*, 304-314.

[5]     G. E. Khalil, A. Chang, M. Gouterman, J. B. Callis, L. R. Dalton, N. J. Turro, S. Jockusch, *Rev. Sci. Instrum.* **2005**, *76*, 054101-1-8.

[6]     J. I. Peterson, R. V. Fitzgerald, *Anal. Chem.* **1984**, *56*, 62-67.

[7]     G. B. Hocker, *Appl. Opt.* **1979**, *18*, 1445-1448.

[8]     X. Lu, I. Manners, M. A. Winnik, in *New Trends in Fluorescence Spectroscopy*, (Eds.: B. Valeur, J.-C. Brochon), Springer, Berlin, **2001,** pp. 229-254.

[9]     J.W. Holmes, *J. Fluoresc.* **1993**, *3*, 179-183.

[10]    R. H. Engler, C. Klein, O. Trinks, *Meas. Sci. Technol.* **2000**, *11*, 1077-1085.

[11]    J. H. Bell, E. T. Schairer, L. A. Hand, R. D. Mehta, *Annu. Rev. Fluid Mech.* **2001**, *33*, 155-206.

[12]    M. A. Woodmansee, J.C. Dutton, *Exp. Fluids* **1998**, *24*, 163-174.

[13]    J. Hradil, C. Davis, K. Mongey, C. McDonagh, B. D. MacCraith, *Meas. Sci. Technol.* **2002**, *13*, 1552-1557.

[14]    K. Nakakita, M. Kurita, K. Mitsuo, S. Watanabe, *Meas. Sci. Technol.* **2006**, *17*, 359-366.

[15]    M. Kameda, N. Tezuka, T. Hangai, K. Asai, K. Nakakita, Y. Amao, *Meas. Sci. Technol*. **2004**, *15*, 489-500.

[16]    S. Nagl, O. S. Wolfbeis, *Analyst* **2007**, *132*, 507-511.

[17]    M. E. Lippitsch, J. Pusterhofer, M. J. P. Leiner, O. S. Wolfbeis, *Anal. Chim. Acta* **1988**, *205*, 1-6.

[18]    M. I. Stich, O. S. Wolfbeis, *Fluorescence Sensing and Imaging Using Pressure-Sensitive Paints and Temperature-Sensitive Paints*, Springer, **2008**.

[19]    R. J. Woods, S. Scypinski, Love, L. J. Cline, H. A. Ashwoth, *Anal. Chem*. **1984**, *56*, 1395-1400.

[20]    S.-K. Lee, I. Okura, *Anal. Sci*. **1997**, *13*, 535-540.

[21]    S.-K. Lee, I. Okura, *Spectrochim. Acta A* **1998**, *54*, 91-100.

[22]    P. M. Gewehr, D. T. Delpy, *Med. Biol. Eng. Comput*. **1993**, *31*, 11-21.

[23]    E. Puklin, B. Carlson, S. Gouin, *J. Appl. Polym. Sci*. **1999**, *77*, 2795-2804.

[24]    R. C. Evans, P. Douglas, J. A. G. Williams, D. L. Rochester, J. Fluoresc. **2006**, *16*, 201-206.

[25]    M. Gouterman, J. Callis, L. Dalton, G. E. Khalil, Y. M´ebarki, *Meas. Sci. Technol*. **2004**, *15*, 1986-1994.

[26]    S. Grenoble, M. Gouterman, G. E. Khalil, *J. Lumin*. **2005**, *113*, 33-44.

[27]    A. Medina-Castillo, J. Fernandez-Sanchez, C. Klein, *Analyst* **2007**, *132*, 929-936.

[28]    S. M. Borisov, I. Klimant, *Anal. Chem.* **2007**, *79*, 7501-7590.

[29]    G. D. Marco, M. Lanza, M. Pieruccini, S. Campagna, *Adv. Mater.* **1996**, *7*, 576-580.

[30]    D. Di Marco, M. Lanza, A. Mamo, I. Stefio, C. Di Pietro, G. Romero and S. Campagna, *Anal. Chem*. **1998**, *70*, 5019-5023.

[31]    L. Huynh, J. Wang, V. Stoeva, A. Lough, I. Manners, M. A. Winnik, *Chem. Mater*. **2005**, *17*, 4765-4773.

[32]    E. Holder, B. M. W. Langeveld, U. S. Schubert *Adv. Mater.* **2005**, *17*, 1109-1121.

[33]    N. Tian, A. Thiessen, R. Schiewek, O. J. Schmitz, D. Hertel, K. Meerholz, E. Holder *J. Org. Chem.* **2009**, *74*, 2718-2725.

[34]    N. Rehmann, C. Ulbricht, A. Köhnen, P. Zacharias, M. C. Gather, D. Hertel, E. Holder, K. Meerholz, U. S. Schubert *Adv. Mater.* **2008**, *20*, 129-133.

[35]    J: F: Fernandez-Sanchez, T. Roth, R. Cannas, Md. K. Nazeeruddin, S. Spichiger, M. Graetzel, U. E. Spichiger-Keller, *Talanta* **2007**, *71*, 242-250.

[36]    J. Brandrup, E. H. Immergut, E. A. Grulke, *Polymer Handbook*, Wiley-VCH, **1999**.

[37]    C. Moore, S. P. Chan, J. N. Demas, B. A. DeGraff, *Appl. Spectrosc.* **2004**, *58*, 603-607.

[38]    M. E. Köse, B. F. Carroll, K. S. Schanze, *Langmuir* **2005**, *21*, 9121-9129.

[39]    G. E. Khalil, C. Costin, J. Crafton, G. Jones, S. Grenoble, M. Gouterman, J. B. Callis, L.R. Dalton, *Sens. Actuators B* **2004**, *97*, 13-21.

[40]    R. Schiewek, M. Lorenz, R. Giese, K. J. Brockmann, T. Benter, S. Gäb, O. J. Schmitz , *Anal. Bioanal. Chem.* **2008**, *329*, 87-96.

[41]    R. Schiewek, M. Schellenträger, R. Mönnikes, M. Lorenz, R. Giese, K. J. Brockmann, S. Gäb, T. Benter, O. J. Schmitz, *Anal. Chem.* **2007**, *79*, 4135-4140.

[42]    S. Lamansky, P. Djurovich, M. E. Thompson, *J. Am. Chem. Soc.* **2001**, *123*, 4304-4312.

[43]    J. I. Kim, I. S. Shin, H. Kim, J. K. Lee, *J. Am. Chem. Soc.* **2005**, *127*, 1614-1615.

# Chapter 7

# Dual Sensing of $p\mathrm{O_2}$ and Temperature Using a Water-Based and Sprayable Fluorescent Paint

**Summary:** Core-shell particles (NPs) composed of a polystyrene core and a poly(vinyl pyrrolidone) shell were dyed with a luminescent platinum(II) porphyrin probe for oxygen. In parallel, microparticles were dyed with a luminescent iridium(III) complex acting as a probe for temperature. The particles were deposited (by spraying) on a surface to enable continuous imaging of the distribution of oxygen (and thus of barometric pressure) and temperature. Unlike most previous paints of this kind, a binder polymer is not needed and water can be used as a dispersant. This makes the paint environmentally friendly and reduces costs in terms of occupational health, clean-up, and disposal. Both indicator probes in the sensor paint can be excited at 405 nm using LEDs or diode lasers, whilst their emission maxima are spectrally separated by about 130 nm. Thus, two independent optical signals are obtained that allow for fluorescent imaging of barometric pressure (in fact oxygen partial pressure) and of temperature, but also to correct the oxygen signal for effects of temperature. The paint was calibrated at air pressures ranging from 50 mbar to 2000 mbar and at temperatures between 1 °C and 50 °C.

## 7.1    Introduction

Pressure and temperature sensitive paints usually are based on volatile and toxic organic solvents (often in large quantities) which causes a substantial effort in terms of clean up and respiratory protection. Also, the level of toxic vapors in test facilities allowed by the Occupational Safety and Health Administration can be heavily exceeded by using such "regular" paints [1]. The use of water soluble paints or aqueous dispersions therefore would represent a highly attractive alternative.

PSPs and TSPs usually consist of a luminescent compound embedded in a polymer matrix [2,3]. The most important factor governing the response characteristics of the probes is the gas permeability of the matrix. Obviously, the matrices for pressure and temperature sensing have to be different in order to achieve optimized sensitivity with respect to the desired dynamic range. Especially the temperature probe has to be shielded from undesired oxygen quenching by applying a very gas impermeable matrix polymer. This of course does not apply for thermographic phosphors which can be used instead of dye-based temperature probes and show virtually no cross-sensitivity to oxygen. Simultaneous imaging of p and T is particularly practicable if particles are being used because this facilitates the adjustment of the ratio of probes, prevents fluorescence energy transfer to occur (which is highly undesirable), and prevents the leakage of the probes into their (micro)environment like the surface of the sensor film or into other adjacent matrices (e.g. the base coat). In contrast to the few previously reported water-based PSPs [1, 4] neither dissolved nor emulsified binders have been used.

Here we report on a water-based sprayable dual sensitive paint for lifetime imaging of p and T on aircraft models in subsonic wind tunnel tests (max. wind speed = 100 m/s). It consists of an aqueous dispersion of two different kinds of well accessible polymer particles that are dyed with appropriate luminescent probes. The resulting sensor paint not only possesses the advantages of being an aqueous paint, but also shows remarkable sensing ranges and response.

## 7.2    Results

### 7.2.1    Sensor Composition

The PSP presented here consists of commercially available poly(styrene)-poly(vinyl pyrrolidone) (PS-PVP) spherical core-shell particles (NPs) with an average size of 240 nm [5] that contain the platinum complex of 5,10,15,20-tetrakis(2,3,4,5,6-pentafluorophenyl)porphyrin (referred to as PtTFPP) which acts as the oxygen (pressure) sensitive probe. The particles were dyed in a simple manner reported previously [6]. Briefly, the beads are swollen in the presence of tetrahydrofurane (THF) and the lipophilic oxygen indicator is added. The dye is incorporated in the core of the beads when THF is removed under reduced pressure. A brightly luminescent iridium complex (referred to as Ir(ppy)$_2$carbac) was used as the probe for T. It was incopoprated into microparticles of poly(acrylonitrile) (PAN) with an average size of 1 µm. PAN microparticles are easily prepared and virtually impermeable to oxygen. Thus, almost no quenching by oxygen is observed. The chemical structures of the two probes are given in Figure 7.1.



**A**                                                 **B**
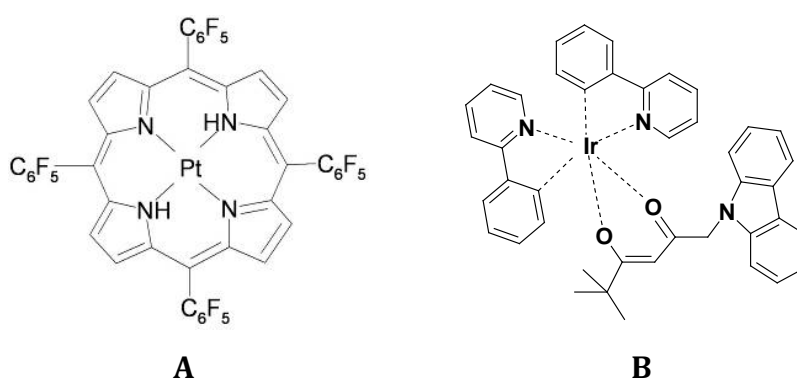
**Figure 7.1**. Chemical structures of the oxygen probe PtTFPP (A) and of the temperature probe Ir(ppy)$_2$carbac (B).

### 7.2.2    Properties of the Paint

The PS-PVP core-shell particles display good adhesion on various surfaces including metals, glass, plastic etc. Excellent adhesion on aluminum is particularly important in context with imaging barometric pressure because this material is widely

used to model aircrafts. We check the adhesion with the so called "Scotch test" were a Scotch® -tape is glued onto the paint and stripped of. In case of this paint no visible destruction was observed which is a sign that the adhesion is definitely sufficient for a subsonic wind tunnel test. Dispersions of such NPs were prepared in concentrations ranging from 10 to 30 % (w/w) in water. Homogeneous films are obtained after drying. The PAN microparticles for temperature imaging are dispersed together with the PS-PVP particles and thus are incorporated in the resulting layer (see Figure7.2). For the paint presented here we used a 10% w/w dispersion of the PS-PVP beads charged with 15 mg of the PAN particles per mL dispersion. We obtained films with a thickness of circa 10 - 15 μm.
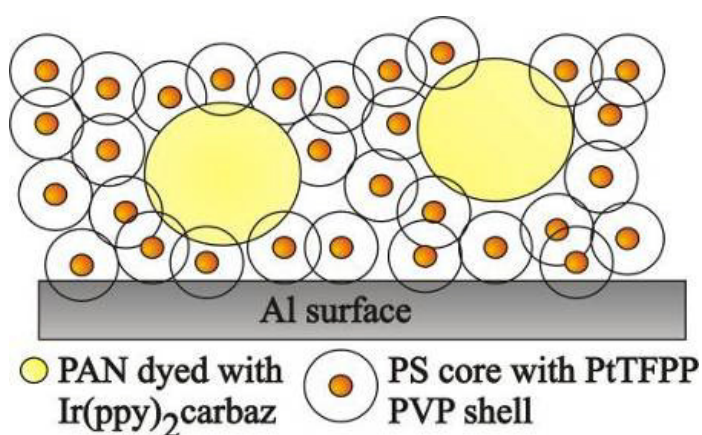


**Figure 7.2.** Schematic of the dually sensitive layer. The poly(styrene)/poly(vinyl pyrrolidone) (PS-PVP) particles dyed with the oxygen probe PtTFPP form a homogeneous film that adheres good to the surface. The poly(acrylonitrile) (PAN) microparticles containing the temperature probe Ir(ppy)$_2$carbac are then dispersed in the layer of PS/PVP particles.
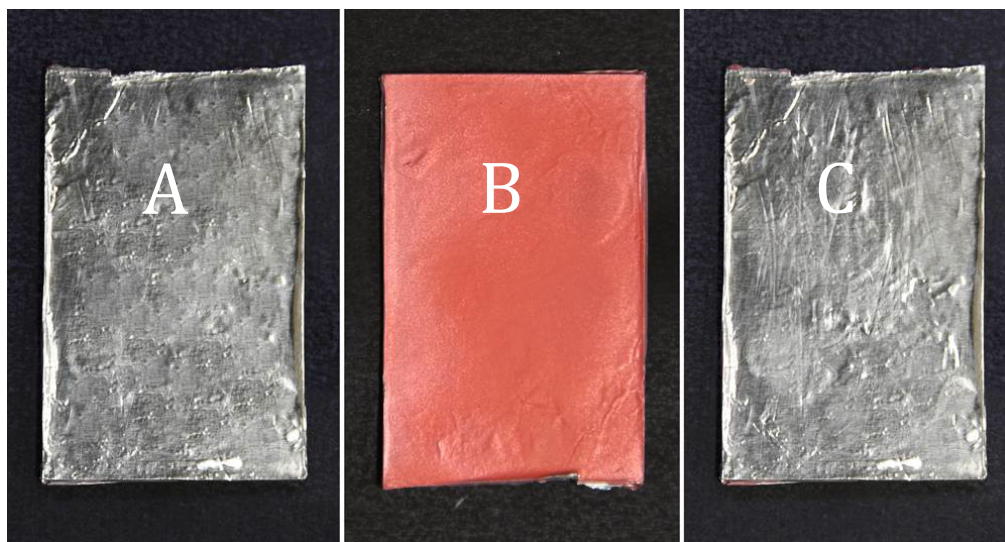
**Figure 7.3.** Images of the aluminum foil before and after coating and washing. (A) before spraying it with the PS-PVP particles; (B) after spraying it with the red paint (dyed with PtTFPP), and (C) after removing the red paint with water.

The sensing layer produced by spraying possesses excellent mechanical stability. Unlike the two previously reported water-based paints , the PSP/TSP presented here can be easily removed from the surface with plain water (see Figure 7.3). The paint also can be reused by collecting the washing water and concentrating it to the desired concentration. This is a most welcome feature and distinguishes this method from others, albeit not dual sensors [1,4]. In fact, these rely on polymerizable compositions with binders that cannot be easily removed.

Figure 7.4 shows an SEM image of the sensor paint containing the oxygen-sensitive beads only. The particles are not densely packed and are well separated. The channels and cavities formed between the individual beads promote fast diffusion of the gas and consequently fast response of the paint to alteration of pressure. The response time is too fast ( <1s) to be determined with our system.
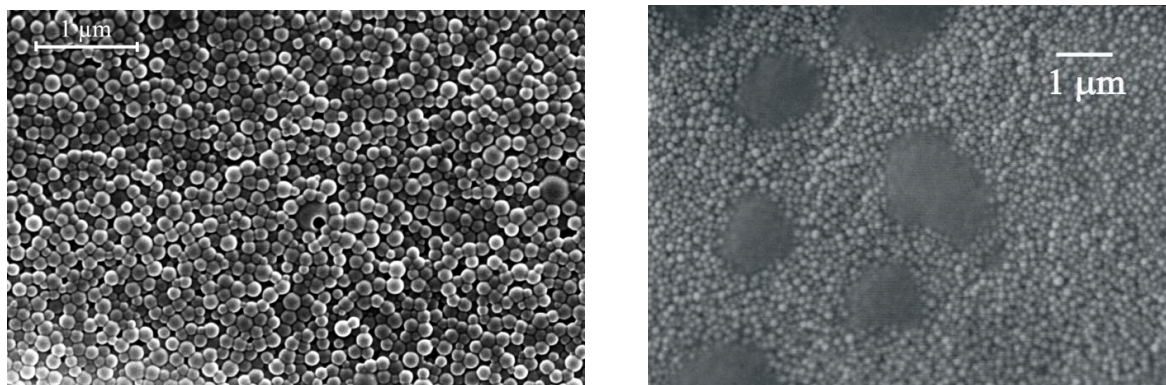
**Figure 7.4.** Scanning Electron microscopy image of (a) the paint based on PtTFPP/PS-PVP beads and (b) of the dual sensitive paint with the (much larger) PAN particles incorporated into the film of PtTFPP/PS-PVP beads.

### 7.2.3   Signal Separation

The luminescence signals for p and T can be separated by optical filters because the two probes have different emission wavelengths. The emission of Ir(ppy)$_2$carbac peaks at 519 nm, that of PtTFPP at 658 mn. The luminescence of Ir(ppy)$_2$carbac is acquired by using a bandpass filter with a 530-nm center wavelength and a 50 nm spectral band width. The barometric signal of the probe PtTFPP was isolated with a second bandpass filter (type BP 680/60). The spectral properties of the dual sensor system are displayed in Figure 7.5.
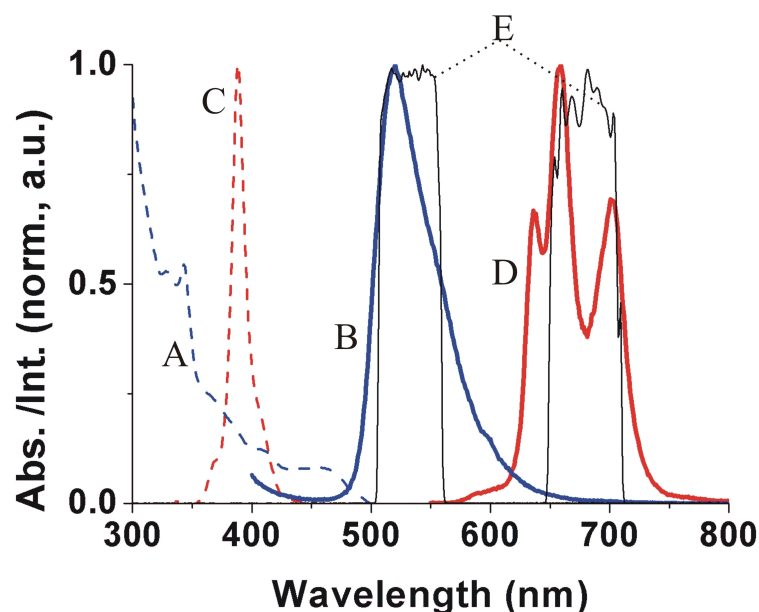
**Figure 7.5.** Absorption and emission spectra of the sensor system. (A) absorption and (B) emission of Ir(ppy)$_2$carbac; (C) absorbance and (D) emission of PtTFPP. (E) Transmittance of the two optical bandpass filters.

### 7.2.4    Data Acquisition

The work function of the sensor was established using time-gated data which were obtained using the RLD method [7,8]. Rather than collecting data at a single point, the data of the whole sensing area were recorded with a CCD camera to yield images of the distribution of pressure and temperature. The luminescence of the dual sensor layer was excited with a 405-nm light pulse from a LED light source. The decay time of the luminescence of PtTFPP ranges from 55 µs at 50 mbar air pressure to 10 µs at 1950 mbar air pressure, that of the iridium complex from 2.6 µs at 1 °C to 1.9 µs at 54 °C. Almost ideally square shaped light pulses can be created with LED light sources in the µs scale.[9] Following photo-excitation, the luminescence intensity was recorded in two precisely timed gates using a triggered CCD camera, this is followed by a dark image that is needed for substraction of dark current (background).[7] Instead of utilizing the luminescence intensities as sensor signal we prefer to use the ratio of the intensities in gate 1 devided by gate 2. The resulting signal consequently is internally referenced and no reference dye is needed. The typical standard deviations for such measurements are

below 4%. A diagramm of the RLD method is given in Figure 2.7. The RLD imaging parameters applied in this work are summarized in Table 7.1.

**Table 7.1.** Basic settings for luminescence lifetime imaging according to the RLD scheme.

| Probe | Excitation pulse width ($\mu$s) | Gate width ($\mu$s) | $t_1$ ($\mu$s) | $t_2$ ($\mu$s) |
|---|---|---|---|---|
| Ir(ppy)$_2$(carbac) | 5 | 1.4 | 0 | 0.7 |
| PtTFPP | 10 | 10 | 0 | 5 |

The RLD method assumes the luminescence decay profile to be mono-exponential. While this is not totally valid in case of the two kinds of particle probes used here, this assumption is justified because the intention here is to rapidly image any changes in T or barometric pressure, rather than the determination of precise (multiple) decay times of probes. The RLD method is fast, intrinsically referenced, and hardly affected by the sources of error sources as listed before. Indeed, we find the results to be highly reproducible and not to be adversely affected by variations in the intensity of the excitation light.

The sensing area typically investigated is 3x3 cm in size, with the paint deposited on an respective aluminum plate mounted inside a calibration chamber where pressure (barometric pressure) can be adjusted to between 50 and 2000 mbar. A temperature-sensing Peltier element in the chamber enables temperatures to be adjusted to values between 1 and 55 °C. Photoexcitation and optical readout are performed from top through a window in the chamber.[7]

### 7.2.5    Response of the Dually Sensitive Paint to Oxygen (Barometric Pressure)

The luminescence decay time of PtTFPP decreases with rising oxygen partial pressure because oxygen acts as a dynamic quencher of luminescence (in terms of intensity and decay time). For situations like the one here (where probes are located in

different microenvironments in the polymer), the Stern-Volmer equation in the form of the so-called "two-site" model [2] is well suited to describe this effect (see eq. 6.1). The lifetimes were normalized to $\tau_0$ at the lowest pressure (50 mbar) for each temperature. The resulting Stern-Volmer plots together with the respective two-site fits are given in Figure 7.6. For calculating the fits according to the two-site model, $f_1$ was set to 0.9 and $f_2$ was set to 0.1. Table 7.2 summarizes the fit parameters.
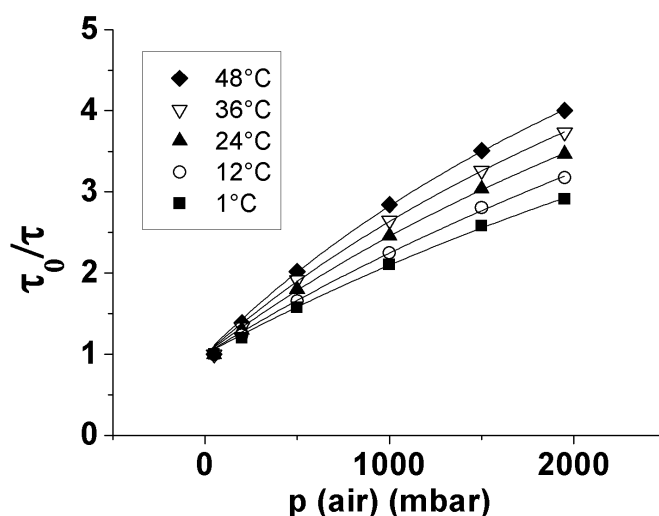


**Figure 7.6.** Stern-Volmer plots of the quenching of the emission of PtTFPP in PS-PVP core-shell particles by oxygen (expressed as air pressure) at various temperatures.

**Table 7.2.** Stern-Volmer constants ($K_{SV}$; in $10^{-4}$ mbar$^{-1}$; mbar refer to air pressure) of the quenching of the luminescence of PtTFPP calculated from the fits according to the two-site model in Figure 6. Fitting parameters $f_1$ and $f_2$ were set to 0.9 and 0.1, respectively.

| T [°C] | $K^1_{SV}$ [$10^{-4}$ mbar$^{-1}$] | $K^2_{SV}$ [$10^{-4}$ mbar$^{-1}$] | $R^2$ |
|---|---|---|---|
| 1 | 13.8 ± 0.8 | 0.11 ± 0.65 | 0.997 |
| 12 | 15.8 ± 0.9 | 0.15± 0.72 | 0.997 |
| 24 | 19.1 ± 0.9 | 0.14 ± 0.48 | 0.998 |
| 36 | 22.1 ± 0.9 | 0.12 ± 0.47 | 0.997 |
| 48 | 25.3± 0.8 | 0.15 ± 0.45 | 0.997 |

The imaging of oxygen partial pressure is demonstrated in Figure 7.7. The ratio images ($A_1/A_2$) of an area of circa 2 x 1.5 cm are depicted as false colour pictures at 30 °C and different air pressures.
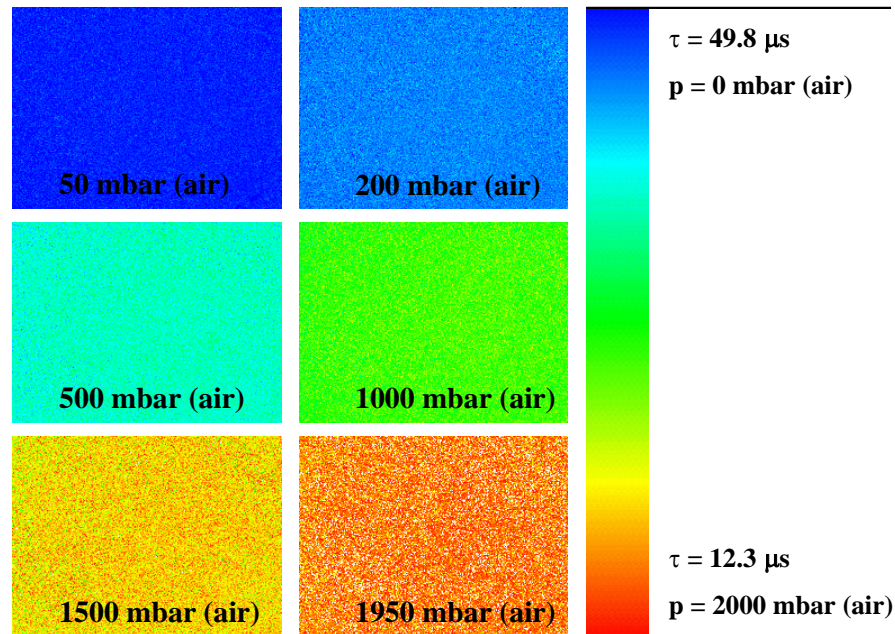


**Figure 7.7.** Ratio images ($A_1/A_2$) of the PSP in the dual sensitive paint at a temperature of 30 °C and at different air pressures.

The influence of humidity of the gas phase on the response of the PSP is very small in general. The humidity in a regular wind tunnel test facility will not have any noteworthy influence on the luminescence lifetime of the PSP. For further details please see the supporting informations to this article.

### 7.2.6    Pesponse of the Dually Sensitive Paint to Temperature

The calibration of the TSP was performed at six different pressures between 50 mbar and 2000 mbar. The resulting plots are given in Figure 7.8. Only the calibration curves at the lowest and the highest pressure are displayed for clarity reasons. The

temperature dependency of the luminescence of Ir(ppy)$_2$carbac is linear over a wide temperature range. The temperature coefficient of the TSP in the dual sensor is 0.01 µs (τ)/°C. The cross-sensitivity towards the air pressure is 0.02 x10$^{-3}$ µs (τ) /mbar (air pressure).
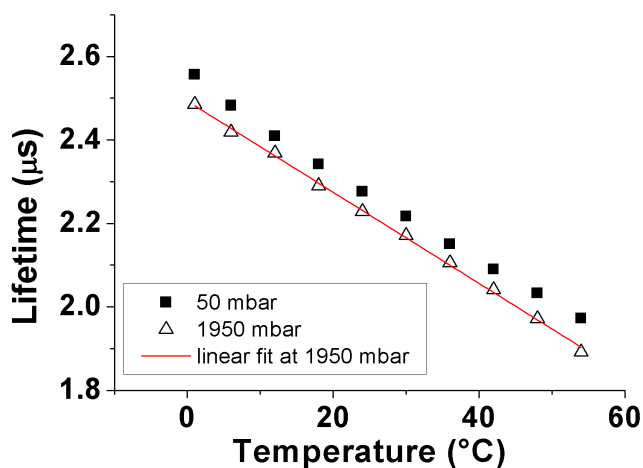


**Figure 7.8.** Temperature dependency of the luminescence lifetime of Ir(ppy)$_2$carbac in PAN micro particles in the dual sensor with linear fit at 1950 mbar air pressure.

### 7.2.7    Data Evaluation

Under operational conditions the data does of course not coincide with the data points of the calibration. For that purpose the calibration data of the paint were plotted in 3D and fitted with a polynomial surface equation (see Figure 7.9). This was done with software called *TableCurve 3D v3.12* according the "Renka II" algorithm.[10,11]
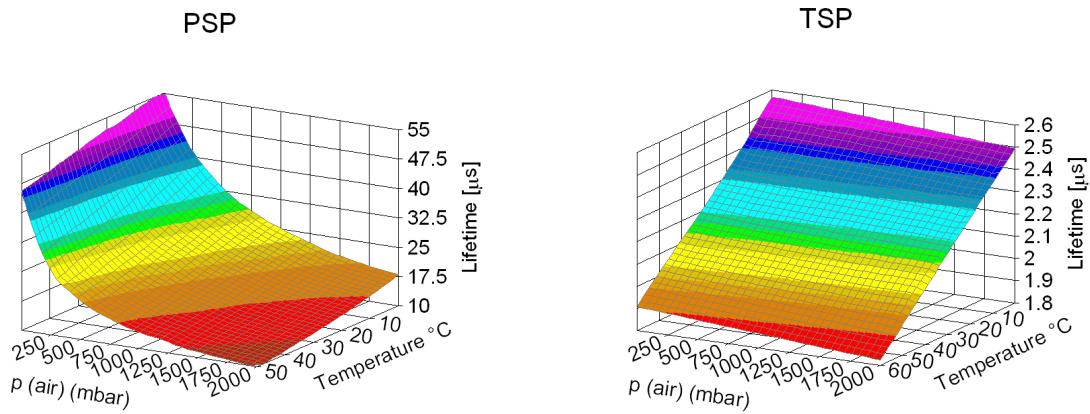
**Figure 7.9.** The 3D surface plot of the PSP and TSP used for data evaluation of random data points.

Specifically, two lifetime values are obtained at any random data point, one for the PSP and one for the TSP. Step one then is to chose a realistic pressure value and calculating the according temperature using the TSP surface plot. In a second step, the PSP lifetime and the temperature value of step 1 are applied to calculate the according pressure with the PSP surface plot. Step one is repeated with the pressure value calculated in step two. Two iterations usually are adequate to determine air pressure and temperature with excellent precision. An example:

Random lifetime values: TSP = 2.2 µs, PSP = 17.4 µs

| Iteration step # | Temperature °C | Air pressure (mbar) | Lifetime (µs) |
|---|---|---|---|
| 1 (TSP) | 28.8 | 1000 | 2.2 |
| 2 (PSP) | 28.8 | 1065 | 17.4 |
| 1 (TSP) | 28.7 | 1065 | 2.2 |
| 2 (PSP) | 28.7 | 1068 | 17.4 |

## 7.2.8    Effect of Humidity

The luminescence of the paint is barely influenced by the humidity of the gas phase. This was proven by applying humid gas mixtures that first were humidified by bubbling them through water. The results were compared with the data obtained with

dry mixtures (Figure 7.10). The lifetime values in this experiment were obtained by phase domain spectroscopy and thus slightly deviate from the values obtained with the RLD method.
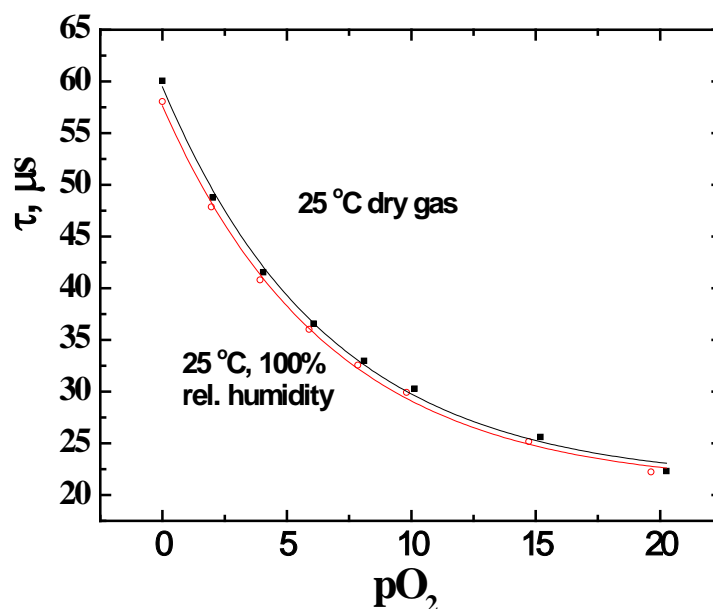


**Figure 7.10.** The oxygen dependence of the luminescence lifetime of PtTFPP in PS-PVP beads acquired in the frequency domain (modulation frequency f = 5kHz). ~ 100% humidity was achieved by bubbling the gas mixtures through a water bottle.

## 7.3    Discussion

As a matter of fact, each and any sensor is sensitive to temperature. Hence, the TSP is not only needed to visualize the temperature distribution but also to correct for the effect of the temperature on the PSP.[12] The temperature probe in turn, has to be shielded from undesired quenching by oxygen. This is achieved by incorporating it into microparticles with very low gas permeability and solubility for oxygen. In this case we used poly(acrylonitrile) (PAN).[13]

The response of the PSP composed of PtTFPP incorporated in the PS-PVP core-shell particles covers the range from 0 to 2000 mbar of air pressure and is perfectly suited for wind tunnel applications. PtTFPP is a popular oxygen probe that has already

been used in various polymer matrices.[14-17] On the one hand, the cross sensitivity towards the temperature can be minimized to a certain extent by using fluoroacrylic polymers like FIB as the matrix.[16] Such materials show oxygen permeabilities that are magnitudes higher compared to PS and PVP. The outcome is a much smaller dynamic range of the PSP [18], meaning the luminescence is almost fully quenched at very low air pressures, which lowers the pressure resolution of the sensor when it comes to pressure values relevant for aerodynamic research. On the other hand, if PtTFPP is applied in a polymer film (e.g. PSAN) that is less oxygen permeable, the dynamic range can be stretched to the same extent as for the PS-PVP core-shell particles. The drawback of using such a matrix material is the resulting higher cross sensitivity towards temperature [19]. Virtually any lipophilic oxygen indicator can be incorporated into PS-PVP beads [6] so that the sensitivity of the resulted pressure-sensitive paint can be tuned over a wide range. Particularly, materials having higher sensitivity are obtained using the corresponding palladium(II) complexes, while those with lower sensitivity can be based on ruthenium(II) polypyridyl complexes and iridium(III) cyclometallated coumarin complexes. Spectral properties can also be tuned over a wide range because NIR-emitting indicators such as metal complexes of porphyrin-ketones[20], meso-porphyrin lactones[21] and tetraphenyl tetrabenzoporphyrins[22] also can be incorporated into PS-PVP beads.

The luminescence of Ir(ppy)$_2$carbac shows a linear temperature dependency over the full range from 1 °C to 55 °C. It is assumed that the probe may also be used for values outside this range. In contrast, most TSPs show nonlinear temperature dependencies making the data evaluation and fitting less convenient.[19,23,24] The TSP exhibited a remarkably low cross sensitivity towards the air pressure. Other TSPs may have higher temperature coefficients but these also display higher cross sensitivities towards oxygen.[19,18,23] Thermographic phosphors such as Mg$_4$FGeO$_6$:Mn$^{4+}$;[25] Y$_3$Al$_5$O$_{12}$:Cr$^{3+}$,[26] ruby [27], as well as La$_2$O$_2$S:Eu [28,29] can also be used.[30] These show virtually no cross-sensitivtiy to oxygen but neither possess high sensitivity nor brightness. The thermographic phosphors usually are prepared in form of micrometer-sized particles which are subsequently entrapped into a PS-PVP layer.

## 7.4      Conclusion

The dye-doped core-shell particles presented here for imaging of oxygen partial pressure (and thus barometric pressure) show excellent adhesion on aluminum, and its aqueous dispersions can be homogeneously sprayed onto such surfaces. The resulting films are of high mechanical stability and thus can function as binder for additional beads. The water based dual sensitive paint for p and T presented here consists exclusively of PS-PVP core-shell particles and poly(acrylonitrile) micro particles without any dissolved binder. Besides the advantages of an aqueous paint like lower health risks for users and environmentally friendly application the paint can be easily removed with plain water. The paint has excellent sensing characteristics for both p and T over the areas of practical interest. The paint can be interrogated by the RLD method which provides all the benefits of an intrinsically referenced imaging method.

## 7.5      Experimental

### Materials

Poly(acrylonitrile) (PAN) was purchased from Polysciences ([www.Polysciences.com](www.Polysciences.com)), PtTFPP from Porphyrin Systems ([www.porphyrin-systems.de](www.porphyrin-systems.de)), and *N,N*-dimethylformamide (DMF) poly(styrene-block-vinylpyrrolidone) dispersion in water (38% w/w) from Sigma-Aldrich ([www.sigmaaldrich.com](www.sigmaaldrich.com)). The temperature-sensitive probe di(2-phenylpyridinato-C2,N)-Iridium(III) (Ir(ppy)$_2$carbac) was synthesized according to ref. [31].

### Synthesis of Sensor Particles

*Polyacrylonitrile (PAN) microparticles doped with [Ir(ppy)$_2$(carbac)].*
200 mg of PAN were dissolved in 40 mL of *N,N*-dimethylformamide (DMF) at 55 °C. After the polymer was fully dissolved (30 min), 7 mg of Ir(ppy)$_2$(carbac) were added. 140 mL of double distilled water were added dropwise under vigorous stirring of the solution. The microparticles formed a precipitate that was separated by centrifugation and washed 4 times with water in order to remove remaining DMF from the solution. As DMF has a high boiling point (153 °C), the particles were then taken up in distilled water

and freeze-dried to remove remaining DMF from the polymer and to fully cure the particles. If the particles are washed with organic solvents without freeze-drying and thus curing them in advance, the amount of dye molecules washed out of the particles is higher and the brightness of the luminescence of the particles is smaller. Prior to use in the dual sensor, the microparticles were washed three times with ethanol and three times with tetrahydrofurane, taken up in distilled water, and freeze-dried again.

*PS-PVP particles doped with PtTFPP*

Five hundred twenty-six milligrams of the PS-PVP polymer aqueous dispersion (at 38 % (w/w) this equals 200 mg of the polymer) were diluted with the mixture of 60 mL of water and 30 mL of tetrahydrofurane. PtTFPP (3 mg) was dissolved in 20 mL of THF, and the solution was added dropwise under vigorous stirring into the dispersion. This process renders the particles doped with PtTFPP. After 30 min all THF and partly water were removed under reduced pressure and the dispersion was concentrated to contain 20% w/w of the beads in water.

### Fabrication of the sensor film

To a 10% w/w dispersion of the PS-PVP beads in water we added 15 mg of the temperature sensitive PAN particles per mL dispersion. This cocktail was sprayed from a distance of circa 15 cm onto a 3 x 3 cm aluminum sample plate. We use a Walther PILOT paint spraying gun ([www.walther-pilot.de](www.walther-pilot.de)) on a Güde compressor (www.guede.ws) for spraying. The pressure applied for spraying was 2.5 bar.

### Setup for sensor calibration

Absorption and emission spectra were recorded on a Lambda 14p Perkin-Elmer UV-vis spectrophotometer (Waltham, MA, USA, [www.perkinelmer.com](www.perkinelmer.com)) and an Aminco AB 2 luminescence spectrometer (Thermo Scientific Inc., Waltham, MA, USA, www.thermo.com), respectively. The $p/T$ calibration chamber was provided by the German Aerospace Center (DLR) in Göttingen (www.dlr.de). Time-resolved measurements were performed with a PCO SensiCam 12 bit b/w CCD camera (PCO, Kelheim, Germany, www.pco.de) equipped with a Schneider-Kreuznach Xenon 0.95/17 lens (Jos. Schneider Optische Werke, Bad Kreuznach, Germany; www.schneiderkreuznach.com) and a 405-66-60 405 nm LED from Roithner Lasertechnik (Vienna, Austria; [www.roithner-laser.com](www.roithner-laser.com)). The excitation light was

focused by a PCX 18_18 MgF2 TS lens (from Edmund Optics, Karlsruhe, Germany: www.edmundoptics.com). It was filtered through a BG 12 long-pass filter (Schott, Mainz, Germany, www.schott.com) with a thickness of 2 mm. Residual light was then passed through a BP 530/50 and a BP 680/60 band pass filter (from AHF Analysentechnik; www.ahf.de).

## 7.6    References

[1]     D. M.Oglesby, J. L. Ingram, J. D. Jordan, A. N. Watkins, B. D. Leighty,  *NASA/TM*

[2]     J. H. Bell, E. T. Schairer, L. A. Hand, R. D. Mehta, *Annu. Rev. Fluid Mech.* **2001**, 33, 155-206.

[3]     O. S. Wolfbeis, *Adv. Mat.* **2008** *20*, 3759–3763

[4]     A. Habibagahi, Y. Mébarki, Y. Sultan, G. P. A. Yap, R. J. Crutchley, *ACS Appl. Mat. Interfaces,* 2009, 1 (8), 1785–1792

[5]     S. M. Borisov, T. Mayr, I. Klimant, *Anal. Chem.*, **2008**, 80, 573-582.

[6]     S. M. Borisov, I. Klimant, *Microchim. Acta,* **2009,** 164, 7-15

[7]     M. I. Stich, O. S. Wolfbeis, *Fluorescence Sensing and Imaging Using Pressure-Sensitive Paints and Temperature-Sensitive Paints*, Springer, **2008; i**n: *Springer Series in Fluorescence*, vol. 5: *Standardization and Quality Assurance in Fluorescence Measurements: vol. 1 (Techniques)*; U. Resch-Genger (ed.), Springer, Berlin – Heidelberg (2008), pp. 429-461;

[8]     C. Moore, S. P. Chan, J. N. Demas, B. A. DeGraff, *Appl. Spectrosc.* **2004**, 58, 603-607.

[9]     P. Hartmann,W. Ziegler, *Anal. Chem.*, **1996**, 68, 4512-4514.

[10]    R. Renka, *ACM Trans. Math. Software*, **1988,** *14*, 139-148.

[11]    R. Renka, *ACM Trans. Math. Software*, **1988,** *14*, 149-150.

[12]    M. A. Woodmansee, J.C. Dutton, *Exp. Fluids* **1998**, 24, 163-174

[13]    J. Brandrup, E. H. Immergut, E. A. Grulke, *Polymer Handbook*, Wiley-VCH, **1999**

[14]    S.-K. Lee, I. Okura, *Anal. Sci.* **1997**, 13, 535-540.

[15]    S.-K. Lee, I. Okura, *Spectrochim. Acta A* **1998**, 54, 91-100.

[16]    E. Puklin, B. Carlson, S. Gouin, *J. Appl. Polym. Sci.* **1999**, 77**,** 2795-2804.

[17]    M. Gouterman, J. Callis, L. Dalton, G. E. Khalil, Y. M´ebarki, *Meas. Sci. Technol.* **2004**, 15, 1986-1994.

[18]    B. Zelelow, G. E. Kahlil, G. Phelan, B. Carlson, M. Gouterman, J. B. Callis, and L. R. Dalton, *Sens. Actuat. B* **2003**, B96, 304-314.

[19]    M. I. Stich, S. Nagl, O. S. Wolfbeis, U. Henne, and M. Schaeferling, *Adv. Funct. Mat.* **2008**, 18**,** 1399-1406.

[20]    D. B. Papkovsky, G. V. Ponomarev, W. Trettnak, P. O´Leary, *Anal. Chem*. **1995,** 67, 4112–4117.

[21]    G. Khalil, M. Gouterman, S. Ching, C. Costin, L. Coyle, S. Gouin, E. Green, M. Sadilek, R. Wan, J. Yearyean, B. Zelelow, *J. Porphyrins Phthalocyanines* **2002**, 6 135–145.

[22]    S. M. Borisov, G. Nuss, I. Klimant, *Anal. Chem*. **2008**, 80, 9435-9442.

[23]    M. E. Köse, B. F. Carroll, K. S. Schanze*, Langmuir* **2005**, 21, 9121-9129.

[24]    G. E. Khalil, C. Costin, J. Crafton, G. Jones, S. Grenoble, M. Gouterman, J. B. Callis, L.R. Dalton, *Sens. Actuators B* **2004**, 97, 13-21.

[25]    Brübach, J.; Patt A.; Dreizler, A, *Appl.Phys. B*. **2006,** *83*, 499–502.

[26]    H. Aizawa, T. Katsumata, Y. Kiyokawa, T. Nishikawa, T. Sasagawa, S. Komuro, T. Morikawa, H. Ishizawa, E. Toba *Meas.* **2006**, *39*, 147–152.

[27]    Aizawa, H.; Ohishi, N.; Ogawa, S.; Katsumata, T.; Komuro, S.; Morikawa, T.; Toba, E. *Rev.Sci. Instrum.* **2002**, 73, 3656–3658.

[28]    L. M. Coyle, M. Gouterman, *Sens. Actuators B* **1999,** *61*, 92–99.

[29]    S. V. Yap, S; R.M. Ranson, W. M. Cranton, D. C. Koutsogeorgis, G. B. Hix, *J. Lumin*. **2009**, *129*, 416–422.

[30]    S. W. Allison, G. T. Gillies, *Rev. Sci. Instrum.* **1997**, 68 (7), 2615-2650.

[31]    N. Tian, A. Thiessen, R. Schiewek, O. J. Schmitz, D. Hertel, K. Meerholz, E. Holder *J. Org. Chem.* **2009**, 74, 2718-2715.

# Chapter 8

# Pressure and Temperature Sensitivity of Cyclometalated Platinum(II) Complexes

**Summary:** Cyclometalated Pt(II) complexes[1-3] have been hardly studied in terms of oxygen sensitivity and temperature sensitivity. The complexes described in this chapter display green luminescence which is important in order to provide a signal that is separable from red emitting indicators. There are very good indicators for temperature (e.g. Eu-complexes) and oxygen (PtTFPP), displaying red emission. In order to prepare a dual sensitive paint providing two signals that can be separated by optical filters, it is necessary to find new blue to green emitting indicators. Herein, five new cyclometalated Pt(II) complexes were studied with respect to the temperature and oxygen sensitivity of their luminescence lifetime. Heteroleptic Pt(II) complexes like these are known to be stable, color tuneable and, to have luminescence lifetimes in the μs range.

## 8.1    Compounds and Calibration

The five complexes investigated are of the general structure of cylometalating C^N-ligand  together with a (2,2,6,6-tetramethylheptane-3,5-dione) ancillary ligand on the Pt(II) central atom. The names of the complexes are [platinum(II)(2-phenylpyridine)(2,2,6,6-tetramethylheptane-3,5-dione)] **1**, [platinum(II)(2,4-difluorophenylpyridine)(2,2,6,6-tetramethylheptane-3,5-dione)] **2,** [Platinum(II)(2-(4-bromophenyl)-5,6,7,8-tetrahydroquinoline)(2,2,6,6-tetramethylheptane-3,5-dione)] **3**, [platinum(II)(2-(4-fluorophenyl)-5,6,7,8-tetrahydroquinoline)(2,2,6,6-tetramethylheptane-3,5-dione)] **4**, and [platinum(II)(2-(4-trifluoromethylphenyl)-5,6,7,8-tetrahydroquinoline)(2,2,6,6-tetramethylheptane-3,5-dione)] **5**. The chemical structures are shown in Figure 8.1.
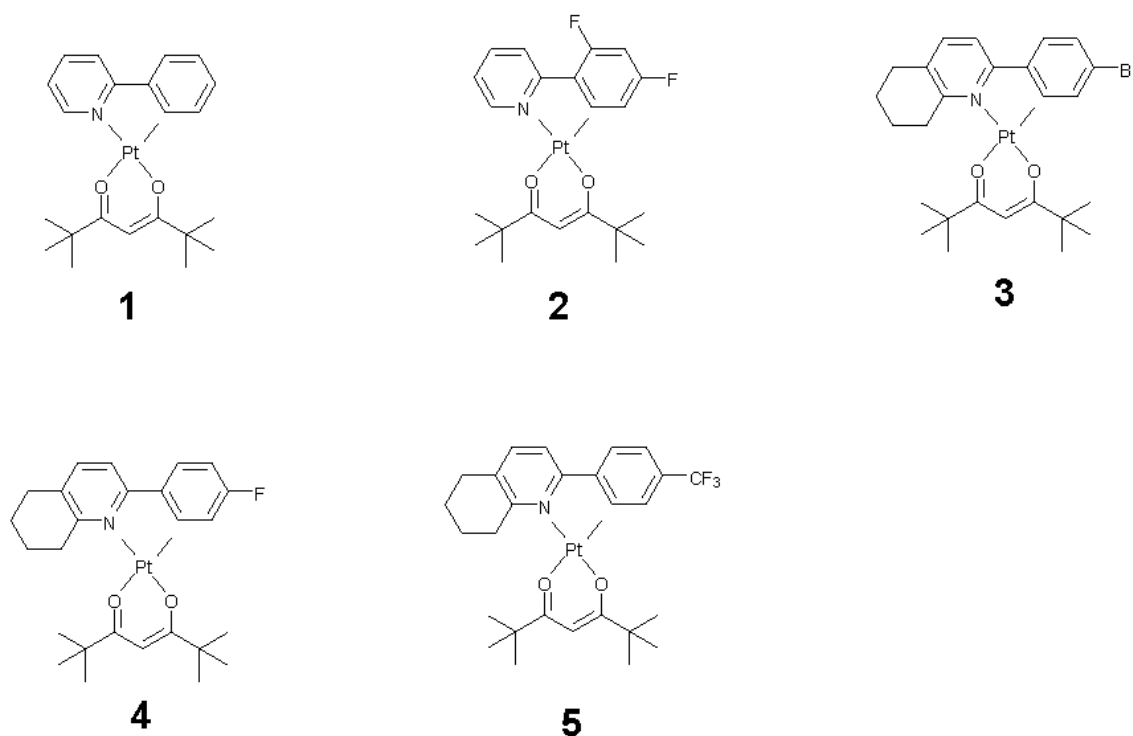


**Figure 8.1.** Chemical Structures of the five cyclometalated Pt(II) complexes investigated. General structure of the complexes is a cyclomeatlating C^N-ligand together with a ancillary ligand at the central Pt(II) atom.

All compounds display green emission which is ascribed to mixed $^3$LC-MLCT states.[1] The absorbance and emission spectra of **1-5** are shown in Figures 8.2 and 8.3. The emission color depends on the C^N-ligand and thus can be tuned from blue to yellow by choosing different ligands. All emission spectra display two maxima. The complexes are well soluble in solvents of medium polarity.
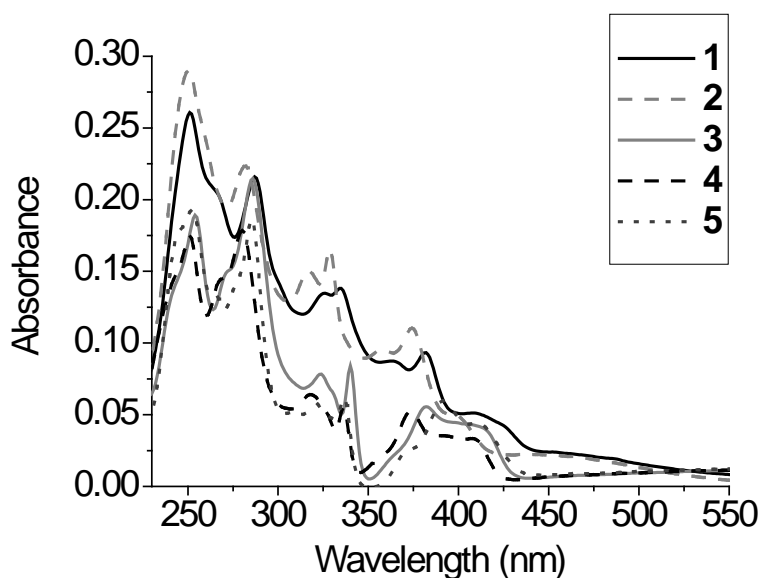
**Figure 8.2.** UV-vis spectra of **1-5** in *n*-hexane solutions (c = 1 × 10$^{-5}$ mol/L) at room temperature.
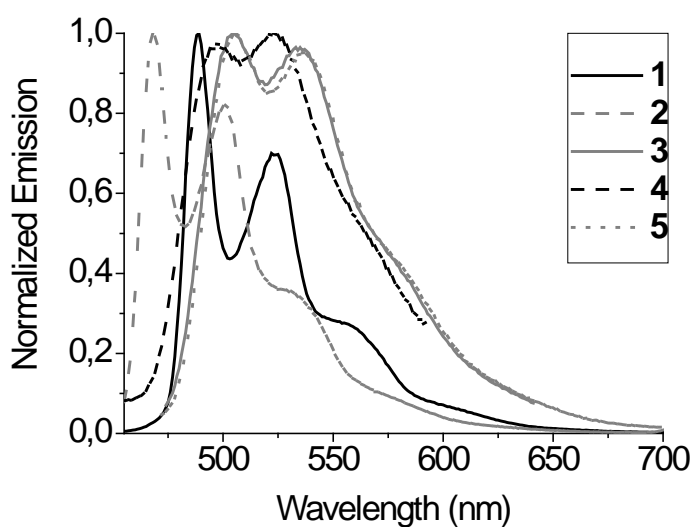
**Figure 8.3.** Luminescence spectra of complexes **1-5** in *n*-hexane (c = 1 × 10$^{-5}$ mol/L).

The complexes **1-5** were incorporated into poly(styrene) (PS) films (thickness 6 μm) and their luminescence lifetimes (Table 1) were determined via the rapid lifetime determination (RLD) method.[4] The light source for excitation is a 405 nm LED and the luminescence intensity is integrated in two precisely timed gates by a triggered CCD camera (see section 2.7). After a short light pulse, the luminescence intensity is acquired in the first gate $A_1$. Likewise, the intensity in the second gate $A_2$ and the dark images are recorded. The whole imaging process has been described in previous works.[5]

However, the RLD only gives correct lifetimes, if the decay of luminescence is monoexponential and both time gates are of the same length. Usually, the condition of monoexponential decay is not fulfilled. Thus, only mean values of $\tau$ can be obtained with this simple process.[6] But RLD is a valuable and fast method to characterize relative changes of $\tau$ responding to luminescence quenching by oxygen or thermal quenching. The ratiometric measurement provides an intrinsically referenced signal, independent from variations in the intensity of the excitation light and other common interferences in luminescence measurements and, therefore, is more accurately than the detection of changes in luminescence intensity. All the imaging measurements were performed with square samples of 3 × 3 cm size of the dyed PS films. The samples were fixed inside a calibration chamber, capable of holding air pressures from 50 to 2000 mbar and temperatures from 1 to 60 °C.

## 8.2     Pressure Sensitivity

The luminescence quenching of the Pt(II) emitters **1-5** by oxygen is depicted in Figure 8.4 in the form of Stern-Volmer plots. Luminescence lifetime is proportional to partial oxygen pressure ($pO_2$) according to the Stern-Volmer equation (eq. 2.6). The excited triplet state is deactivated by a collision with oxygen. The presence of oxygen quenches the luminescence lifetime and intensity likewise. The Stern-Volmer constants and the temperature coefficients obtained from these measurements are shown in Table 8.1.
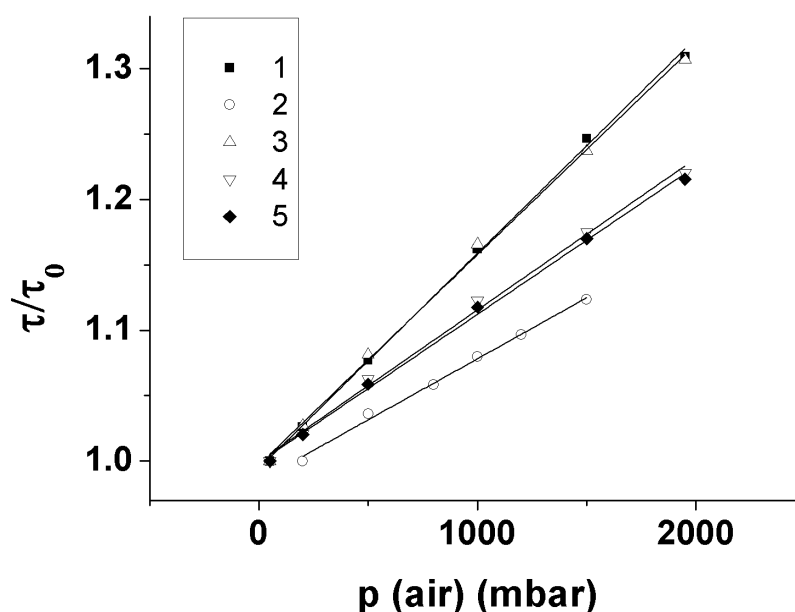
**Figure 8.4.** Response of the luminescence lifetimes of ppy **1**, 2,4-Fppy **2**, Brph-thq **3**, Fph-thq **4** and CF$_3$ph-thq **5** in PS to oxygen at a temperature of 30 °C displayed as Stern-Volmer plots with linear fits according to eq. 2.6. $\tau_0$ refers to the lifetime at 10 kPa pO$_2$ and 30 °C. Also see Table 8.1.

## 8.3    Temperature Sensitivty

The calibration plots for the temperature response are nonlinear and can be fitted by an Arrhenius-type equation (Eq. 5.1).[7] The response of the luminescence of the studied complexes to increasing temperature is shown in Figure 8.4. All measurements were performed using PS as matrix polymer. It displays a moderate oxygen permeability P of $1.9 \times 10^{-13}$cm$^3$ (STP) cm (cm$^2$sPa)$^{-1}$ (STP = standard temperature and pressure).[8] The temperature dependency of Brph-thq **3** is fitted exemplarily in Figure 8.5.
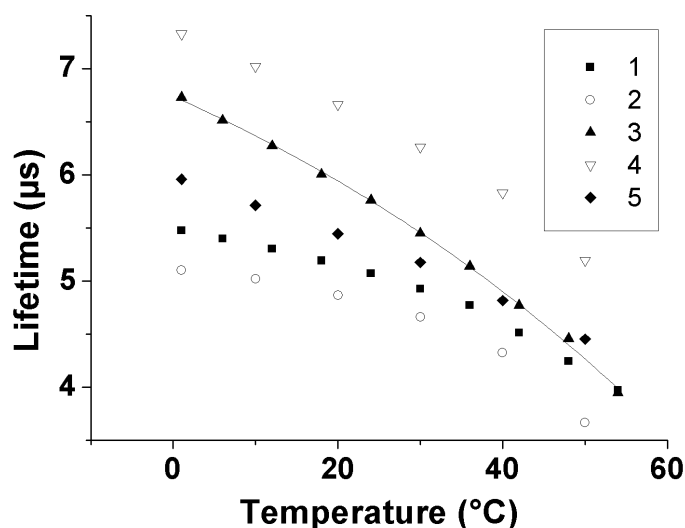
**Figure 8.5.** Temperature dependence of the luminescence lifetime of the cyclometalated Pt(II) complexes ppy **1**, 2,4-Fppy **2**, Brph-thq **3**, Fph-thq **4** and CF$_3$ph-thq **5** in PS at 1000 mbar air pressure. The values for Brph-thq are fitted according to Eq. 5.1 for demonstration. Also see Table 8.1.

## 8.4    Discussion

Generally, the oxygen sensitivity of the studied platinum complexes is very weak in contrast to other phosphorescent metal complexes such as platinum(II)-porphyrins,[9,10] ruthenium(III)-,[11] or some iridium(III) complexes. These represent typical luminescent oxygen indicators with Stern-Volmer constants that are significantly higher compared to the complexes presented here. With the exception of 2,4-Fppy **2** and Brph-thq **3**, also thermal quenching is weakly pronounced. Hence, these luminophores are promising candidates for inert reference complex that can be applied e.g. in optical sensors or for ratiometric dual-wavelength fluorescence measurements. Particularly, complex **4** and **5** are rather insensitive to either thermal or oxygen quenching. The latter can be further suppressed in gas blocking polymer materials. The blue to green emission of these complexes is separable from red emitting indicators. Additionally the green

emission of Br-phthq matches the green channel of a RGB camera. This complex is applied in a dually sensitive paint for color camera readout described in chapter 9.

**Table 8.1.** Stern-Volmer constants $K_{SV}$ and temperature coefficients of the cyclometalated Pt(II) complexes **1-5** in 6 μm PS films

| Complex | $K_{SV}$ | T-coeff. |
|---------|----------|----------|
|         | **[10$^{-4}$ mbar$^{-1}$]$^b$** | **[%τ/°C]$^{a,b}$** |
| **1**   | 1.6      | 0.54     |
| **2**   | 0.9      | 0.66     |
| **3**   | 1.6      | 0.76     |
| **4**   | 1.2      | 0.58     |
| **5**   | 1.1      | 0.51     |

$^a$ at 30 °C and 1000 mbar air pressure; $^b$ in PS.

In terms of optical sensor applications, complex **3** is interesting as temperature-sensitive probe. Its temperature coefficient is almost as high as that of typical luminescent indicators for T such as ruthenium and europium complexes.[12-14] Thus, **3** was incorporated in a gas blocking polymer matrix of poly(vinylidene chloride-*co*-acrylonitrile) (PVDCAN). The results of the response to temperature are shown in Figure 8.6. Additionally, it is possible to synthesize micro particles dyed with complex **3** as shown in chapter 9.

It is evident that the resulting optical temperature sensor is virtually inert to oxygen quenching and exhibits a constant luminescence in a very broad air pressure range from 50 to 1950 mbar. In contrast to the established luminescent indicators for temperature, the emission of **3** is comparably short-waved enabling a combination with a second red emitting indicator such as platinum(II)-porphyrins for simultaneous detection of oxygen in dual sensors.
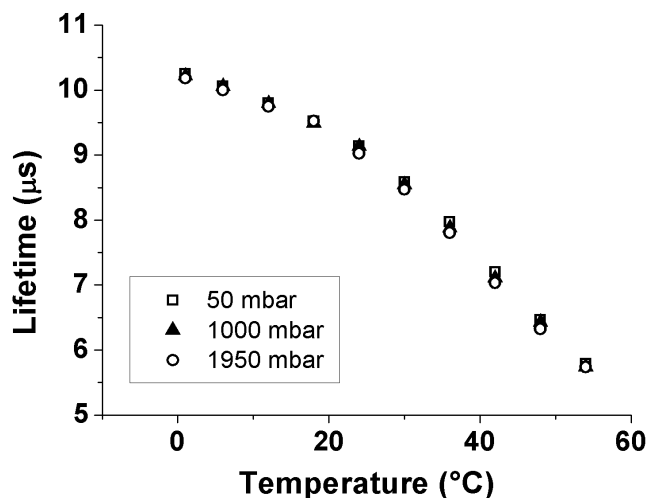
**Figure 8.6.** Temperature dependence of the luminescence lifetime of Brph-thq **3** in PVDCAN at various air pressures.

## 8.5    Conclusion

A series of five heteroleptic Pt(II) complexes was investigated. The complexes display luminescence lifetimes of several µs and the response of the lifetime to oxygen and temperature was calibrated. In general, the compounds are rather insensitive towards oxygen and temperature as well. Such dyes are promising candidates to be used as reference dyes. However, Brph-thq **3** displayed pronounced temperature sensitivity. Additionally, this dye can be combined with red emitting indicators because of its green emission. Brph-thq **3** is applied as temperature indicator in the first dually sensitive paint for color camera read out which is described in the chapter 9.

**8.6    Experimental**

All complexes were synthesized by the group of Prof. Elisabeth Holder at the university of Wuppertal. UV-vis spectra were measured with a JASCO V-550 UV-vis spectrometer (1 cm cuvettes) at concentrations of $1 \times 10^{-5}$ mol/L. The emission spectra were performed using a CARY Eclipse fluorescence spectrophotometer at concentrations of $1 \times 10^{-5}$ mol/L. Absorption and emission spectra for the determination of pressure and temperature sensitivity were recorded on a Lambda 14p Perkin-Elmer UV-vis spectrophotometer (Waltham, MA, USA, www.perkinelmer.com) and an Aminco AB 2 luminescence spectrometer (Thermo Scientific Inc., Waltham, MA, USA, www.thermo.com), respectively. The $p/T$ calibration chamber was provided by the German Aerospace Center (DLR) in Göttingen.[9]

All time-resolved measurements were performed with a PCO SensiCam 12 bit b/w CCD camera (PCO, Kelheim, Germany, www.pco.de) equipped with a Schneider-Kreuznach Xenon 0.95/17 lens (Jos. Schneider Optische Werke, Bad Kreuznach, Germany, www.schneiderkreuznach.com) and a 405-66-60 405 nm LED from Roithner Lasertechnik (Vienna, Austria, www.roithner-laser.com). The excitation light was focused by a PCX 18_18 MgF2 TS lens from Edmund Optics (Karlsruhe, Germany, www.edmundoptics.com). It was filtered through a BG 12 filter (Schott, Mainz, Germany, www.schott.com) with a thickness of 2 mm. Emission was detected through a GG 475 high pass filter purchased from AHF Analysentechnik (www.ahf.de). The PS films and the PVDCAN films containing the Pt(II) complexes **1-5** were prepared with a knife coating device on a solid poly(ethylene-terephtalate) (PET) support. The concentration of the polymer solutions was 5% (w/w) in THF. The polymers were purchased from Sigma-Aldrich (www.sigmaaldrich.com). In order to increase the luminescence intensity recorded by the camera, the backside of the PET foils was coated with a highly reflective layer of $TiO_2$ in silicone.

## 8.7    References

[1]     J. Brooks, Y. Babayan, S. Lamansky, P. I. Djurovich, I. Tsyba, R. Bau, M. E. Thompson, *Inorg. Chem.* **2002**, *41*, 3055.

[2]     B. Hirani, J. Li, P. I. Djurovich, M. Yousufuddin, J. Oxgaard, P. Persson, S. R. Wilson, R. Bau, W. A. Goddard, M. E. Thompson, *Inorg. Chem.* **2007**, *46*, 3865.

[3]     G. Minghetti, M. I. Pilo, G. Sanna, R. Seeber, S. Stoccoro, F. Laschi, *J. Organomet. Chem.* **1993**, *452*, 257.

[4]     C. Moore, S. P. Chan, J. N. Demas, B. A. DeGraff, *Appl. Spectrosc.* **2004**, *58*, 603.

[5]     L. H. Fischer, M. I. J. Stich, O. S. Wolfbeis, N. Tian, E. Holder, M. Schaferling, *Chem. Eur. J.* **2009**, *15*, 10857.

[6]     K. K. Sharman, A. Periasamy, H. Ashworth, *Anal. Chem.* **1999**, *71 No.5*.

[7]     J. N. Demas, B. A. Degraff, *Anal. Chem.* **1991**, *63*, A829.

[8]     Y. Amao, Y. Ishikawa, I. Okura, *Anal. Chim. Acta* **2001**, *445*, 177.

[9]     S. K. Lee, I. Okura, *Anal. Commun.* **1997**, *34*, 185.

[10]    I. M. P. de Vargas-Sansalvador, A. Martinez-Olmos, A. J. Palma, M. D. Fernandez-Ramos, L. F. Capitan-Vallvey, *Microchim. Acta* **2011**, *172*, 455.

[11]    E. R. Carraway, J. N. Demas, B. A. Degraff, J. R. Bacon, *Anal. Chem.* **1991**, *63*, 337.

[12]    S. M. Borisov, O. S. Wolfbeis, *Anal. Chem.* **2006**, *78*, 5094.

[13]    H. S. Peng, M. I. J. Stich, J. B. Yu, L. N. Sun, L. H. Fischer, O. S. Wolfbeis, *Adv. Mater.* **2010**, *22*, 716.

[14]    X. D. Wang, X. H. Song, C. Y. He, C. J. Yang, G. N. Chen, X. Chen, *Anal. Chem.* **2011**, *83*, 2434.

# Chapter 9

# Referenced Dual Pressure and Temperature Sensitive Paint for Digital Color Camera Read Out

**Summary:** The first fluorescent material is presented for referenced simultaneous RGB imaging of barometric pressure (oxygen partial pressure) and temperature. This dual sensitive coating consists of two platinum(II) complexes as indicators and a reference dye, each incorporated in appropriate polymer nanoparticles. These particles are dispersed in a polyurethane hydrogel and spread onto a solid support. The emissions of the pressure (oxygen) indicator PtTFPP matches the red channel of a RGB color camera while the emission of the temperature indicator [Pt(II)(Br-thq)(acac)] matches the green channel. The reference dye 9,10-diphenylanthracene emits in the blue channel. In contrast to other dual sensitive materials, this new coating allows for simultaneous imaging of both indicator signals and the reference signal in one RGB color picture without having to separate the signals with additional optical filters. All dyes are excitable with a 405 nm LED and display good photostability under continuous illumination. With this novel composite material barometric pressure can be determined with a resolution of 22 mbar. The temperature can be determined with a resolution of 4.3 °C.

## 9.1    Introduction

The dual imaging of barometric pressure and temperature was already accomplished with intensity imaging[1,2] and lifetime imaging[3,4]. For intensity imaging the emissions of indicators and reference have to be separated by appropriate optical filters[5]. This means that at least two pictures have to be taken. If using a single camera the emission filters have to be exchanged in between of taking the two pictures. During that time the temperature and the pressure have to remain constant. If using two cameras, taking pictures simultaneously, the images have to be aligned afterwards by sophisticated software in order to provide correct measurements. For lifetime imaging pretty elaborate hardware is necessary.[6] The camera has to feature fast shutter technique for gated lifetime measurements. Camera and light source need to be connected to a computer, precisely triggering both devices. Recently, the use of digital color cameras for luminescence imaging[7] has gained rising interest.[8,9] The photosensitive chip of a color camera records three images at once. The pixels on the chip are coated with optical filters for red, green and blue light (RGB) according a certain pattern[10] (see Figure 2.9). The three color channels of the camera can be used to simultaneously photograph up to three different emissions of luminescent indicators, matching the color channels. The emission of one of the dyes can be a reference signal. After taking the picture the channels are split and the intensities or intensity ratios are evaluated by software. This color camera read out supersedes the use of optical filters for each emission as well as elaborate and bulky hardware like cooled fast shutter cameras or triggered light sources. Furthermore, the RGB camera does not have to be connected to a computer and portable LED light sources can be easily mounted on the camera. This really makes it a cheap, convenient, and hand-held imaging method.

## 9.2      Results

### 9.2.1    Synthesis and Preparation of Sensitive Paints

The chemical structures of the three dyes used are displayed in Figure 9.1.
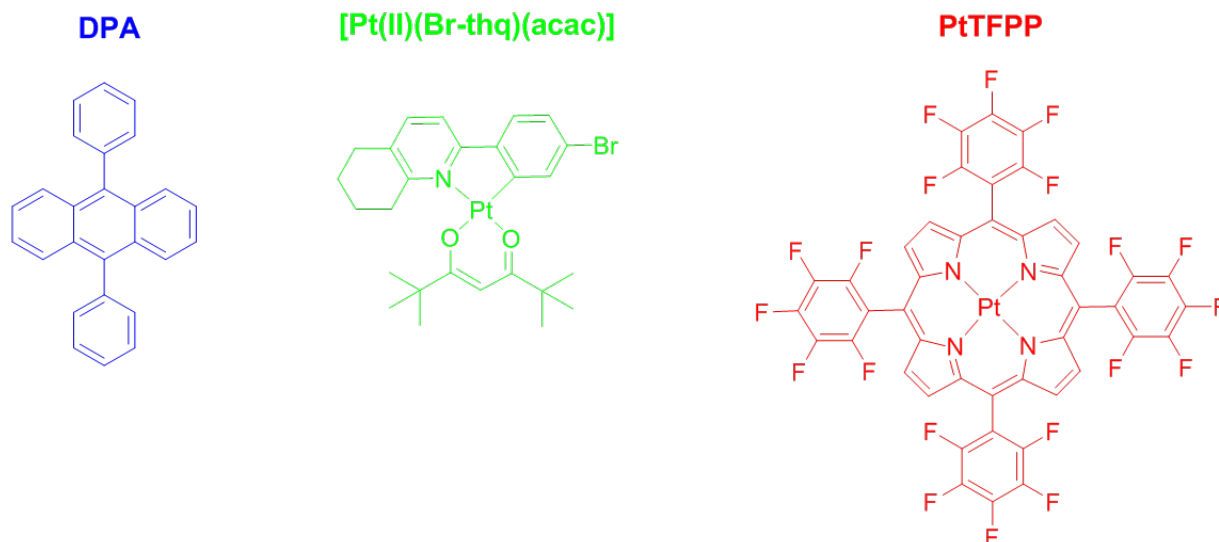


**Figure 9.1**. Chemical structures of the dyes applied in the sensor. DPA is used as a reference dye and its emission matches the blue channel of the camera with an emission maximum of 440 nm. The temperature indicator [Pt(II)(Br-thq)(acac)] matches the green channel emitting at 497 nm and 532 nm. PtTFPP acts as oxygen indicator recorded in the red channel emitting at 650 nm.

The emission of every dye is temperature dependent. The reference dye should display small temperature dependence and has to be insensitive towards $pO_2$ (air pressure). If the temperature dependence of the reference is similar to that of the temperature indicator, the ratio of the two emissions does not change with temperature. The emission of DPA shows only a small temperature dependency and is insensitive towards air pressure ($pO_2$). Together with its blue emission matching the blue channel of the camera, DPA is a very suiting reference dye. The emission spectrum and the response to pressure and temperature of DPA is shown in Figure 9.2.
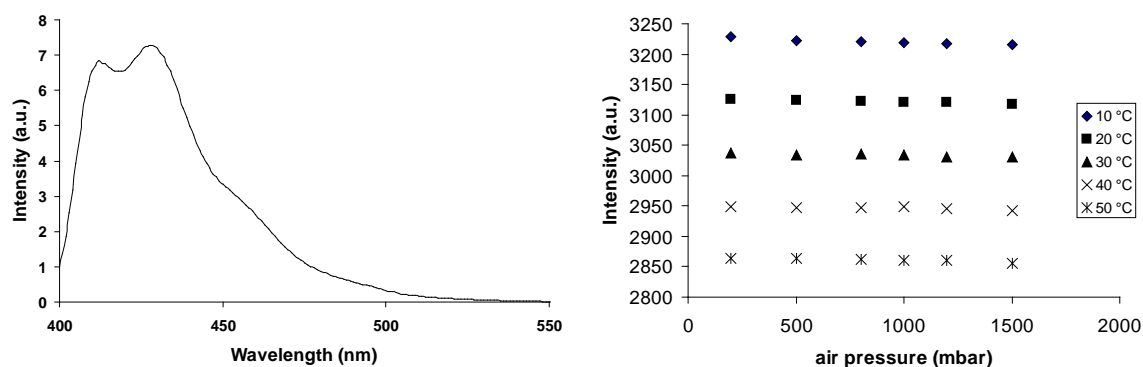
**Figure 9.2.** Emission spectrum of the reference dye DPA (left) and the response of DPA incorporated in poly(acrylonitrile) nanoparticles, to various temperatures and air pressures (right). DPA displays small temperature dependence and is insensitive towards air pressure (pO$_2$) when incorporated in poly(acrylonitrile).

The emission spectra of the two indicator dyes in the respective polymer particles embedded in a film of polyurethane hydrogel (see description below for further information) at various air pressures and temperatures are shown in Figure 9.3. The emission of the temperature indicator [Pt(II)(Br-thq)(acac)] is virtually insensitive towards the air pressure.
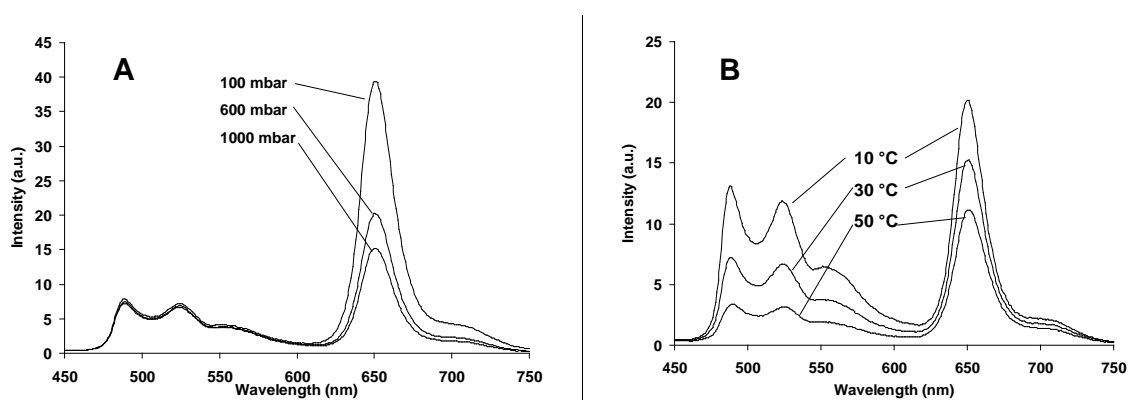


**Figure 9.3.** Emission spectra of the temperature indicator [Pt(II)(Br-thq)(acac)] and the oxygen indicator PtTFPP in the sensor film recorded at (A) various air pressures and 30 °C and, (B) at various temperatures and 1000 mbar air pressure.

The dual sensitive coating consists of three different nanoparticles dispersed in a film of polyurethane hydrogel. The reference 9,10-diphenylanthracene (DPA) is

incorporated in poly(acrylonitrile) (PAN) nanoparticels. The temperature indicator [platinum(II)(2-(4-bromophenyl)-5,6,7,8-tetrahydroquinoline)(2,2,6,6-tetramethylheptane-3,5-dione)] [Pt(II)(Br-thq)(acac)] is enclosed in poly(vinylidene chloride-*co*-acrylonitrile) (PVDCAN). For this, the Pt(II) temperature probe was firstly synthesized by using a straight-forward synthetic method[4,13-18]. Modifying the Lewis-method for the first step of the synthesis, 2-(4-bromophenyl)-5,6,7,8-tetrahydroquinoline (Br-thq)[19] and $K_2PtCl_4$ were heated in order to receive the $\mu$-chloro-bridged precursor dimer and subsequently in a second step, by introducing ligand 2,2,6,6-tetramethylheptane-3,5-dione (acac) the target complex [platinum(II)(2-(4-bromophenyl)-5,6,7,8-tetrahydroquinoline)(2,2,6,6-tetramethylheptane-3,5-dione)] was isolated in a yield of 65%. For oxygen sensing, nanoparticles made of poly(styrene-*co*-1-vinylpyrrolidone) (PS-*co*-PVP)[20] were doped with platinum(II)-5,10,15,20-*tetrakis*(2,3,4,5,6-pentafluorophenyl)porphyrin (PtTFPP). This copolymer forms a core-shell-like structure with the nonpolar polystyrene units building the core which is doped with PtTFPP. The more polar PVP shell ensures a very stable emulsions of the particles in water and ethanol[21], the two solvents used for preparing the sensor film. The structures of the polymers applied are shown in Figure 9.4 and electron microscopy images that display the size distribution of the resulting nanoparticles are shown in Figure 9.5.
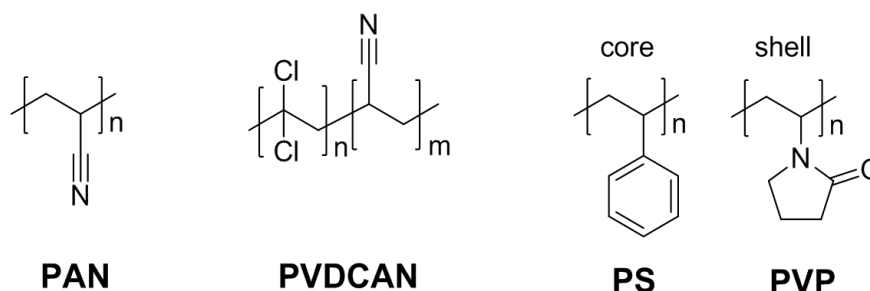


**Figure 9.4.** The chemical structures of the polymers used to prepare the nanoparticulate dye matrixes. DPA is incorporated in PAN nanoparticles; [Pt(II)(Br-thq)(acac)] is incorporated in PVDCAN copolymer nanoparticles; and PtTFPP is incorporated in PS-*co*-PVP nanoparticles.

**(A)**                      **(B)**                      **(C)**
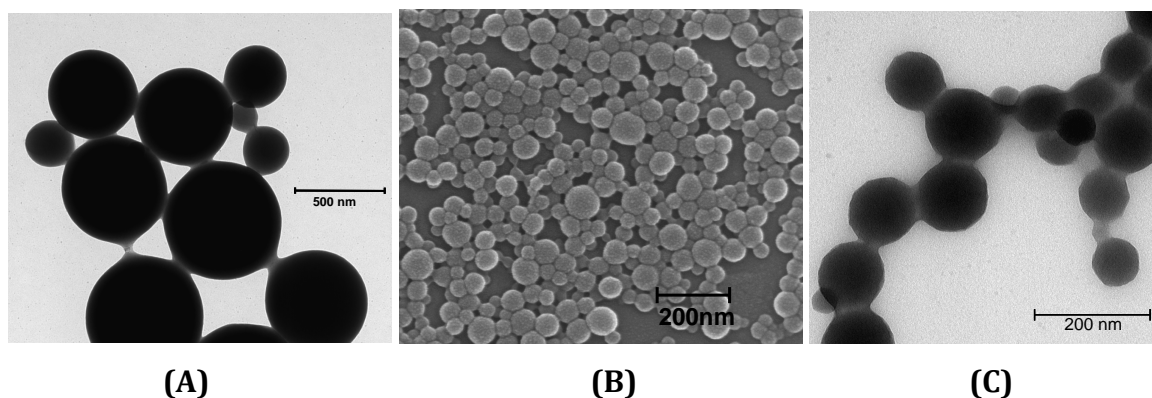
**Figure 9.5.** (A) TEM image of the PAN particles doped with the reference dye DPA. (B) SEM image of the PVDCAN particles dyed with the temperature indicator [Pt(II)(Br-thq)(acac)] and (C) TEM image of the PS-*co*-PVP particles hosting the pressure indicator PtTFPP.

The sensor film was cast on a solid poly(ethylene terephthalate) (Mylar®) foil and placed in a calibration chamber. In this chamber, the temperature can be adjusted from 1 °C to 60 °C and the barometric pressure from 50 mbar to 2000 mbar. All dyes can be excited with a circular 405 nm LED array mounted in front of the lens. In order to block reflections of the blue excitation light the lens was covered with a 325 nm high pass filter. The film inside the chamber was photographed with a digital color camera, the channels were split and the ratios of indicators and reference were calculated.

### 9.2.2    Lifetime Imaging of the Sensor Film

The sensor film presented in this work is designed for imaging with a RGB color camera but the two indicator dyes are suited for lifetime imaging as well. Lifetime imaging was performed according the rapid lifetime determination (RLD)[22]. Herein the luminescence is recorded in two precisely timed gates by a fast shutter CCD camera after a pulse of excitation light. The luminescence lifetime can be estimated by the intensity ration of these two gates. The calibration plots of the pressure indicator and the temperature indicator are given in Figure 9.6.

**(A)**                                                    **(B)**
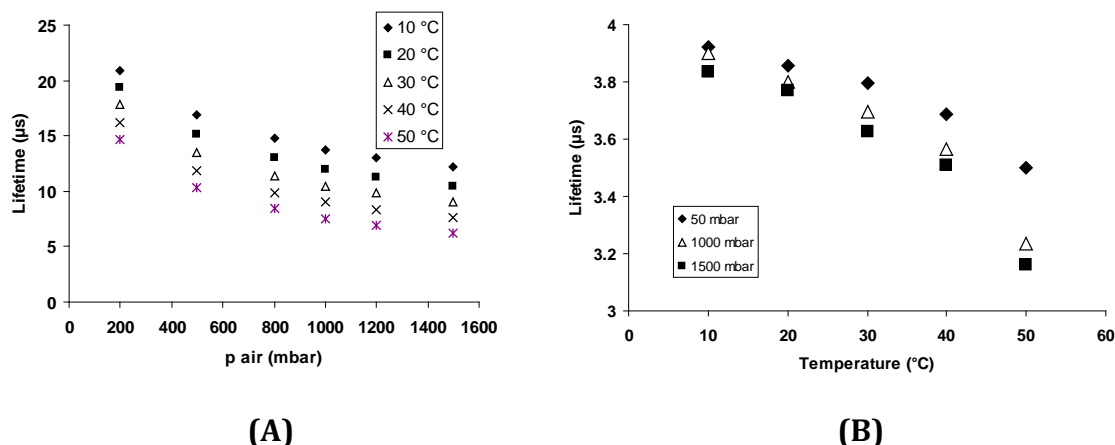
**Figure 9.6.** Calibration plots of the lifetime imaging of (A) the pressure indicator and (B) the temperature indicator. Measurements were performed according the RLD method.

Lifetime measurements provide an intrinsically referenced signal. Compared to RGB imaging, lifetime imaging achieves a better resolution in terms of analyte concentration. The drawback is the bulky and expensive hardware required. Cooled fast shutter cameras and precisely triggered light sources are necessary.

### 9.2.3    Color Camera Imaging

In this work the barometric pressure ($pO_2$ respectively) and the temperature are imaged with a RGB camera. The emission of the reference dye matches the blue channel, the temperature indicator matches the green channel, and the oxygen indicator matches the red channel. This is the first composite material that enables for simultaneous imaging of barometric pressure and temperature by means of a digital color camera. This supersedes the use of optical filters to separate the emissions of the three dyes. Additionally no bulky and expensive hardware is required. The RGB imaging system is cheap and readily portable including the LED light source mounted on the camera.

The emission intensities of the indicators decrease with rising temperature and pressure, respectively. The dual sensitive film is photographed during excitation after the desired pressure and temperature values are set. The change in color is depicted in Figure 9.7.
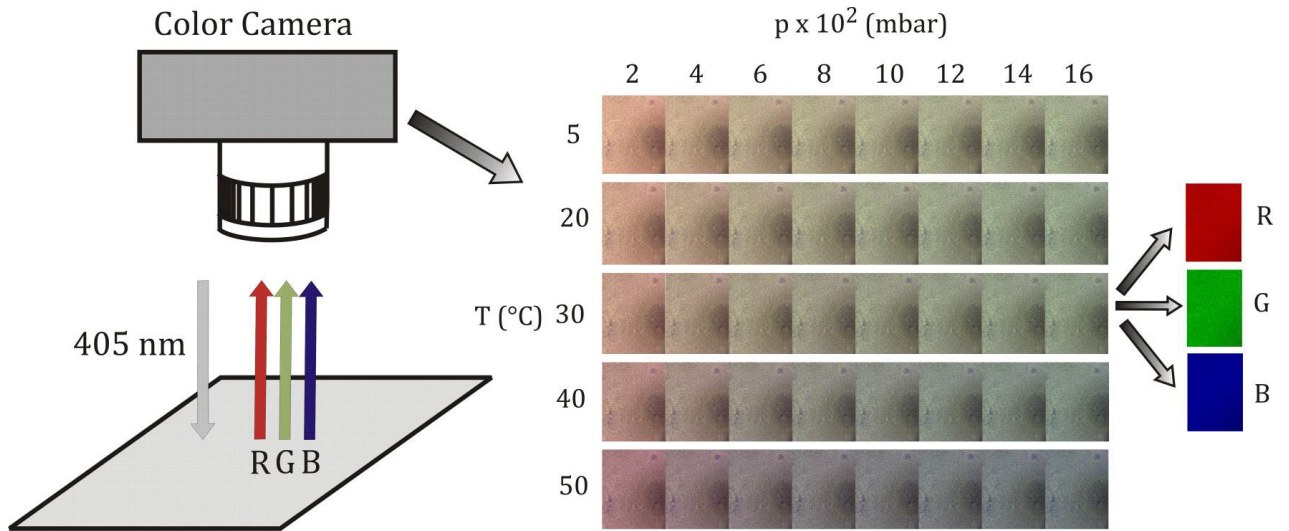
**Figure 9.7.** The dual sensitive coating is photographed under excitation at a certain pressure and temperature. The RGB pictures are then split into the three color channels and processed for evaluation.

The temperature signal is the ratio of the green channel divided by the blue channel (G/B). The pressure signal is the ratio of the red channel divided by the blue channel (R/B). The calibration plots are shown in Figure 9.8 and Figure 9.9. Of course, the pressure sensor displays cross- sensitivity towards temperature but it is small in the range from 15 °C to 35 °C. The effect of temperature on the pressure sensor can be corrected by determining the temperature simultaneously.
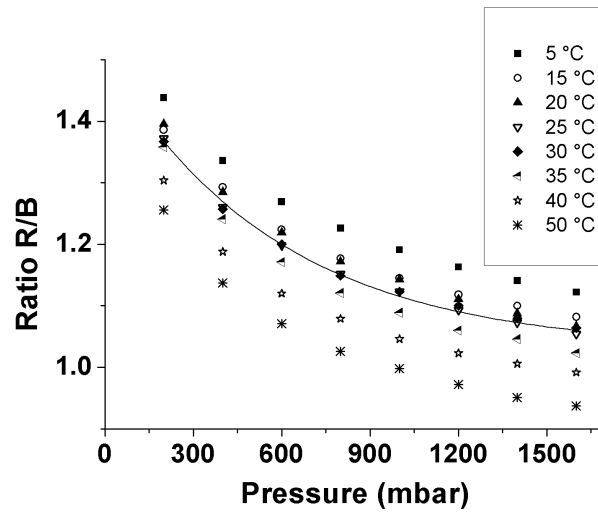
**Figure 9.8.** Calibration plots of the intensity ratio of the pressure indicator in the red channel divided by the reference intensity in the blue channel (R/B) at various temperatures. The experimental data at 25 °C was fitted exemplarily according a mono exponential fit. The pressure sensor displays only a small cross-sensitivity towards temperature between 15 °C and 35 °C.
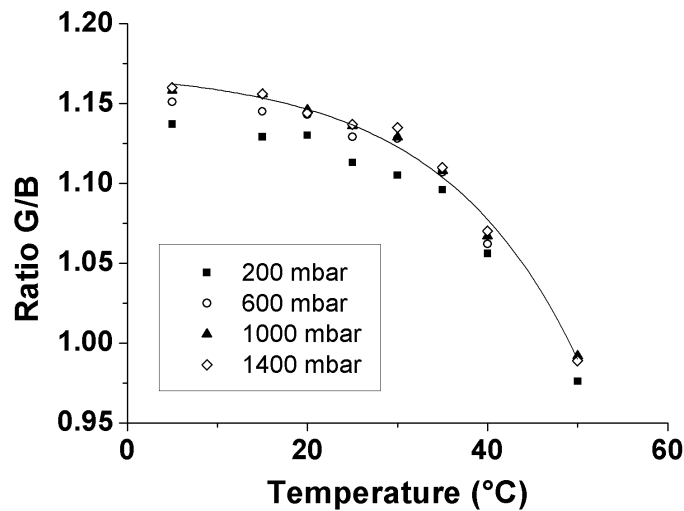


**Figure 9.9.** Calibration plots of the intensity ratio of the temperature indicator in the green channel divided by the reference intensity in the blue channel (G/B) at various air pressures. The experimental data at 1000 mbar air pressure was fitted exemplarily according a mono exponential fit.

Both plots can be fitted according the following mono exponential decay function:

$$y = y_0 + A \, e^{-x/t}$$

The pressure curve was fitted at 25 °C and the temperature curve at 1000 mbar air pressure. The fitting parameters are given in Table 9.1.

**Table 9.1.** The parameters used for fitting of the calibration curves at 25 °C and 1000 mbar, respectively.

|  | $y_0$ | $A$ | $t$ | $R^2$ |
|---|---|---|---|---|
| Pressure Sensor at 25 °C | 1.03 | 0.48 | 583 | 0.996 |
| Temperature Sensor at 1000 mbar | 1.17 | $-6.8 \times 10^{-3}$ | -15.25 | 0.988 |

A very important parameter for a sensor is the resolution. Herein, the resolution is defined as the absolute value of the ratio of the standard deviation (stdev) divided by the slope of the calibration curve. As the calibration plots are not linear the slope of the curve has to be calculated by differentiating the curve at the respective pressure or temperature value. If the calibration curve is not linear, the resolution changes with the analyte concentration. The stdev is determined from five consecutive calibrations. The values refer to a temperature of 25 °C and 1000 mbar air pressure. The values are summarized in Table 9.2.

**Table 9.2.** The standard deviations, the slopes of the calibration curves, and the resolutions of the pressure and temperature probe at 25 °C and 1000 mbar air pressure.

|  | Stdev % | Stdev | Slope | Resolution |
|---|---|---|---|---|
| Pressure Sensor | 0.3 | $3.5 \times 10^{-3}$ | $-1.6 \times 10^{-4}$ mbar$^{-1}$ | 22 mbar |
| Temperature Sensor | 1.2 | $13.8 \times 10^{-3}$ | $-3.2 \times 10^{-3}$ °C$^{-1}$ | 4.3 °C |

The referencing of the signals is very important to correct errors resulting from inhomogeneous paint thickness and inhomogeneous excitation. The effect of inhomogeneous excitation and its correction by referencing is displayed in Figure 9.10. The upper graph (A) shows the intensity (z-axis) of the temperature indicator in the green channel at 25 ° C and 1000 mbar air pressure. The right corner of the area is less illuminated than the rest. By dividing the green channel by the reference in the blue channel the effect is corrected. The distribution of the ratio G/B is displayed in graph (B).
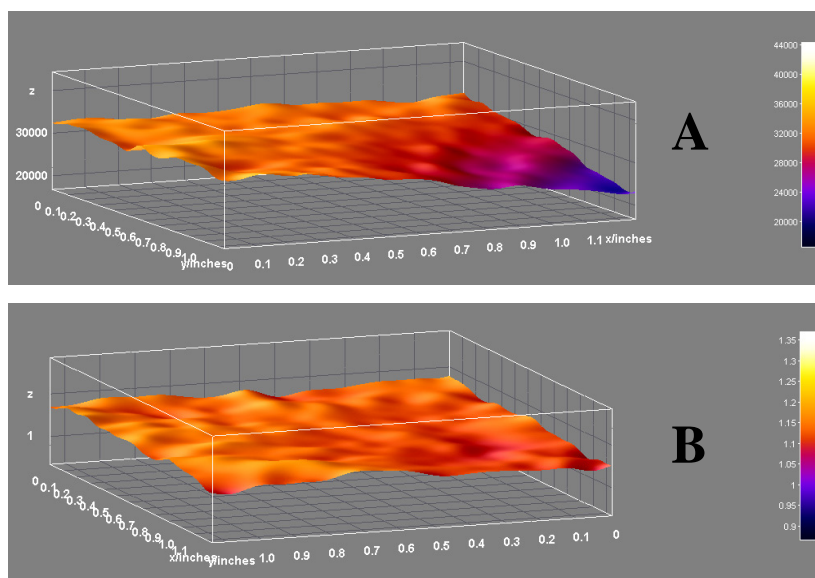


**Figure 9.10.** The upper graph (A) shows the distribution of intensity in the green channel over the sensor area. The right corner is less illuminated than the rest. The effect of inhomogeneous illumination is corrected by dividing it by the reference signal in the blue channel. Graph (B) displays the resulting distribution of the ratio G/B.

## 9.3    Conclusion and Outlook

It is demonstrated that the different RGB sensitive pixels of a digital color camera can be used to efficiently separate three fluorescence signals of different emission wavelength. This enables the simultaneous read out of dual optical sensors combined with an internal reference. For that purpose, a novel green emitting temperature indicator [Pt(II)(Br-thq)(acac)] was synthesized and characterized. This

was combined with PtTFPP as red emitting oxygen indicator and the insensitive DPA as blue emitting reference. Such materials are of high interest as pressure and temperature sensitive paints in aerodynamic research and fluid mechanics.

The most important characteristic of this referenced imaging method using RGB cameras is that only simple hardware is required. A digital color camera on which a LED light source is mounted is portable and cheap compared to the setup required for referenced fluorescence lifetime imaging with time gated CCD cameras. Moreover, RGB measurements are fast and easy to carry out. Of course, RGB imaging is not limited to oxygen and temperature. Any luminescent probes matching the color channels of the RGB chip can be imaged. These features make RGB imaging a very promising technique for applications where no bulky and expensive hardware can be employed. The resolutions of the read out with an RGB camera are not as good as in case of a read out by lifetime imaging. The improvement of the resolution and therefore the accuracy of a quantitative determination is subject for further research. Especially the search for appropriate blue and green emitting indicators is promising for further advancements.

## 9.4    Experimental

**Materials, Instrumentation and Methods.** All reagents were used as purchased from commercial suppliers without further purification. All reactions were carried out by using standard Schlenk techniques under an atmosphere of dry argon. Solvents were used as purchased without further purification. $^1$H NMR and $^{13}$C NMR spectra were performed on a BRUKER III AVANCE 600. Chemical shifts were quoted relative to the internal standard tetramethylsilane (Me$_4$Si) in CDCl$_3$ solutions. For $^1$H (s = singlet, d = doublet, t = triplet, q = quartet and m = multiplet), $^{13}$C NMR data, J values are given in Hertz (Hz). Mass spectrometry was carried out by using electrospray ionization (ESI) techniques on a Bruker Daltonics MICROTOF instrument, respectively. Fourier transform infrared (FT-IR) spectra were recorded on a JASCO FT/IR-4200. Elemental analysis (EA) was performed on a Perkin Elmer 240 B. UV-vis spectra were measured with a JASCO V-550 UV-vis spectrometer (1 cm cuvettes) at concentrations of $1 \times 10^{-5}$ mol/L. The emission spectra were performed using a CARY Eclipse fluorescence spectrophotometer at concentrations of $1 \times 10^{-5}$ mol/L. Absorption and emission spectra for the determination of pressure and temperature sensitivity were recorded on a

Lambda 14p Perkin-Elmer UV-vis spectrophotometer (Waltham, MA, USA, www.perkinelmer.com) and an Aminco AB 2 luminescence spectrometer (Thermo Scientific Inc., Waltham, MA, USA, www.thermo.com), respectively. The *p/T* calibration chamber was provided by the German Aerospace Center (DLR) in Göttingen. All time-resolved measurements were performed with a PCO SensiCam 12 bit b/w CCD camera (PCO, Kelheim, Germany, www.pco.de) equipped with a Schneider-Kreuznach Xenon 0.95/17 lens (Jos. Schneider Optische Werke, Bad Kreuznach, Germany, www.schneiderkreuznach.com) and a 405-66-60 405 nm LED from Roithner Lasertechnik (Vienna, Austria, www.roithner-laser.com). The excitation light was focused by a PCX 18_18 MgF2 TS lens from Edmund Optics (Karlsruhe, Germany, www.edmundoptics.com). The concentration of the polymer solutions was 5% (w/w) in THF. The polymers including poly(1-vinylpyrrolidone-*co*- styrene) emulsion in water (38% w/w emulsion in water), 9,10-Diphenylanthracene, and platinum(II)-5,10,15,20-*tetrakis*(2,3,4,5,6-pentafluorophenyl)porphyrin (PtTFPP) were purchased from Sigma-Aldrich (www.sigmaaldrich.com). In order to increase the luminescence intensity recorded by the camera, the backside of the PET foils was coated with a highly reflective layer of $TiO_2$ in silicone. Chromatography: Separations were carried out on Geduran Si 60 (0.063-0.200 mm). Thin layer chromatography (TLC) was performed on Analtech uniplate silica gel GF plates (500 micron, 20 × 20 cm) and developed with (*n*-hexane/ethyl acetate:10/3).

2-(4-Bromophenyl)-5,6,7,8-tetrahydroquinoline[19], as well as the dimer[18] and the complex[4,13-18] were synthesized according to partly modified literature procedures.

*PVDCAN particles doped with [Pt(II)(Br-thq)(acac)].* The particles were prepared following the precipitation method.[23] Typically, 40 mg of PVDCAN and 3 mg [Pt(II)(Br-thq)(acac)] were dissolved in 20 mL of tetrahydrofuran. With rigorous stirring, 60 mL of double distilled water was poured into the solution, and the acetone was removed at reduced pressure. Particles were freeze-dried before storage. [Pt(II)(Br-thq)(acac)] was synthesized and characterized as above-described.

*PS-co-PVP particles doped with PtTFPP.* Five hundred twenty-six milligrams of the PS-*co*-PVP polymer aqueous dispersion (at 38 % (w/w) this equals 200 mg of the polymer) were diluted with the mixture of 60 mL of water and 30 mL of tetrahydrofurane. PtTFPP

(3 mg) was dissolved in 20 mL of THF, and the solution was added drop-wise under vigorous stirring into the dispersion. This process renders the particles doped with PtTFPP. After 30 min all THF and partly water were removed under reduced pressure and the dispersion was concentrated to contain 20% w/w of the beads in water. Particles were freeze-dried before storage.

*Preparation of the sensor film.* 0.4 mg of DPA/PAN, 8 mg of [Pt(II)(Br-thq) (acac)]/ PVDCAN, and 1.5 mg of PtTFPP/PS-*co*-PVP were dispersed in 0.5 ml of a 1% (w/w) solution of D4 polyurethane hydrogel in 9:1 (v/v) ethanol:water. The dispersion was spread onto a solid poly(ethylene terephthalate) (Mylar®) foil by knife coating.

*Hardware and Software.* The RGB imaging setup[8] consists of a standard digital camera (Canon EOS50D), a modified ring light with 28 LEDs (405 nm peak wavelength; UV5TZ-405-15 BIVAR), and a GG435 emission filter (www.Schott.com). Camera parameters were set as follows: Raw+jpg; ISO 160; white balance 2450 K. Excessive ambient light is to be avoided. The image data were stored as 16-bit TIFs using the Adobe Camera Raw plug-in for Adobe Photoshop and data were further processed with ImageJ software. The images are split into the three color channels. The ratios of R/B and G/B are calculated and plotted vs. the air pressure or temperature respectively. Lifetime imaging was performed with a PCO SensiCam 12 bit b/w CCD camera (PCO, Kelheim; www.pco.de) equipped with a Schneider- Kreuznach Xenon 0.95/17 lens (Schneider Optische Werke; www.schneiderkreuznach.com) and a 405-66-60 405 nm LED from Roithner Lasertechnik (Vienna; www.roithner-laser.com).

The pressure/temperature calibration chamber was provided by the German Aerospace Center (DLR) in Göttingen (www.dlr.de).

## 9.5    References

[1]     M. Gouterman, J. Callis, L. Dalton, G. Khalil, Y. M´ebarki, *Meas. Sci. Technol.* **2004**, *15*, 1986-1994.

[2]     M. E. Köse, B. F. Carroll, K. S. Schanze, *Langmuir* **2005**, *21*, 9121-9129.

[3]     M. I. J. Stich, S. Nagl, O. S. Wolfbeis, U. Henne, M. Schaeferling, *Adv. Funct. Mater* **2008**, *18*, 1399-1406.

[4]     L. H. Fischer, M. I. J. Stich, O. S. Wolfbeis, N. Tian, E. Holder, M. Schaferling, *Chem. Eur. J.* **2009**, *15*, 10857-10863.

[5]     M. I. J. Stich, L. H. Fischer, O. S. Wolfbeis, *Chem. Soc. Rev.* **2010**, *39*, 3102-3114.

[6]     K. Mitsuo, K. Asai, A. Takahashi, H. Mizushima, *Meas. Sci. Technol.* **2006**, *17*, 1282-1291.

[7]     M. I. J. Stich, S. M. Borisov, U. Henne, M. Schaferling, *Sens. Actuat. B-Chem.* **2009**, *139*, 204-207.

[8]     R. J. Meier, S. Schreml, X. D. Wang, M. Landthaler, P. Babilas, O. S. Wolfbeis, *Angew. Chem. Int. Ed.* **2011**, *50*, 10893-10896.

[9]     X. D. Wang, R. J. Meier, M. Link, O. S. Wolfbeis, *Angew. Chem. Int. Ed.* **2010**, *49,* 4907-4909.

[10]    B. E. Bayer, U. P. 3971065  1976.

[11]    C. M. L. Burnett; Bayer pattern on Sensor; Wikimedia Commons: 2006.

[12]    Antaya; Leucanthemum-vulgare, Wikimedia Commons: 2006.

[13]    N. Tian, D. Lenkeit, S. Pelz, L. H. Fischer, D. Escudero, R. Schiewek, D. Klink, O. J. Schmitz, L. Gonzalez, M. Schaferling, E. Holder, *Eur. J. Inorg. Chem.* **2010**, 4875-4885.

[14]    N. Tian, A. Thiessen, R. Schiewek, O. J. Schmitz, D. Hertel, K. Meerholz, E. Holder, *J. Org. Chem.* **2009**, *74*, 2718-2725.

[15]    N. Tian, Y. V. Aulin, D. Lenkeit, S. Pelz, O. V. Mikhnenko, P. W. M. Blom, M. A. Loi, E. Holder, *Dalton Trans.* **2010**, *39*, 8613-8615.

[16]    N. Tian, D. Lenkeit, S. Pelz, D. Kourkoulos, D. Hertel, K. Meerholz, E. Holder, *Dalton Trans.* **2011**, *40*, 11629-11635.

[17]    J. Brooks, Y. Babayan, S. Lamansky, P. I. Djurovich, I. Tsyba, R. Bau, M. E. Thompson, *Inorg. Chem.* **2002**, *41*, 3055-3066.

[18]    B. N. Cockburn, D. V. Howe, T. Keating, B. F. G. Johnson, J. Lewis, *J. Chem. Soc. Dalton* **1973**, 404-410.

[19]    D. Sielemann, R. Keuper, N. Risch, *J. Prak. Chem-Chem. Ztg.* **1999**, *341*, 487-491.

[20]    S. M. Borisov, T. Mayr, I. Klimant, *Anal. Chem.* **2008**, *80*, 573-582.

[21]    R. Nagarajan, M. Barry, E. Ruckenstein, *Langmuir* **1986**, *2*, 210-215.

[22]    M. I. Stich, O. S. Wolfbeis *Fluorescence Sensing and Imaging Using Pressure-Sensitive Paints and Temperature-Sensitive Paints; Standardization and Quality Assurance in Fluorescence Measurements I* Springer, 2008; Vol. 5.

[23]    S. M. Borisov, T. Mayr, G. Mistlberger, K. Waich, K. Koren, P. Chojnacki, I. Klimant, *Talanta* **2009**, *79*, 1322-1330.

[24]    X. D. Wang, X. H. Song, C. Y. He, C. J. Yang, G. N. Chen, X. Chen, *Anal. Chem.* **2011**, *83*, 2434-2437.

# Chapter 10

# Summary

## 10.1  Summary in English

This thesis describes the preparation and evaluation of new materials for imaging of barometric pressure and temperature using so-called luminescent paints. The historical background and the motivation for the research conducted are given in Chapter 1. Chapter 2 summarizes the basic principles of photoluminescence involved in imaging of partial oxygen pressure and temperature, the fundamentals of the design of pressure and temperature sensitive paints. It also summarizes the effects of luminescence quenching by oxygen and temperature together with the respective equations. An overview of materials used in such pressure sensitive paints (PSPs) and temperature sensitive paints (TSPs) is given, this is followed by an explanation of various methods for the readout of such paints together with a description of the hardware needed and used for those methods. These methods of readout are compared in terms of standard deviation, lateral signal homogeneity and resolution in Chapter 3. The advantages and disadvantages of the different techniques also are discussed, especially for lifetime imaging and RGB color camera imaging. Referenced intensity imaging is another method of readout. This method utilizes a reference dye which is insensitive towards the analyte or displays a different sensitivity compared to the indicator dye. In Chapter 4 such reference dyes are characterized, calibrated and compared. A general problem in dually sensitive paints is the separation of two luminescent signals. The spectral overlap of the emissions of two indicators should be a small as possible. Most established indicators for $pO_2$ and temperature display red emission. Therefore, new complexes that have not yet been evaluated for indicator purposes were searched for and investigated. Chapter 5 is dealing with homoleptic and heteroleptic iridium(III) complexes with respect to their ability as pressure or

temperature indicator. The complexes are calibrated via lifetime imaging and the results are compared. They provide blue to green emission which is separable from red emitting indicators. The best temperature indicator and the best pressure (oxygen) indicator amongst them were combined to demonstrate the applicability in a dually sensitive paint which is described in Chapter 6. The composition, the separation of the two luminescent signals, and the calibration of this dual paint is described in detail. One of the iridium(III) complexes evaluated above was applied in a dually sensitive paint base on water instead of organic solvents (see Chapter 7). It is the first dually sensitive paint working like emulsion paint. The preparation and calibration of this material is described in detail. Cyclometalated platinum(II) complexes were found to be fairly unstudied in terms of indicator applications. The applicability of various Pt(II) complexes is investigated in Chapter 8. The spectra of the compounds and the sensitivity of their luminescence lifetime towards oxygen and temperature were measured and compared. The performance of PtTFPP for sensing air pressure in the range of atmospheric pressure was mot surpassed by any of the investigated dyes. The temperature indicator has to display blue to green emission if applied together with PtTFPP in a dually sensitive paint. The aim of further research should be the discovery of blue to green emitting temperature indicators with improved temperature resolution. The emission of one of the cyclometalated Pt(II) dyes is not only temperature dependent and separable from the red PtTFPP, it also matches the green channel of a RGB color camera. Based on the results of Chapter 4 and Chapter 8, the first dually sensitive paint appropriate for color camera read out was prepared. This novel material is specified in Chapter 9. Its oxygen and temperature response was calibrated. The standard deviation, the influence of inhomogeneous illumination and the resolution was determined.

## 10.2 Summary in German

In dieser Arbeit wird die Herstellung und Kalibration neuer Materialien für die bildgebende Messung von Luftdruck und Temperatur mittels lumineszenter Farben beschrieben. Der historische Hintergrund und die Motivation der durchgeführten Forschung sind in Kapitel 1 dargelegt. In Kapitel 2 sind die dabei zu beachtenden Grundlagen der Photolumineszenz erklärt. Dieses Kapitel beschreibt außerdem den grundsätzlichen Aufbau von Druck- und Temperatur-sensitiven Farben und es fasst die Effekte der Lumineszenzlöschung durch Sauerstoff und Temperatur anhand der zugehörigen Gleichungen zusammen. Anschließend an einen Überblick über die Materialien, die in solchen Druck- und Temperatur-sensitiven Farben zum Einsatz kommen, werden verschiedene Methoden des Auslesens solcher Farben erläutert, inklusive der dafür benötigten Instrumente und Komponenten. Die Methoden des Auslesens werden in Kapitel 3 hinsichtlich der Standardabweichung, der lateralen Signalhomogenität und der Auflösung verglichen. Ferner werden die Vor- und Nachteile der verschiedenen Techniken diskutiert, speziell die der Messung der Lumineszenzlebenszeit und der Messung mittels digitaler RGB Farbkameras. Eine weitere Methode des Auslesens ist die referenzierte Intensitätsmessung. Bei dieser Technik kommt ein Referenzfarbstoff zum Einsatz, dessen Emission insensitiv von der Analytkonzentration ist oder eine deutlich unterschiedliche Sensitivität zeigt verglichen mit dem Indikatorfarbstoff. Derartige Referenzfarbstoffe werden in Kapitel 4 charakterisiert, kalibriert und verglichen. Ein generelles Problem bei dual sensitiven Farben ist die Trennung der lumineszenten Signale. Die spektrale Überlappung der Emissionen beider Indikatoren sollte so gering wie möglich sein. Die etablierten Indikatoren für Sauerstoff (z.B. PtTFPP) und für Temperatur (z.B. Eu-Komplexe) zeigen rote Emissionen. Darum wurden neue Komplexe, die bisher nicht auf ihre Eignung als Indikatoren untersucht wurden, ermittelt und charakterisiert. In Kapitel 5 werden homo- und heteroleptische Iridium(III) Komplexe hinsichtlich der Druck- und Temperatursensitivität ihrer Lumineszenzlebenszeit untersucht und verglichen. Die blauen bis grünen Emissionen der Farbstoffe kann von der roten Emission eines zweiten Indikators abgetrennt werden. Der Komplex mit der höchsten Drucksensitivität (Sauerstoffsensitivität) und der Komplex mit der größten Temperaturabhängigkeit wurden in einer dual-sensitiven Farbe kombiniert, die in Kapitel 6 beschrieben ist. Darin

sind die Zusammensetzung der Farbe, die Trennung der beiden Signale und die Kalibration dieser dualen Farbe beschrieben. Einer der Iridium (III) Komplexe kommt in einer dual sensitiven Farbe auf Wasserbasis, anstatt basierend auf organischen Lösungsmitteln, zum Einsatz, der in Kapitel 7 beschrieben wird. Es handelt sich dabei um die erste dual-sensitive Farbe, die wie eine Dispersionsfarbe funktioniert. Die Herstellung und die Kalibration dieses Materials werden hier im Detail beschrieben. Die Eignung verschiedener Platin(II) Komplexe als Druck- beziehungsweise Temperaturindikator wird in Kapitel 8 untersucht. Die Absorptions- und Emissionsspektren der Komplexe wurden gemessen und die Druck- und Temperaturabhängigkeit der Lumineszenzlebenszeiten wurden bestimmt und verglichen. Die Eignung des rot emittierenden PtTFPP zur Messung des Luftdrucks im Bereich des Atmosphärendrucks wurde von keinem der in dieser Arbeit untersuchten Komplexe übertroffen. Ein Temperaturindikator, der mit PtTFPP in einer dualen Farbe verwendet werden soll, muss folglich im blauen bis grünen Spektralbereich emittieren. Das Ziel weiterer Forschungen sollte die Entdeckung eines blau bis grün emittierenden Temperaturindikators mit verbesserter Temperaturauflösung sein. Die Emission eines der Pt(II) Komplexe aus Kapitel 8 ist temperaturabhängig und kann spektral von der Emission von PtTFPP getrennt werden. Die grüne Emission des Farbstoffes passt außerdem in den spektralen Bereich des grünen Kanals einer RGB Farbkamera. Basierend auf den Ergebnissen von Kapitel 4 und Kapitel 8 wurde die erste dual-sensitive Farbe, die mit einer RGB Farbkamera ausgelesen werden kann, hergestellt. Dieses neue Material wird in Kapitel 9 beschrieben. Die Druck- und Temperaturabhängigkeit des Materials wurde kalibriert, die Standardabweichung der Signale ermittelt, der Einfluss inhomogener Beleuchtung wurde untersucht und die Auflösung bestimmt.

# Chapter 11

# Curriculum Vitae

| | |
|---|---|
| **Name** | Fischer |
| **First Name** | Lorenz Heinrich |
| **Date of Birth** | March 8, 1983 |
| **Place of Birth** | Regensburg |
| **Nationality** | German |

### Education

| | |
|---|---|
| 09/1993 – 06/2002 | Goethe – Gymnasium Regensburg |

### Civil Service

| | |
|---|---|
| 10/2002 – 07/2003 | Regensburger Kranken Transporte RKT |

### Studies

| | |
|---|---|
| 10/2003 – 10/2008 | Chemistry (Diploma), University of Regensburg |
| 01/2009 – 06/2012 | PhD Thesis, Institute of Analytical Chemistry, Chemo-and Biosensors, University of Regensburg |

# Chapter 12

# List of Publications

## 12.1 Journal Articles

1. Lorenz H. Fischer, Matthias I. J. Stich, Otto S. Wolfbeis, Nan Tian, Elisabeth Holder, Michael Schäferling, ***Red- and Green-Emitting Iridium(III) Complexes for a Dual Barometric and Temperature-Sensitive Paint***; Chemistry – A European Journal, **2009**, 15, 41, 10857–10863

2. Lorenz H. Fischer, Sergey M. Borisov, Michael Schaeferling, Ingo Klimant, Otto S. Wolfbeis, ***Dual Sensing of pO$_2$ and Temperature Using a Water-Based and Sprayable Fluorescent Paint***, Analyst, **2010**,135, 1224-1229

3. Lorenz H. Fischer, Gregory S. Harms, Otto S. Wolfbeis, ***Upconverting Nanoparticles for Nanoscale Thermometry***, Angewandte Chemie International Edition, **2011**, 50, 20, 4546–4551

4. Lorenz H. Fischer, Cüneyt Karakus, Robert J. Meier, Otto S. Wolfbeis, Elisabeth Holder, Michael Schäferling, ***Referenced Dual Pressure and Temperature Sensitive Paint for Digital Color Camera Read Out***, **2012**, *submitted*

5. Lorenz H. Fischer, Robert J. Meier, Otto S. Wolfbeis, Michael Schäferling, ***Referenced Fluorescence Imaging with Digital Color Cameras: A Comparative Study***, **2012**, *in preparation*

6. Matthias I. J. Stich, Lorenz H. Fischer, Otto S. Wolfbeis, ***Multiple Fluorescent Chemical Sensing and Imaging***, Chemical Society Reviews, **2010**, 39, 3102-3114

7. Hongshang Peng, Matthias I. J. Stich, Jiangbo Yu, Li-ning Sun, Lorenz H. Fischer, Otto S. Wolfbeis, ***Luminescent Europium(III) Nanoparticles for Sensing and Imaging of Temperature in the Physiological Range***, Advanced Materials, **2010**, 22, 6, 716–719

8. Nan Tian, Daniel Lenkeit, Simon Pelz, Lorenz H. Fischer, Daniel Escudero, Ralf Schiewek, Dennis Klink, Oliver J. Schmitz, Leticia González, Michael Schäferling, Elisabeth Holder, ***Structure–Property Relationship of Red- and Green-Emitting Iridium(III) Complexes with Respect to Their Temperature and Oxygen Sensitivity***, European Journal of Inorganic Chemistry, **2010**, 30, 4875–4885

9. Daniela E. Achatz, Robert J. Meier, Lorenz H. Fischer, Otto S. Wolfbeis, ***Luminescent Sensing of Oxygen Using a Quenchable Probe and Upconverting Nanoparticles***, Angewandte Chemie International Edition, **2011** 50, 1, 260–263

10. Joanna Napp, Thomas Behnke, Lorenz Fischer, Christian Würth, Marieke Wottawa, Dörthe M. Katschinski, Frauke Alves, Ute Resch-Genger, Michael Schäferling, ***Targeted Luminescent Near-Infrared Polymer-Nanoprobes for In Vivo Imaging of Tumor Hypoxia***, Analytical Chemistry, **2011**, 83, 23, 9039–9046

11. Anne Heller, Lorenz H. Fischer, Otto S. Wolfbeis, Achim Göpferich, ***Long Time Monitoring of the Respiratory Activity of Isolated Mitochondria***, Experimental Cell Research, **2012**, *in press*

12. Cüneyt Karakus, Lorenz H. Fischer, Sebastian Schmeding, Johanna Hummel, Nikolaus Risch, Michael Schäferling, Elisabeth Holder, ***Oxygen and Temperature Sensitivity of Blue to Green to Yellow Light-Emitting Pt(II) Complexes***, Dalton Transactions, **2012**, *in press, DOI:10.1039/C2DT30835E*

13. Andreas Sedlmeier, Daniela E. Achatz, Lorenz H. Fischer, Hans H. Gorris, Otto S. Wolfbeis, ***Photon Upconverting Nanoparticles for Luminescent Sensing of Temperature***, **2012**, *in preparation*

14. Xudong Wang, Robert J. Meier, Lorenz H. Fischer, Otto S. Wolfbeis, ***Review: Optical Probes and Nanoparticles for Sensing Temperature***, **2012**, *in preparation*

## 12.2 Posters

1. Lorenz H. Fischer, Nan Tian, Elisabeth Holder, Otto S. Wolfbeis,Michael Schäferling, *Red and Green Emitting Ir(III) Probes for Lifetime Imaging of Barometric Pressure and Temperature,* 2nd German-Japanese Seminar: Molecular Imaging for Interdisciplinary Research*,* Regensburg*,* **2009**

2. Lorenz H. Fischer, Nan Tian, Daniel Escudero, Leticia González, Elisabeth Holder, Otto S. Wolfbeis, Michael Schäferling*, Oxygen and Temperature Sensitivities of Cyclometalated Ir(III) Triplet Emitters,* Europtrode Conference on Optical Chemical Sensors and Biosensors, Prague, **2010**

3. Lorenz H. Fischer, Robert J. Meier, Otto S. Wolfbeis, Michael Schäferling, *Fluorescence Imaging with Digital Color Cameras: Limits for Quantitative Analysis*, Europtrode Conference on Optical Chemical Sensors and Biosensors, Barcelona, **2012**

4. Nan Tian, Lorenz H. Fischer, Matthias I. J. Stich, Otto S. Wolfbeis, Michael Schäferling, Elisabeth Holder, *Red and Green Emitting Ir(III) Complexes for Dual Barometric and Temperature Sensors,* GDCh-Frühjahrskolloquium, Wuppertal, **2009**

5. Cüneyt Karakus, Lorenz H. Fischer, Michael Schäferling, Elisabeth Holder, *Cyclometalated Green Platin(II) Complexes: Temperature-Sensitive Sensor Materials,* 3rd EuCHEMS Chemistry Congress, Nürnberg, **2010**

6. Michael Schäferling, Lorenz H. Fischer, Cüneyt Karakus, Elisabeth Holder, *Luminescent Properties of Green Emitting Cyclometalated Platinum(II) Complexes,* Conference on Methods and Applications of Fluorescence, Strasbourg, **2011**

# Erklärung

Hiermit erkläre ich, dass ich die vorliegende Arbeit selbst verfasst, und keine anderen als die angegebenen Hilfsmittel und Quellen verwendet habe.

Regensburg, den 30. Mai 2012

_____

Lorenz Fischer